

Evaluation of ECHAM5/MESSy2

Patrick Jöckel^{1,2}, Astrid Kerkweg³,
Andrea Pozzer⁴, Rolf Sander¹, Holger Tost¹,
Hella Riede¹, Andreas Baumgaertner¹,
Sergey Gromov¹, Bastian Kern¹

¹ Air Chemistry Department, Max-Planck Institute of Chemistry, PO Box 3060,
55020 Mainz, Germany

² Deutsches Zentrum für Luft- und Raumfahrt, Institut für Physik der
Atmosphäre, Oberpfaffenhofen, 82230 Wessling, Germany

³ Institute for Atmospheric Physics, University Mainz, 55128 Mainz, Germany

⁴ Cyprus Institute, EEWRC, P.O. Box 27456, 1645 Nicosia, Cyprus
Patrick.Joeckel@dlr.de

This document is part of the electronic supplement of our article “Development Cycle 2 of the Modular Earth Submodel System (MESSy2)” in Geosci. Model Dev. (2010), available at: <http://www.geoscientific-model-development.net>

Contents

1 Biomass burning emissions	3
2 Global views	4
3 Vertical profiles	7
3.1 C ₂ H ₄	8
3.2 C ₂ H ₆	11
3.3 C ₃ H ₆	14
3.4 C ₃ H ₈	16
3.5 CH ₃ COCH ₃	19
3.6 CH ₃ OH	21
3.7 CO	22
3.8 H ₂ O ₂	26
3.9 HCHO	29
3.10 HNO ₃	31
3.11 HNO ₃ + NO ₃ ⁻ (cs)	34
3.12 O ₃	37
3.13 ²¹⁰ Pb	40
4 Time series	41
4.1 CO	42
4.2 ²¹⁰ Pb	55
4.3 ²²² Rn	83
References	87

1 Biomass burning emissions

Table 1: Total annual biomass burning emissions (in Tg(species)/year, NOx emissions in Tg(N)/year) applied from the Global Fire Emission Database (GFED v2.1, Randerson et al., 2007; Van der Werf et al., 2006). The climatological averages (clim.) have been used for the years 2007 and 2008. The values in parentheses list the corresponding emissions of the year 2000 as incorporated in the EDGAR3.2FT2000 emission inventory, which has been used for all years in the previous study (Jöckel et al., 2006; Pozzer et al., 2007, see supplement).

substance	1997	1998	1999	2000	2001	2002	2003	2004	2005	2006	clim.
C ₂ H ₄	6.73	6.65	4.32	3.58 (4.84)	3.94	4.60	4.25	4.62	4.70	4.46	4.79
C ₂ H ₆	3.84	3.79	2.47	2.04 (2.76)	2.25	2.62	2.42	2.63	2.68	2.54	2.73
C ₃ H ₆	3.01	2.97	1.93	1.60 (2.16)	1.76	2.06	1.90	2.07	2.10	1.99	2.14
C ₃ H ₈	1.19	1.17	0.76	0.63 (0.86)	0.69	0.81	0.75	0.82	0.83	0.79	0.84
C ₄ H ₁₀	1.52	1.50	0.98	0.81 (1.10)	0.89	1.04	0.96	1.04	1.06	1.01	1.08
CH ₃ CHO	2.69	2.65	1.72	1.43 (1.93)	1.57	1.83	1.69	1.84	1.87	1.78	1.91
CH ₃ COCH ₃	2.44	2.41	1.57	1.30 (1.76)	1.43	1.67	1.54	1.68	1.70	1.62	1.74
CH ₃ COOH	8.61	8.50	5.53	4.58 (6.18)	5.03	5.88	5.43	5.90	6.00	5.70	6.12
CH ₃ OH	8.64	8.53	5.54	4.59 (6.24)	5.05	5.90	5.45	5.92	6.02	5.72	6.14
CO	554.60	588.39	389.65	335.77 (452.36)	364.06	416.60	395.33	404.22	409.97	389.49	424.81
HCHO	4.60	4.54	2.95	2.45 (3.31)	2.69	3.14	2.90	3.15	3.21	3.05	3.27
HCOOH	4.70	4.64	3.01	2.50 (3.37)	2.75	3.21	2.96	3.22	3.27	3.11	3.34
MEK	5.81	5.74	3.73	3.09 (4.19)	3.40	3.97	3.67	3.99	4.05	3.85	4.13
NOx	14.04	16.09	11.39	10.39 (9.28)	11.18	12.08	11.68	11.37	11.54	10.77	12.05

2 Global views

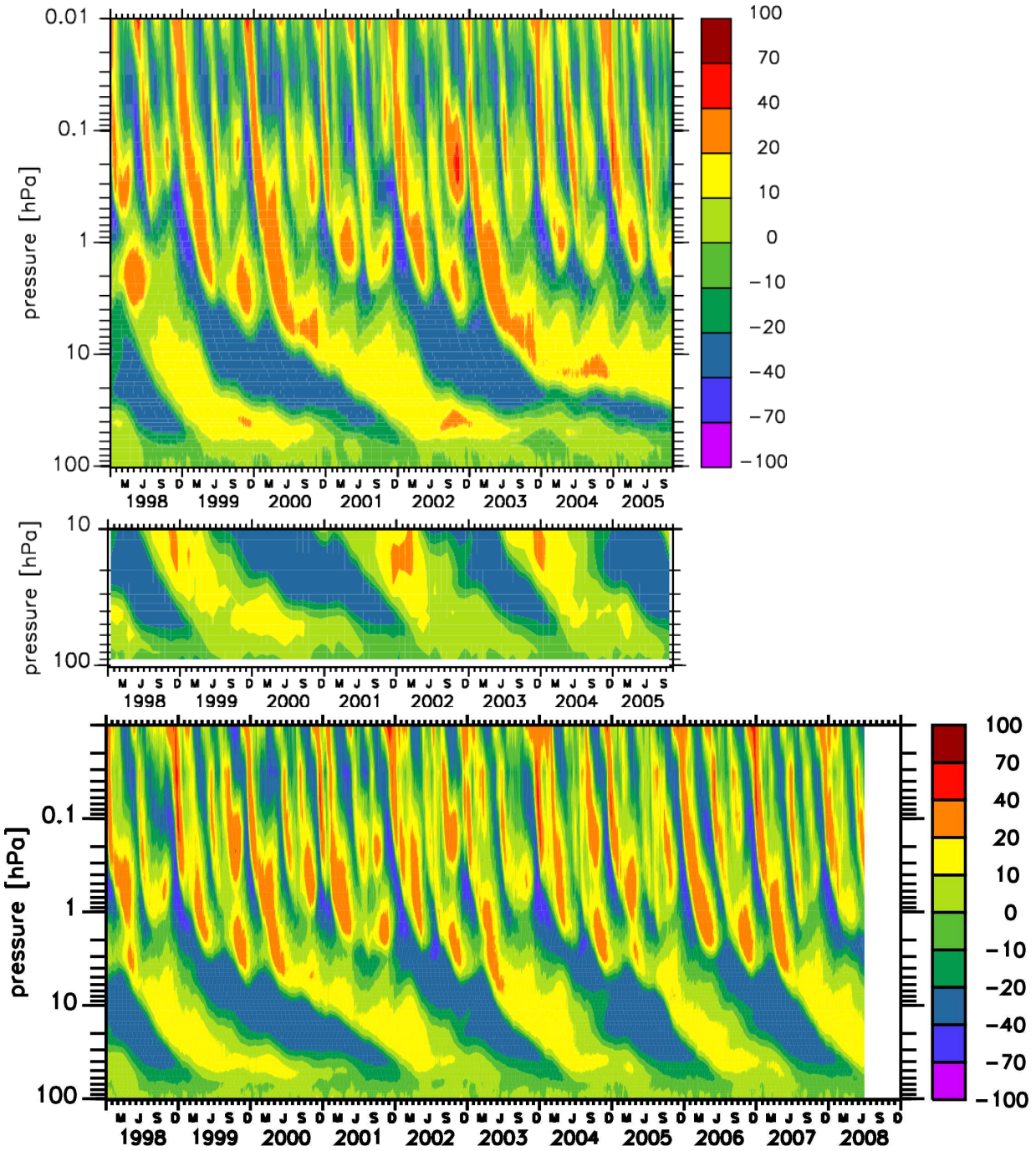


Figure 1: Tropical zonal wind average between 2°S and 2°N (in m/s) and its quasi-biennial oscillation. Upper panel: EMAC1 reference simulation (S1, see Jöckel et al., 2006, Fig. 2); middle panel: observations; lower panel: EMAC2 simulation of this study.

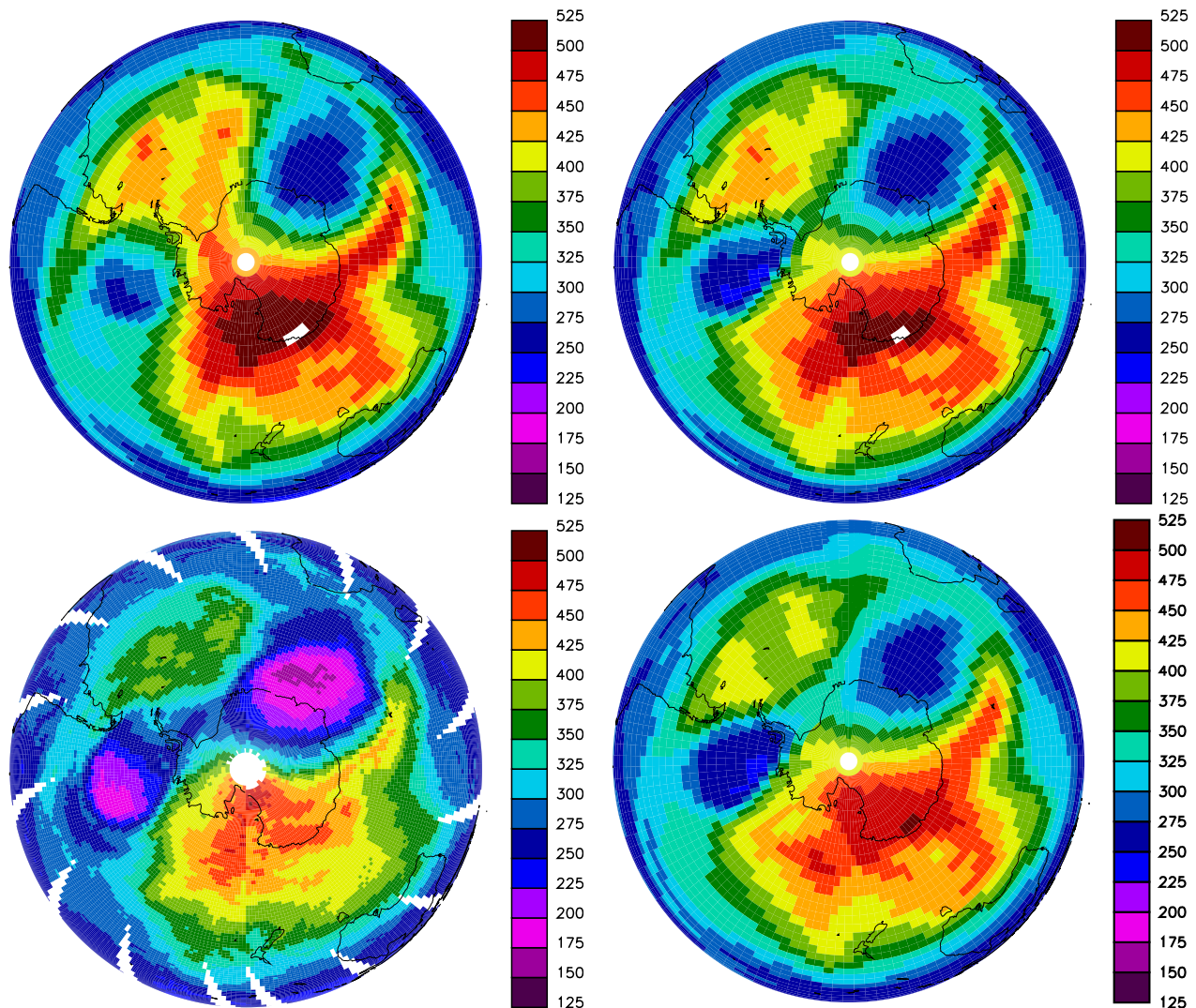


Figure 2: Total ozone (in DU) on 26 September 2002. Upper: simulated by EMAC1 (see Jöckel et al., 2006, Fig. 7) (left: S1, right: S2); lower left: observed by TOMS; lower right: EMAC2 simulation of this study.

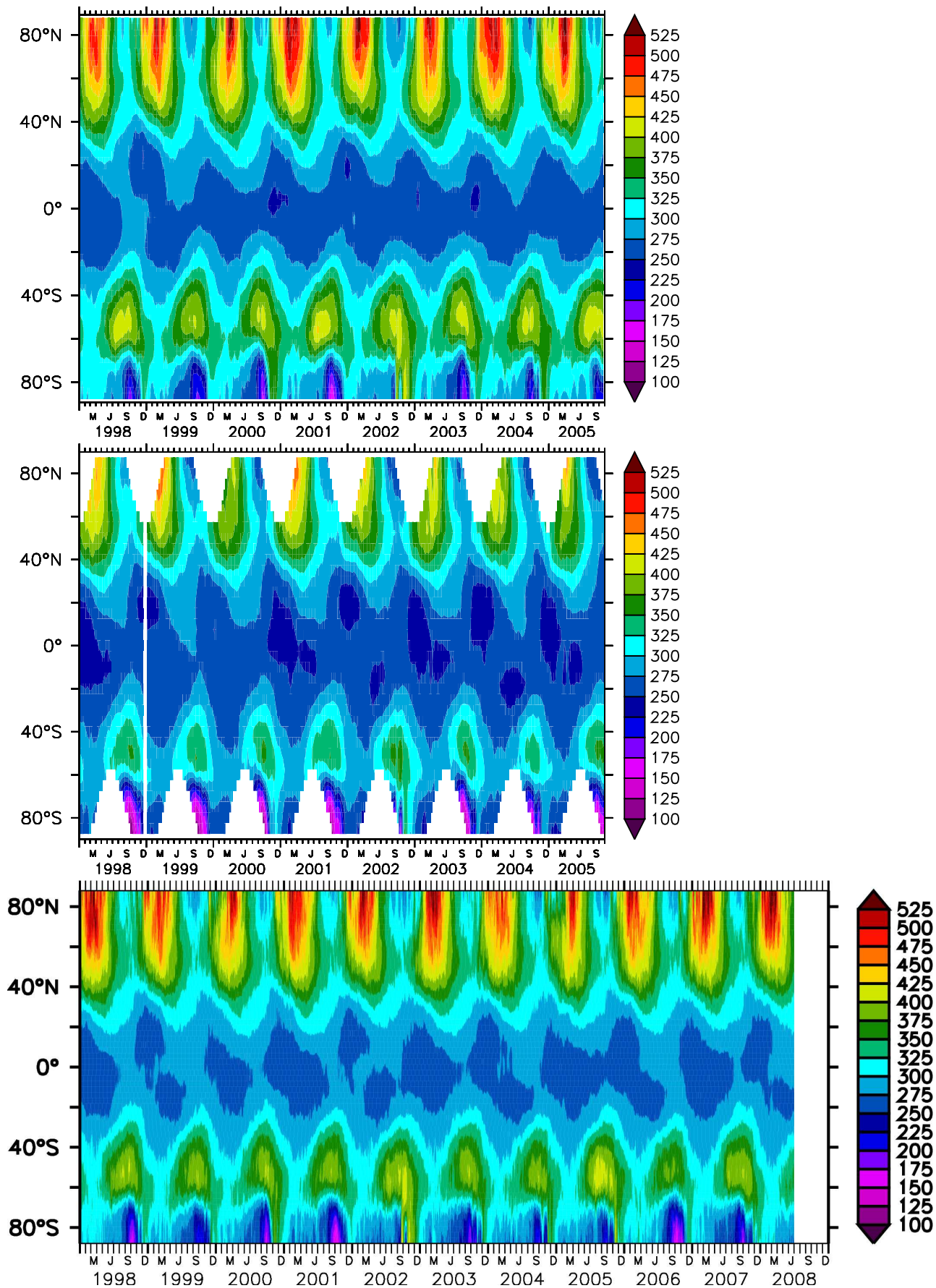


Figure 3: Time series of total ozone (zonally averaged, in DU). Upper panel: EMAC1 reference simulation (S1, see Jöckel et al., 2006, Fig. 9); middle panel: TOMS satellite data; lower panel: EMAC2 simulation of this study.

3 Vertical profiles

The simulated vertical profiles (for the year 2000) are compared to the compilation of observational data (mainly from aircraft campaigns) by Emmons et al. (2000). The geographical areas of the individual campaigns are listed above the panels. The left vertical axes show the altitude (in km), the horizontal axes show the mixing ratio (in the indicated units). Numbers close to the right vertical axes list the number of measurements, the asterisks show the mean values of the measurements, the boxes indicate the corresponding standard deviation. The blue lines are the results of the S1 simulation (Jöckel et al., 2006), the red lines those of the new simulation. The lines denote the average within the geographical area and during the time of the year of the respective campaign, the dashed lines the corresponding (plus / minus) spatio-temporal standard deviations.

3.1 C₂H₄

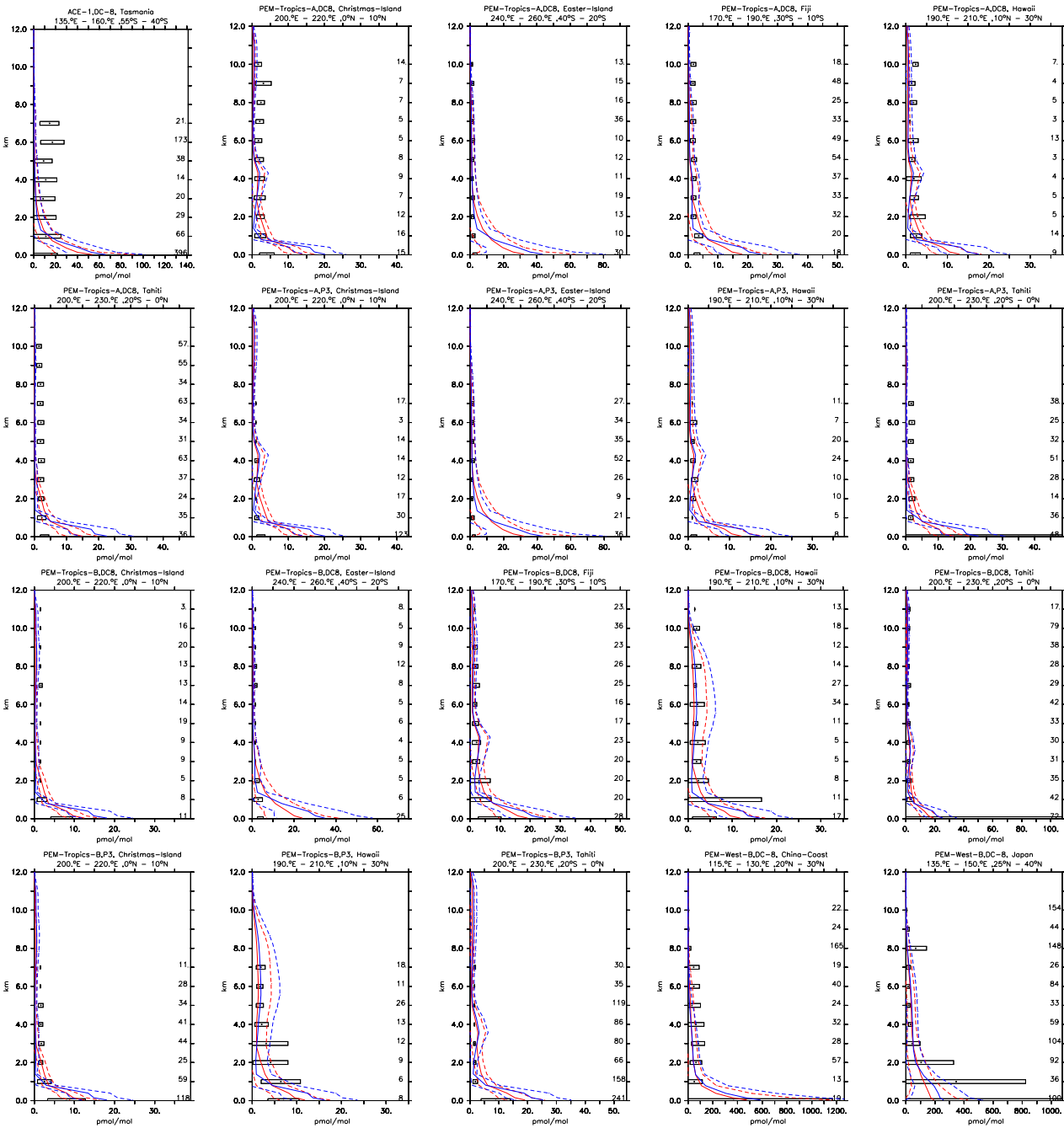


Figure 4:

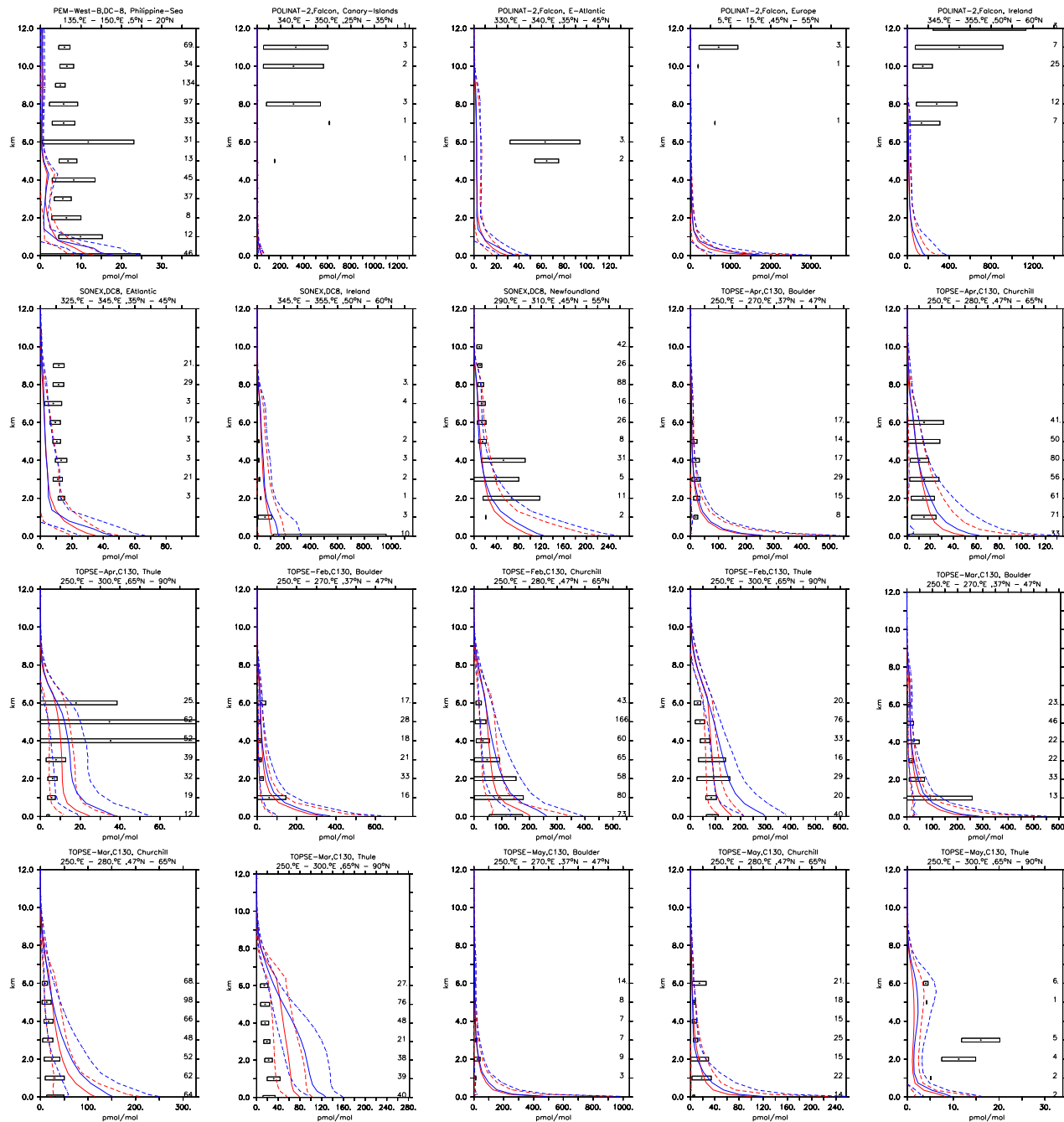


Figure 4: continued

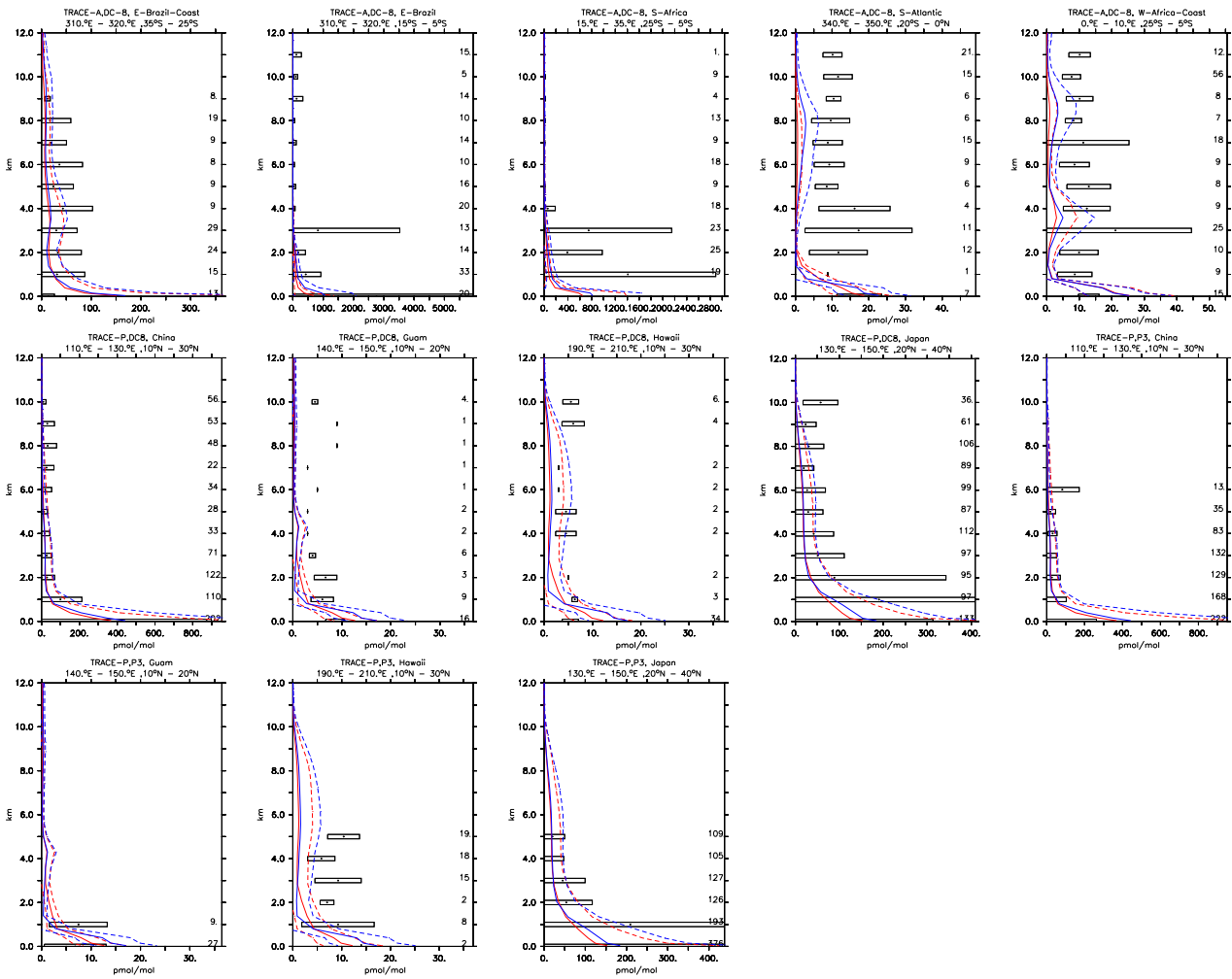


Figure 4: continued

3.2 C₂H₆

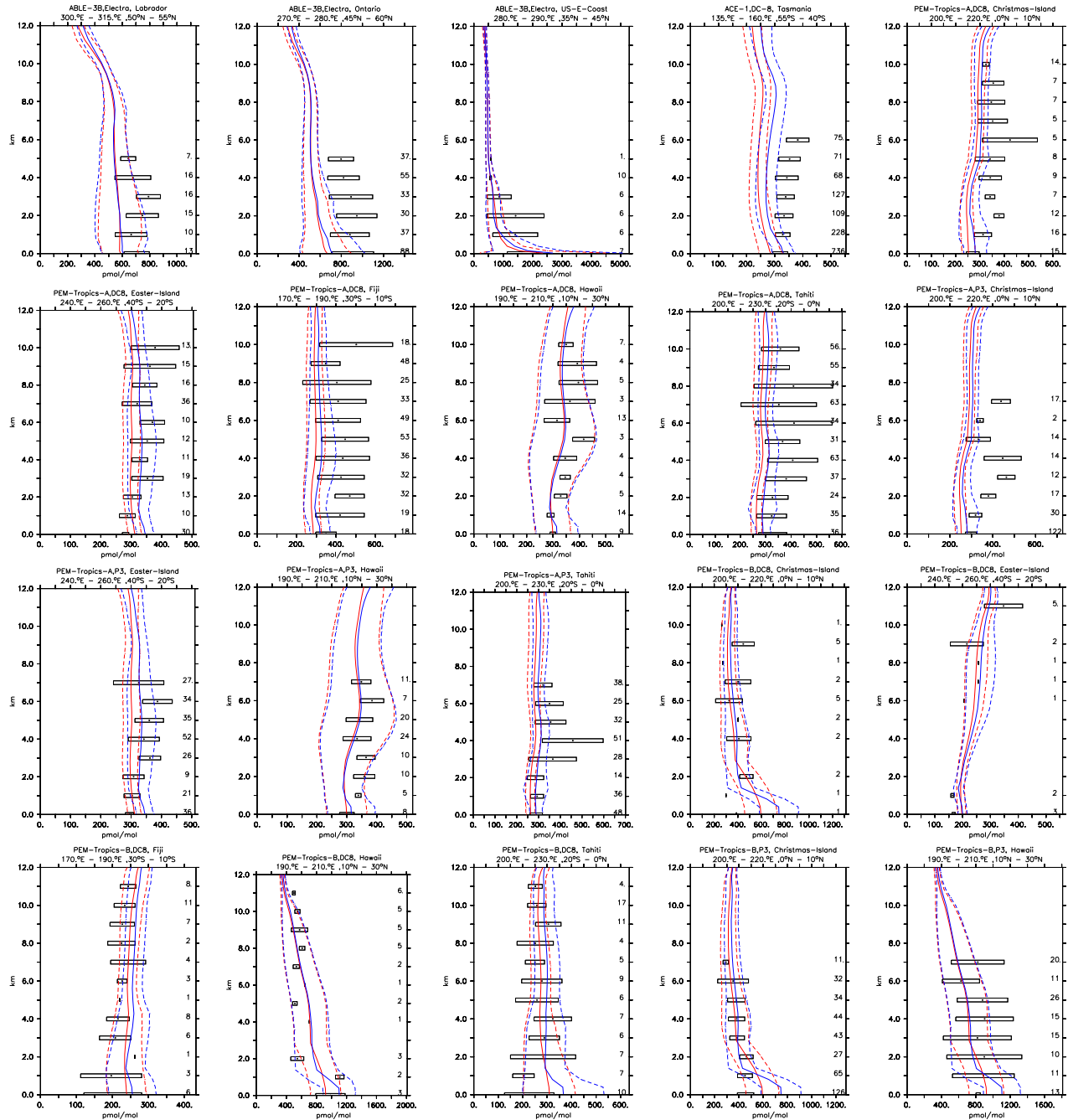


Figure 5:

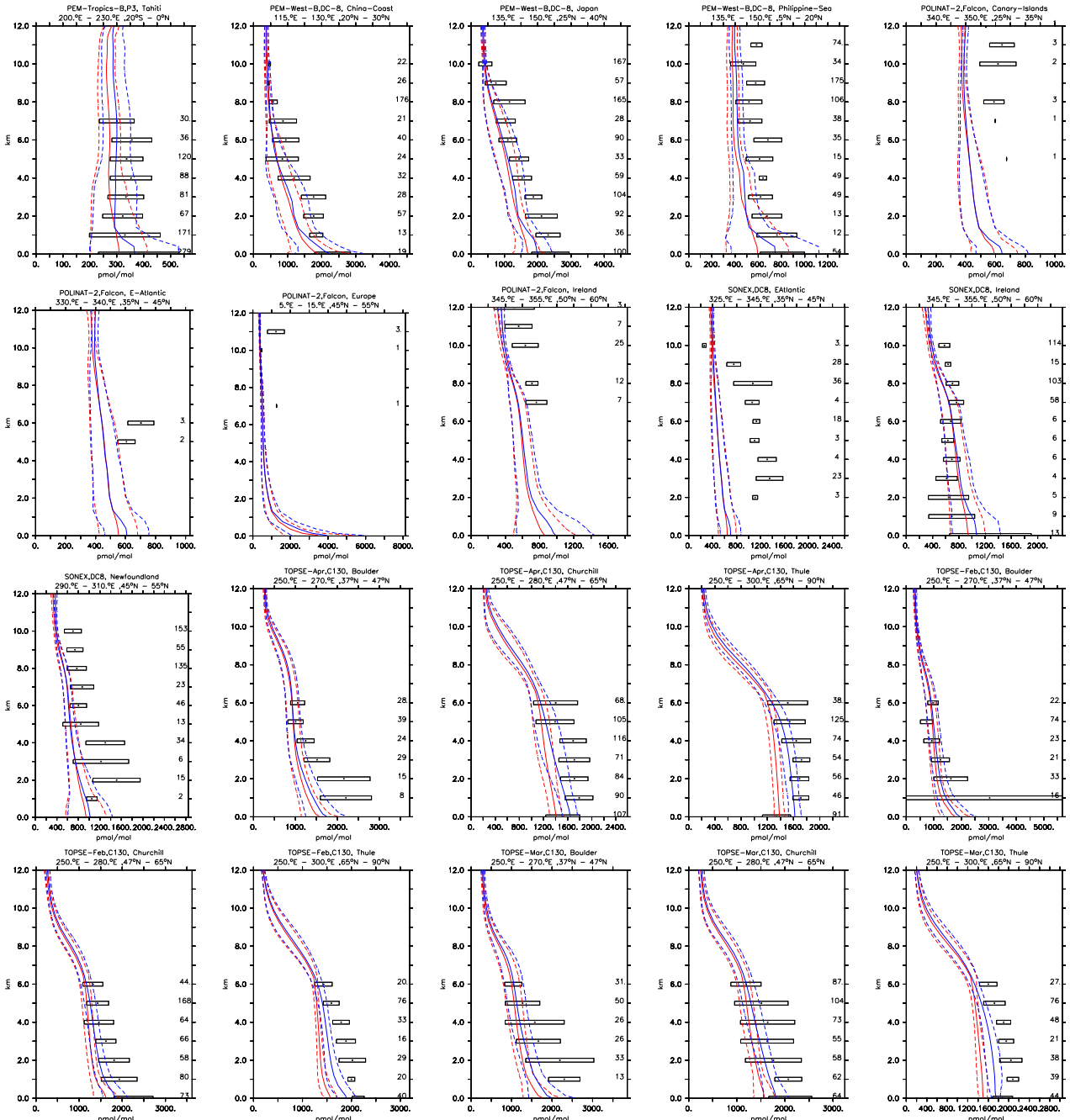


Figure 5: continued

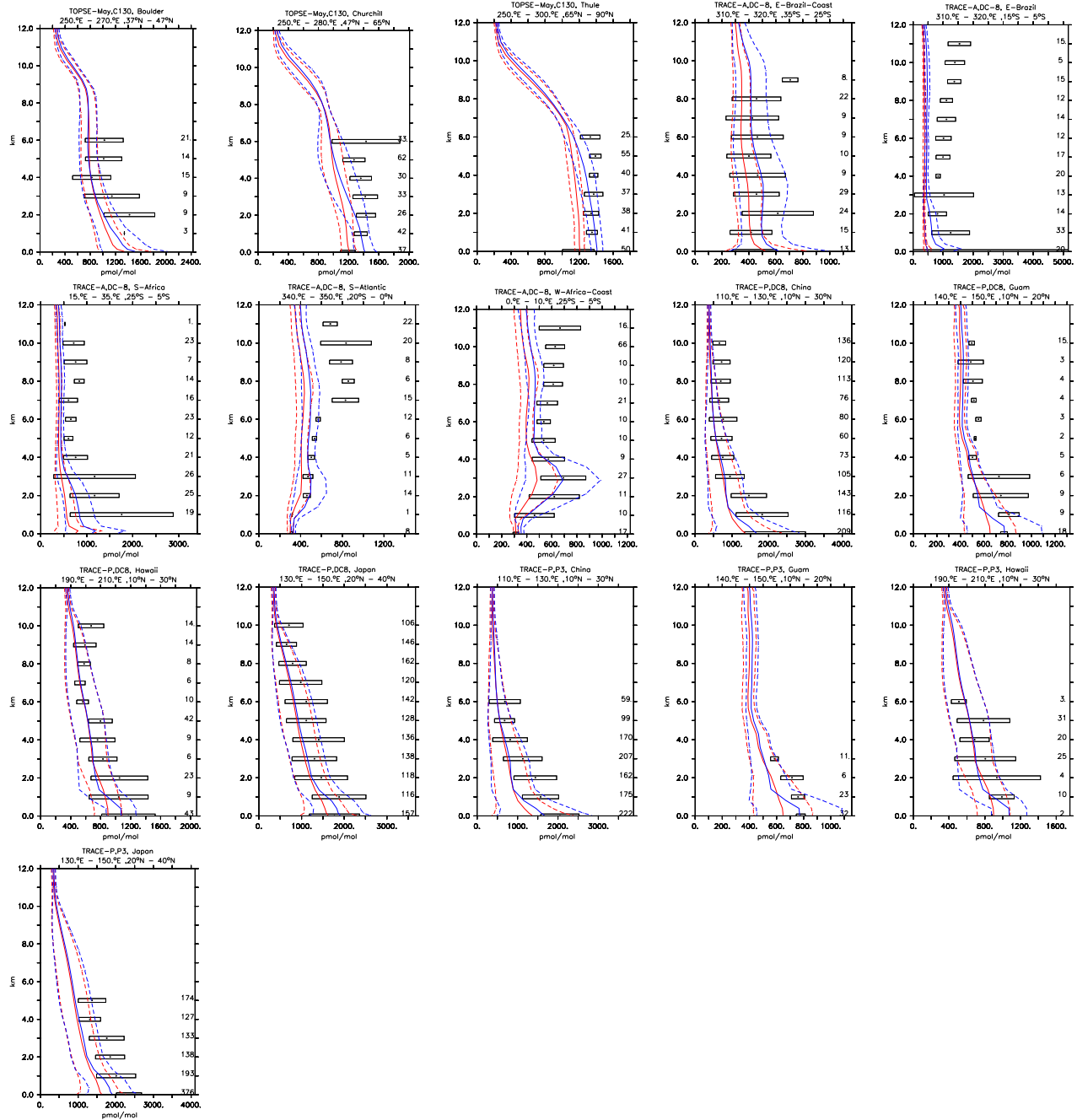


Figure 5: continued

3.3 C₃H₆

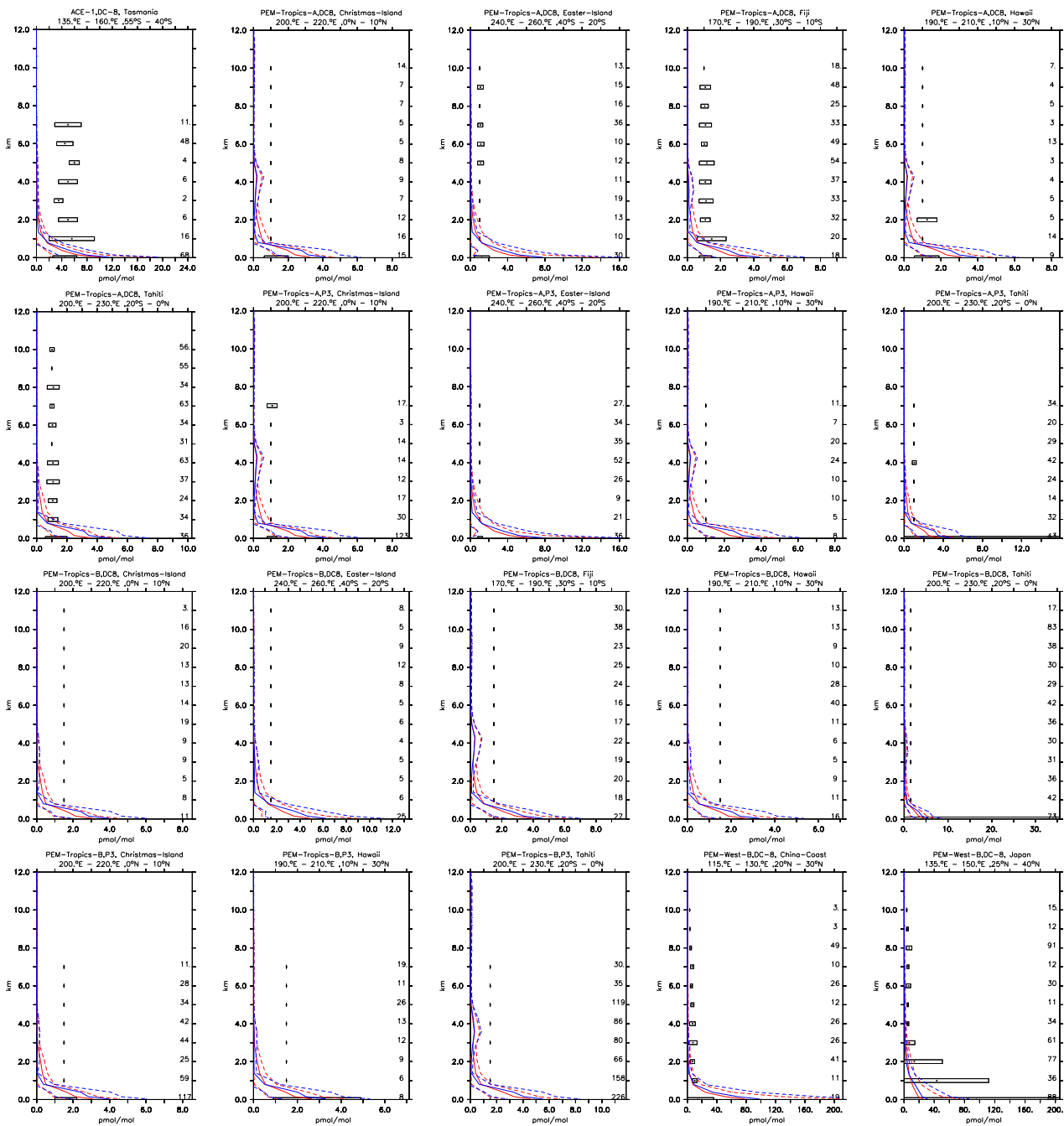


Figure 6:

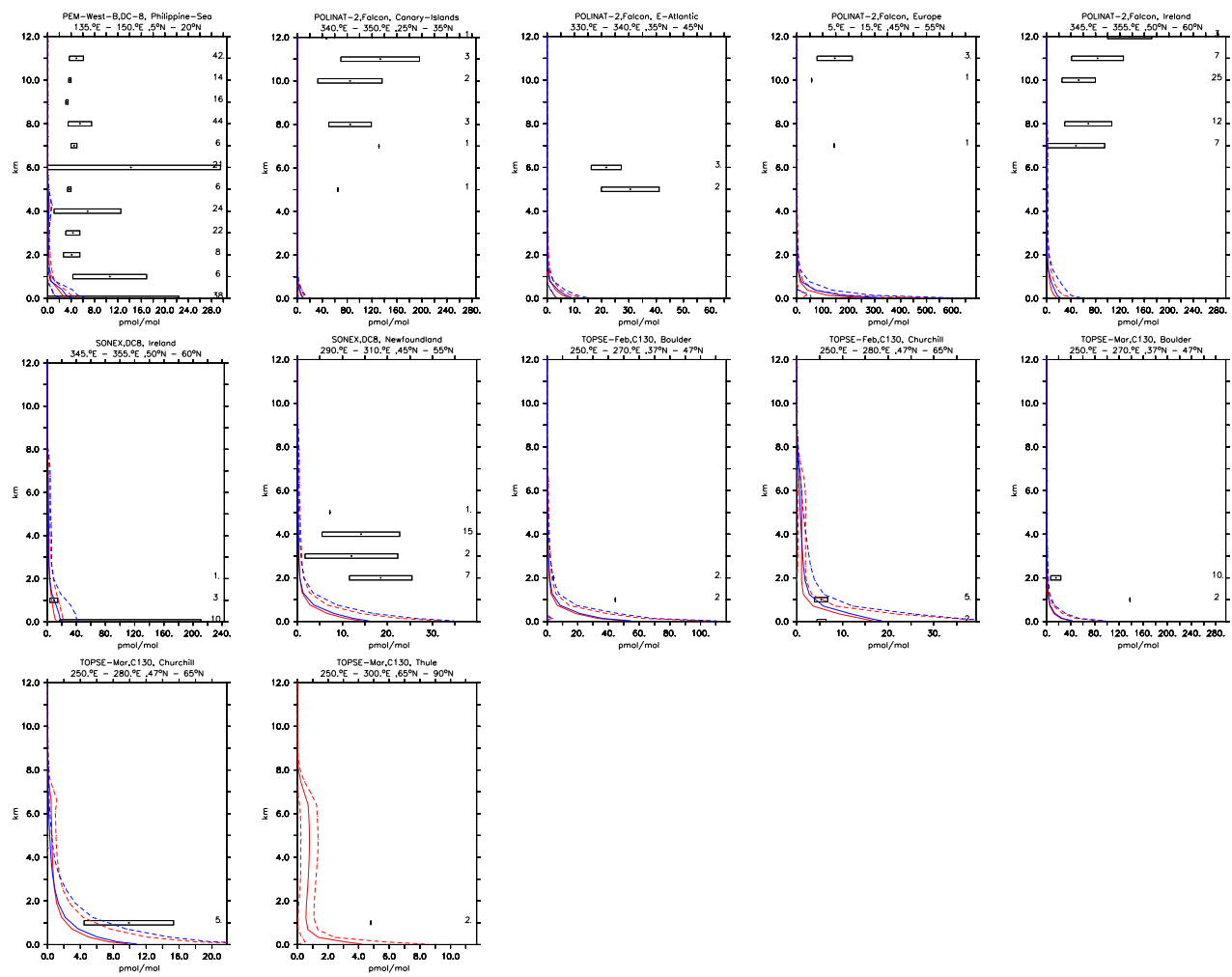


Figure 6: continued

3.4 C₃H₈

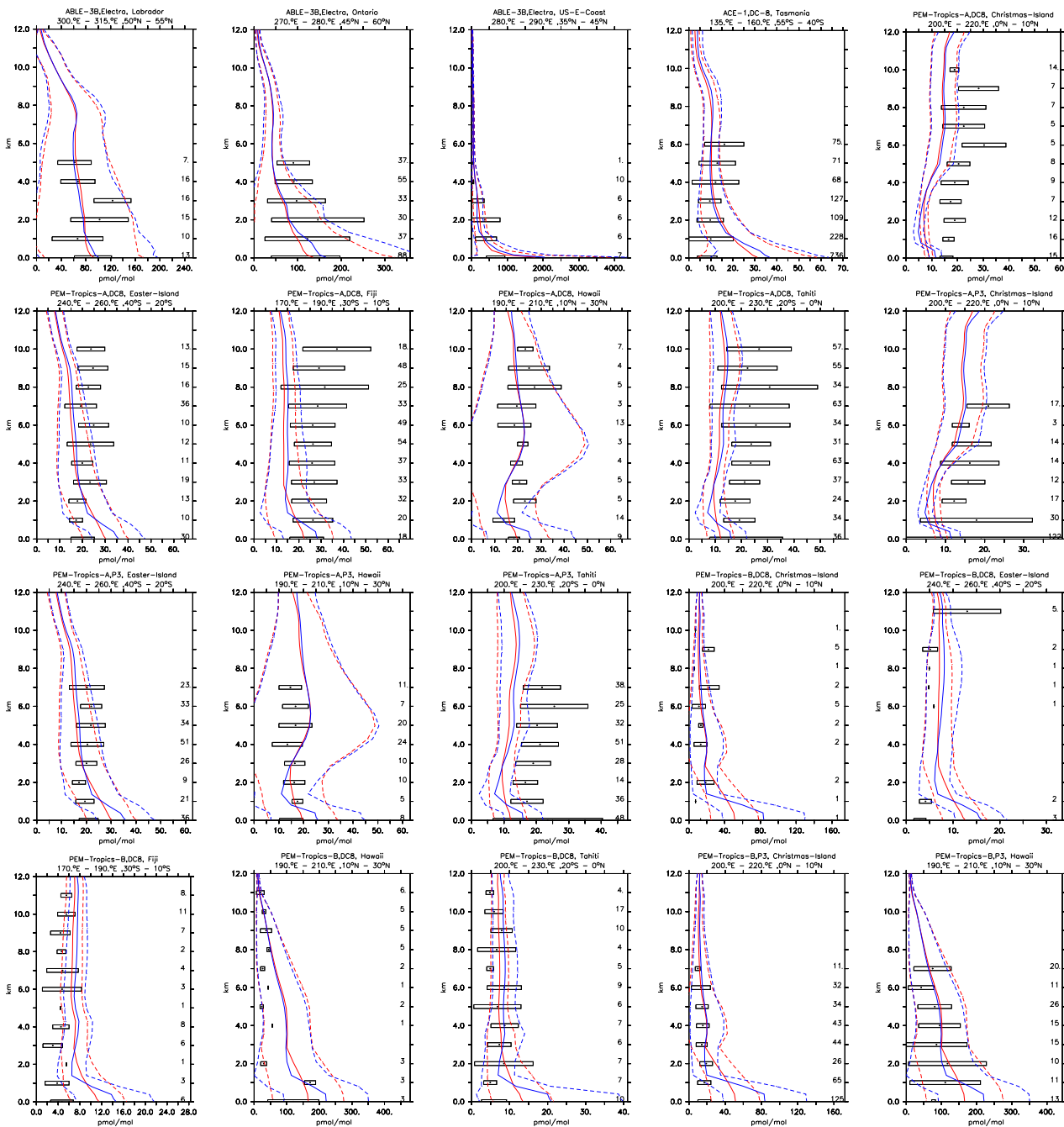


Figure 7:

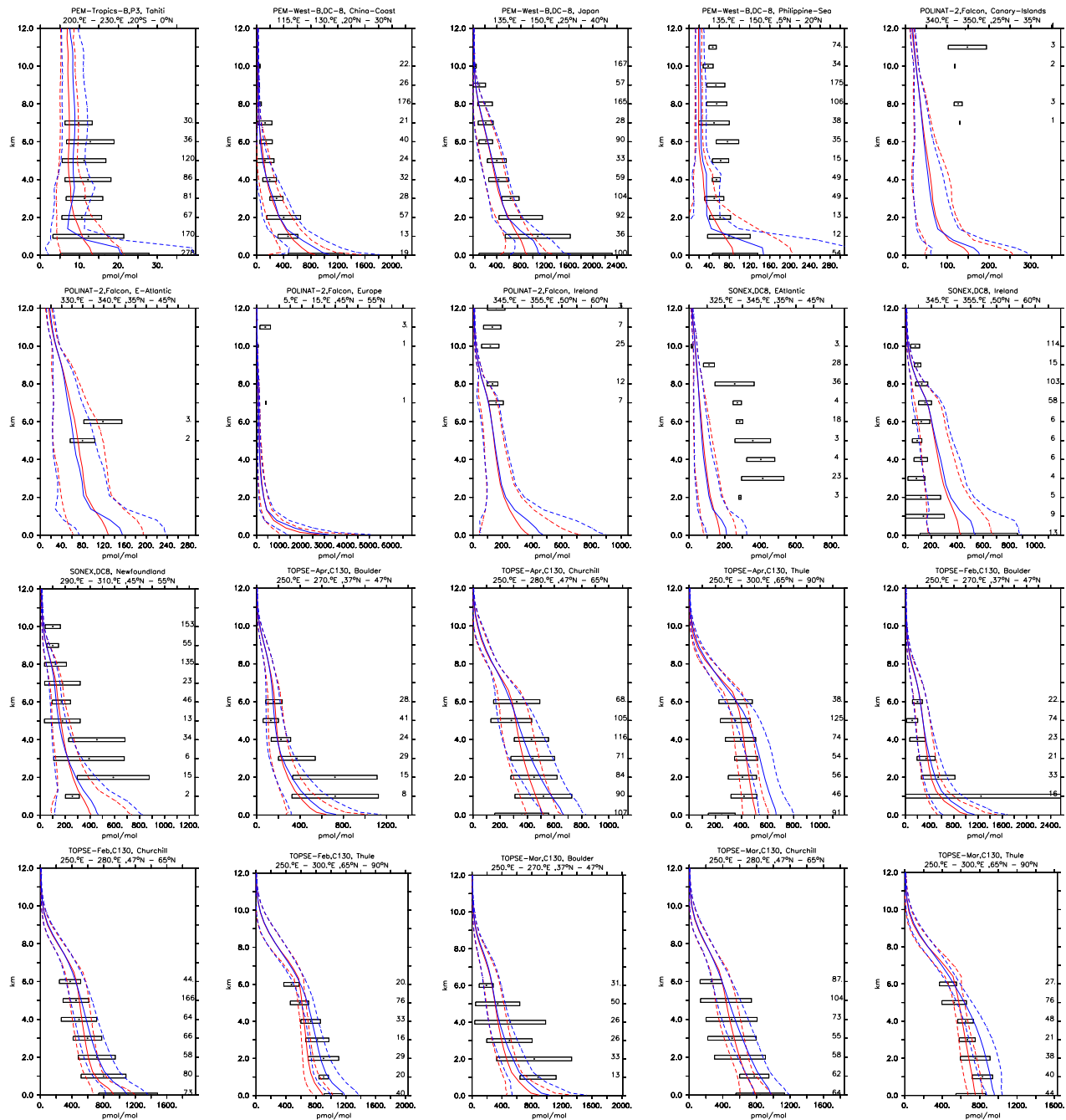


Figure 7: continued

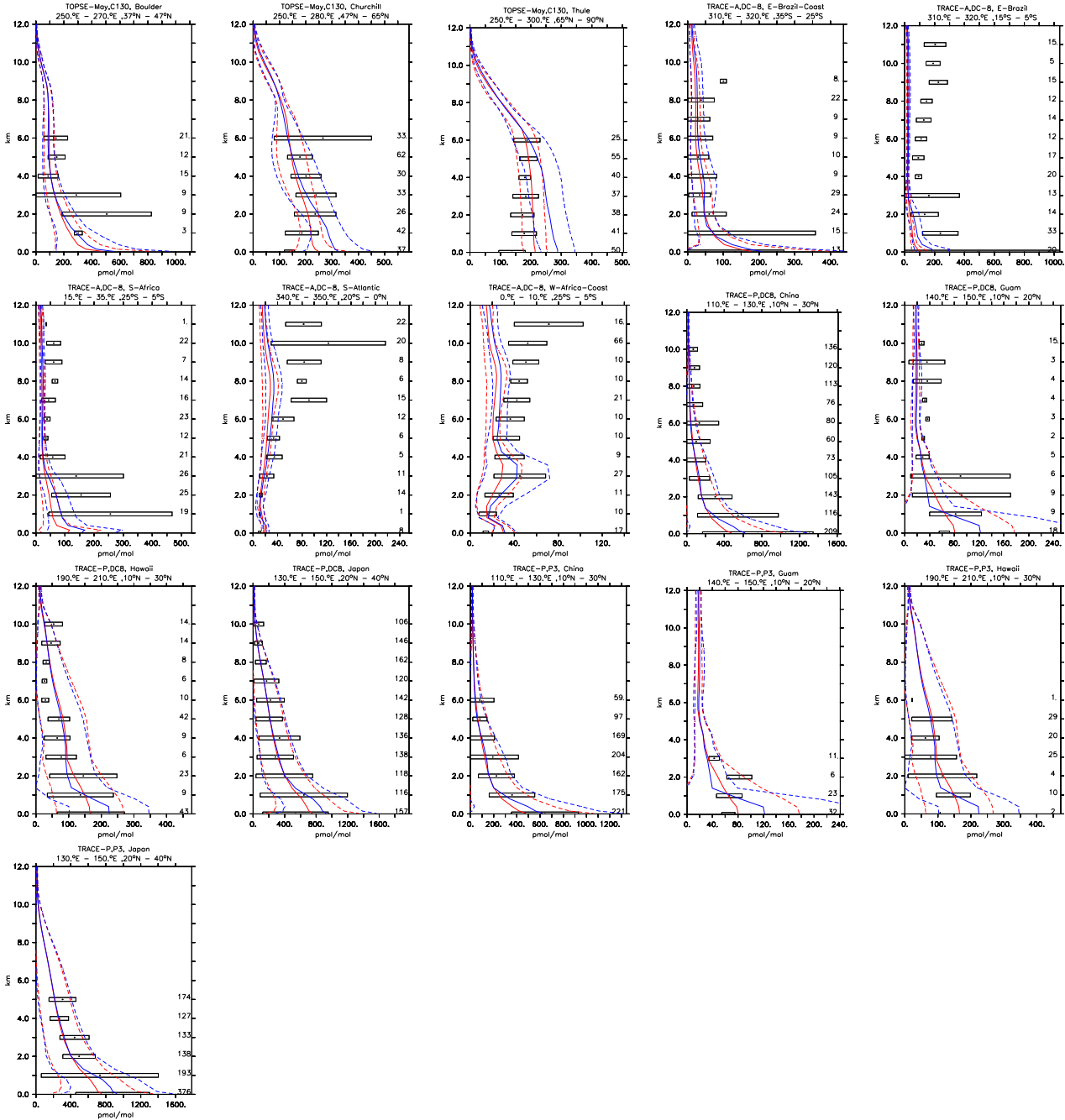


Figure 7: continued

3.5 CH_3COCH_3

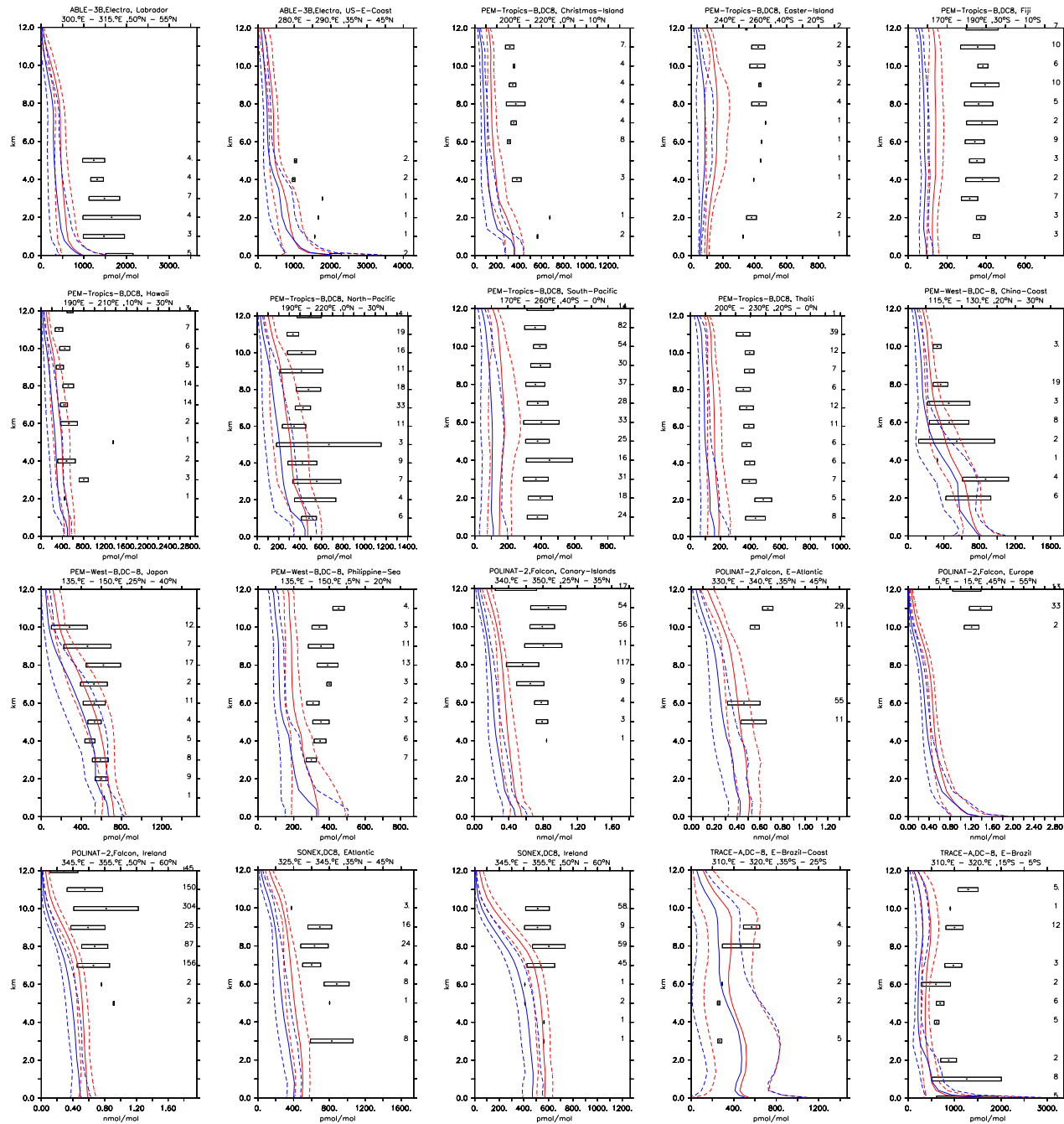


Figure 8:

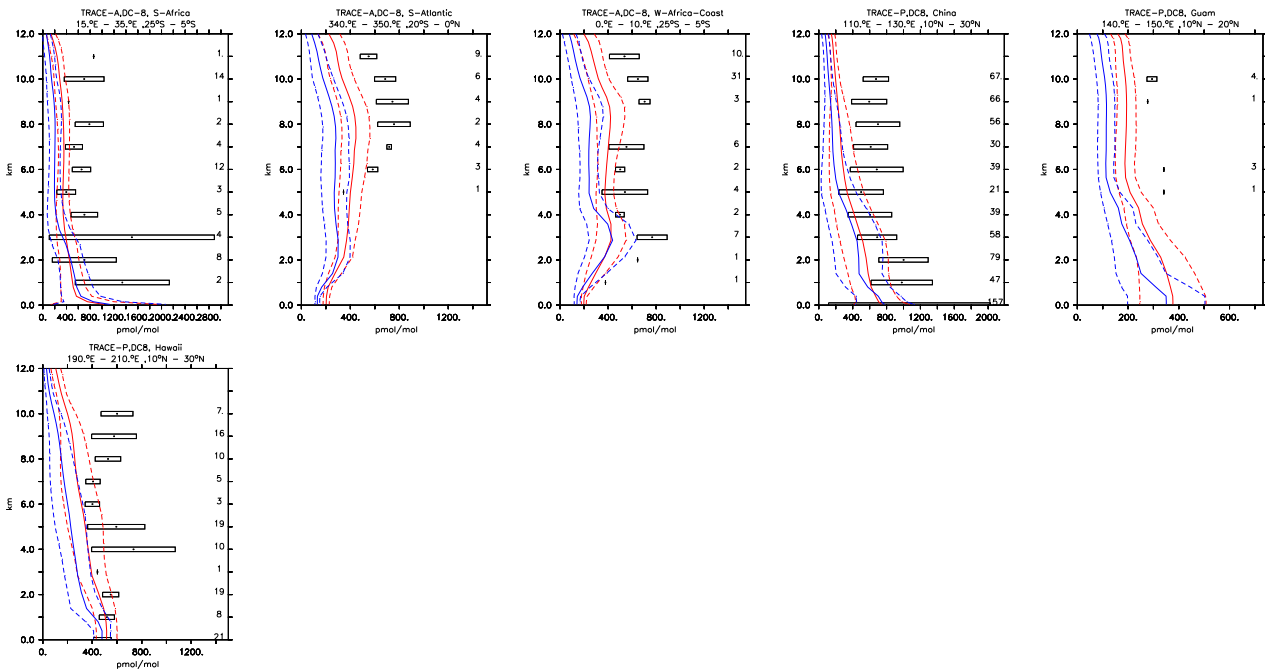


Figure 8: continued

3.6 CH₃OH

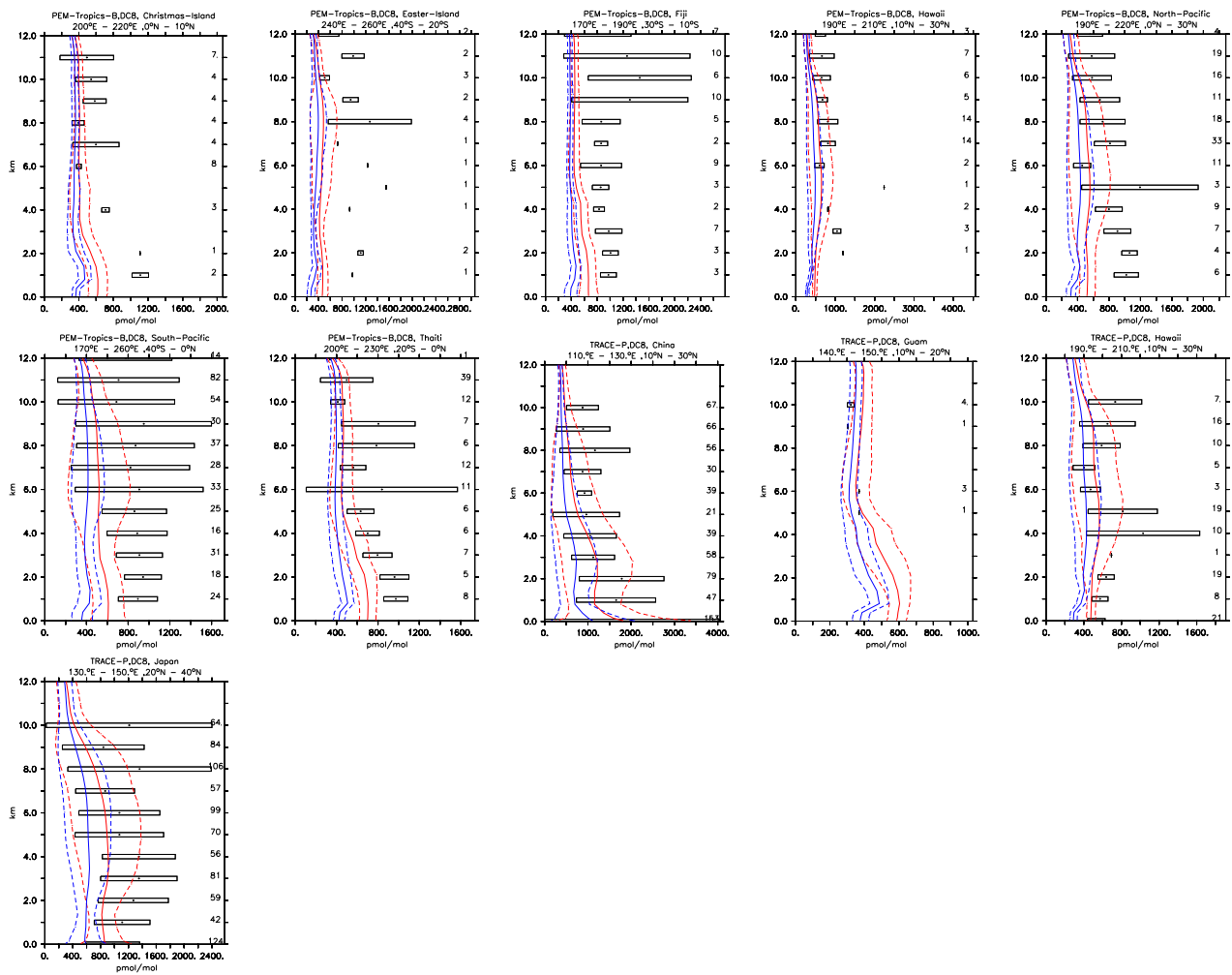


Figure 9:

3.7 CO

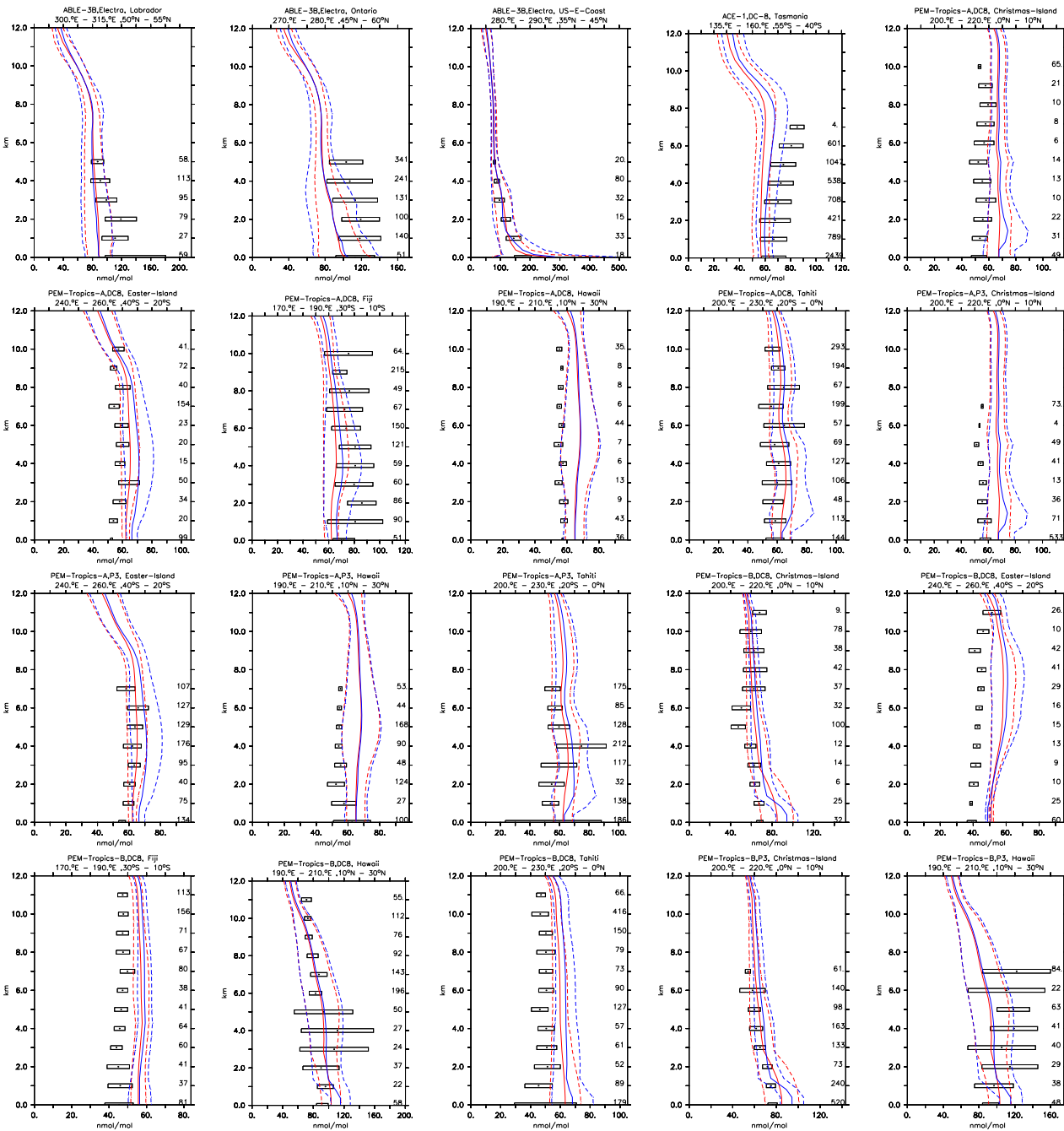


Figure 10:

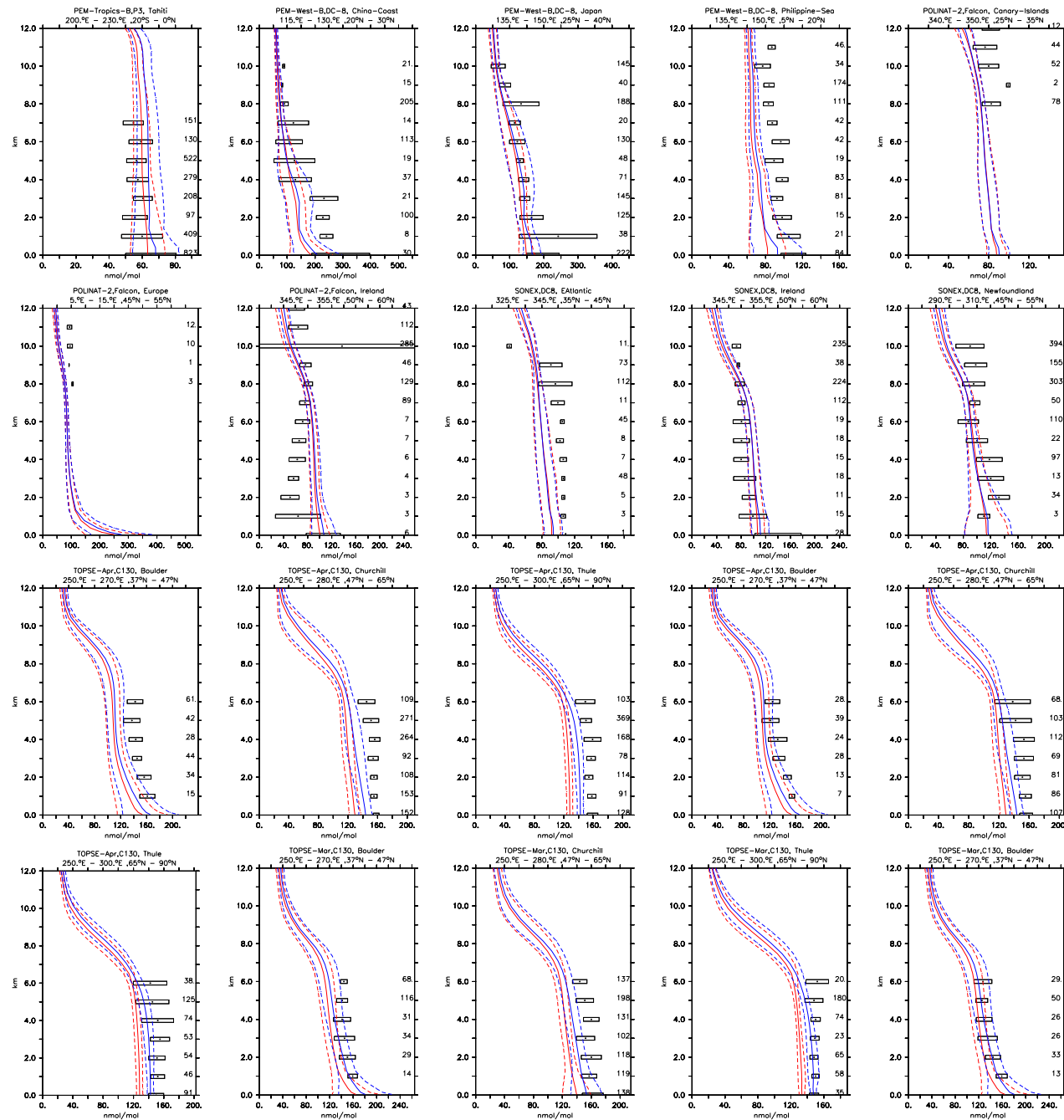


Figure 10: continued

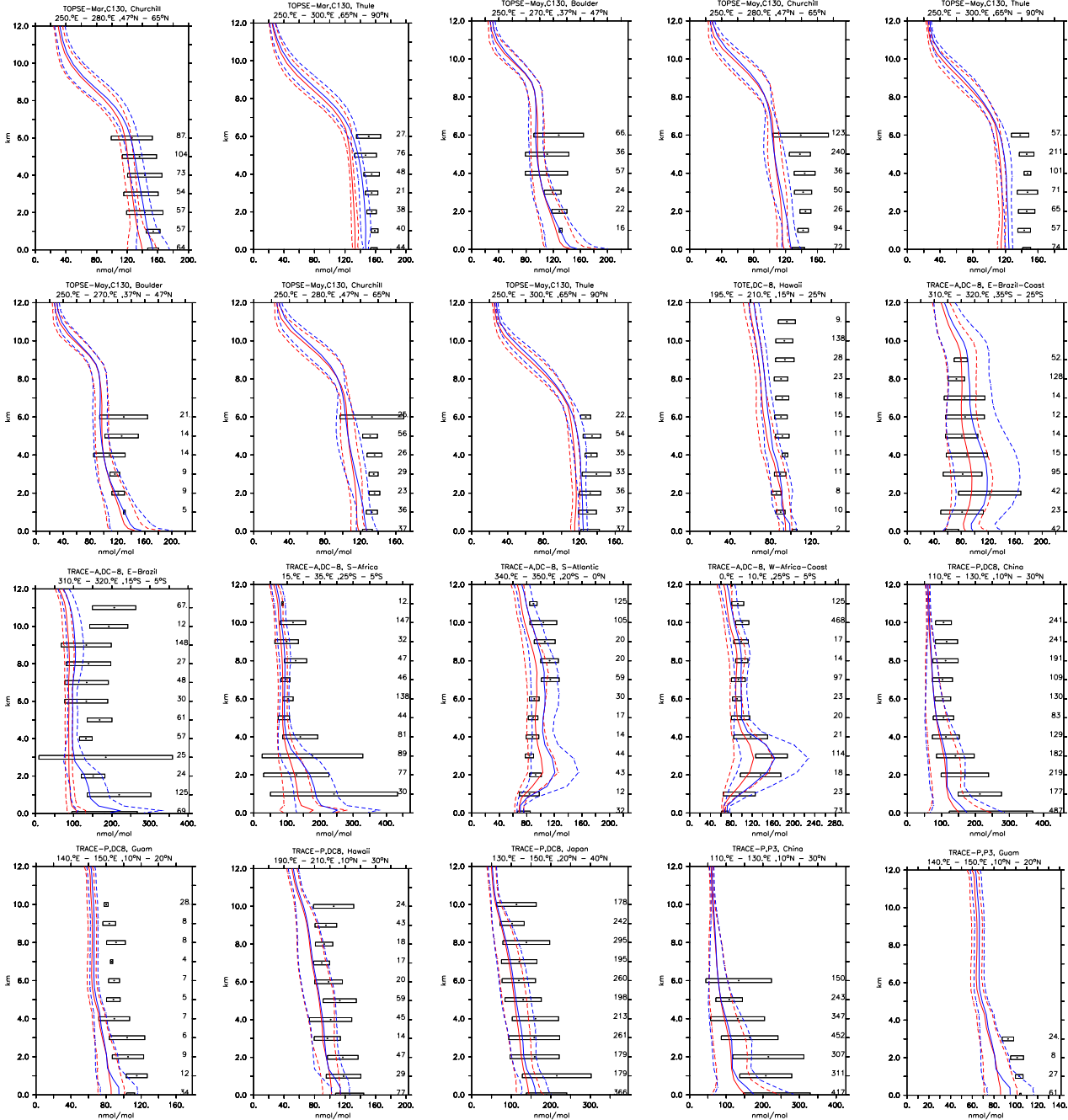


Figure 10: continued

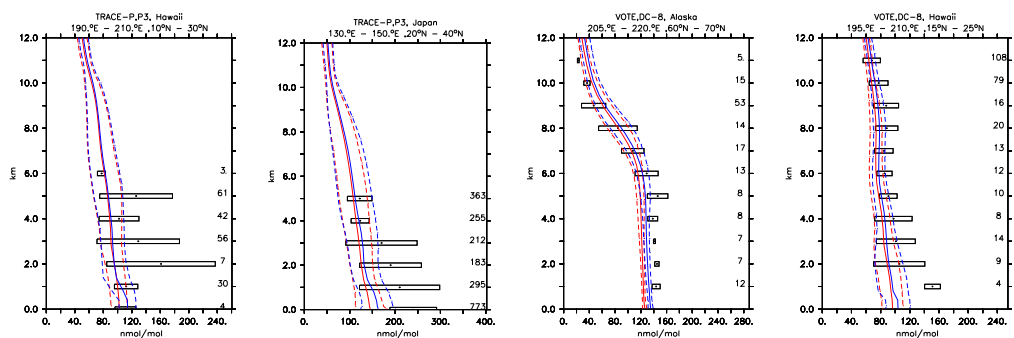


Figure 10: continued

3.8 H₂O₂

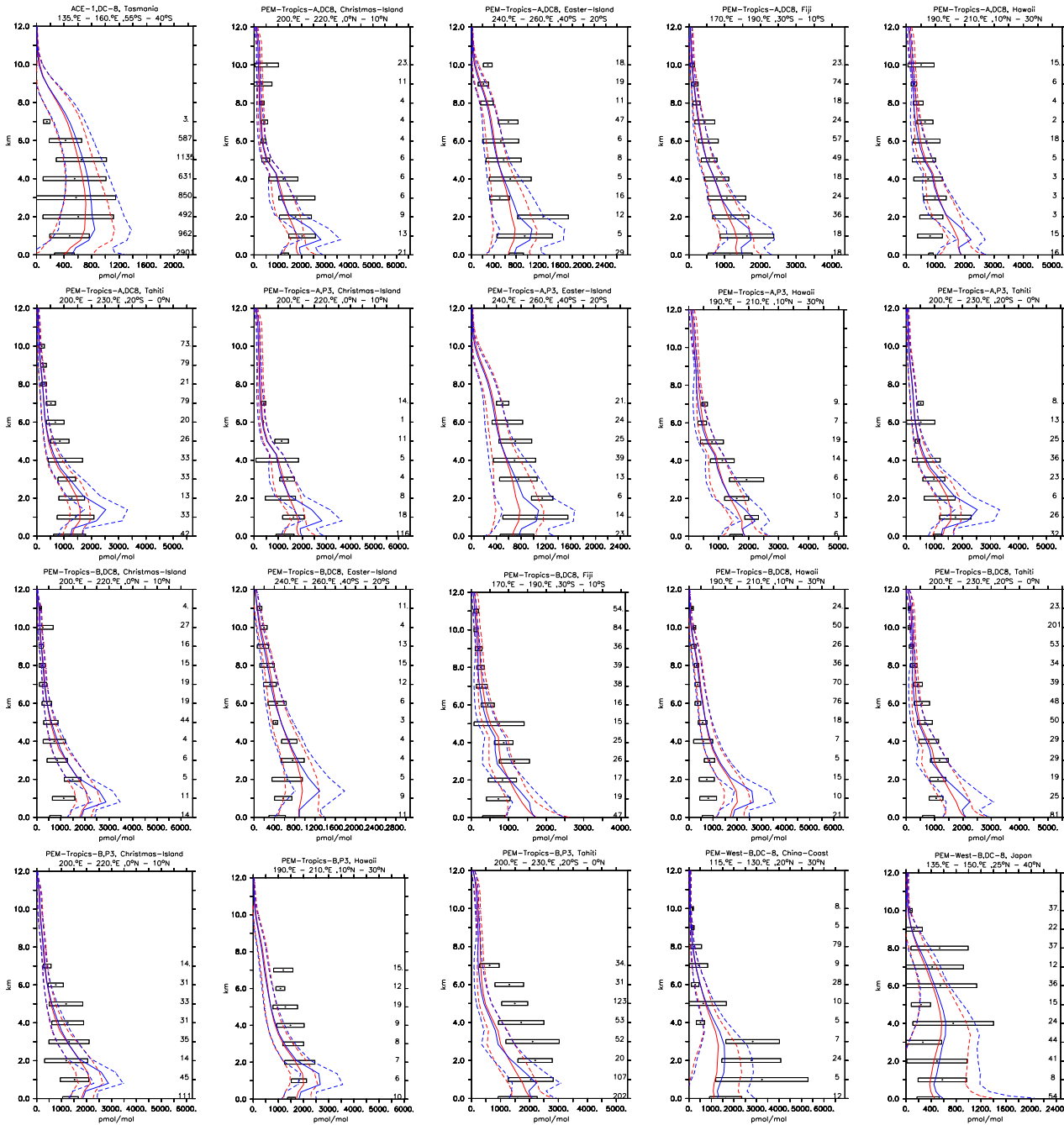


Figure 11:

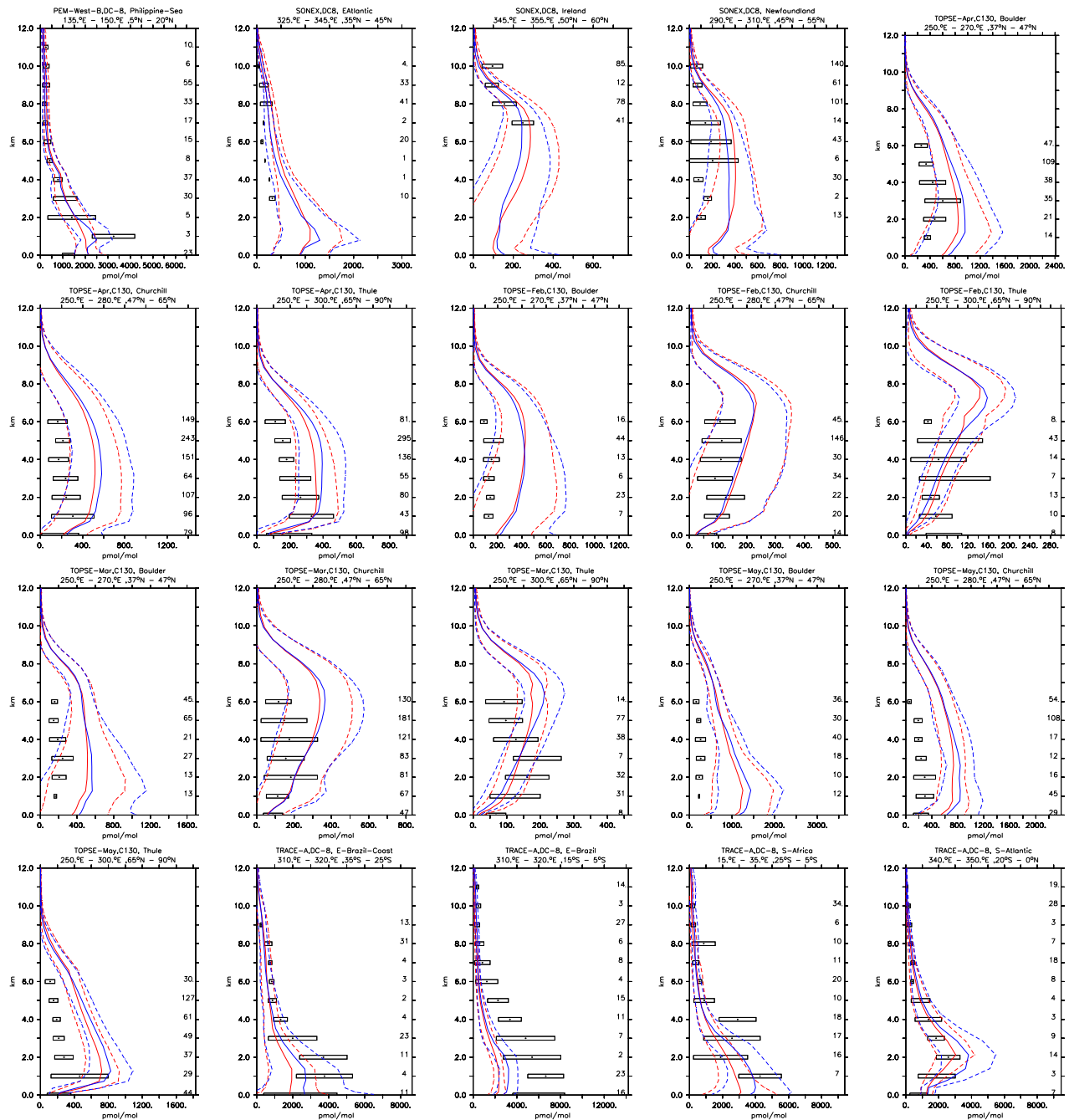


Figure 11: continued

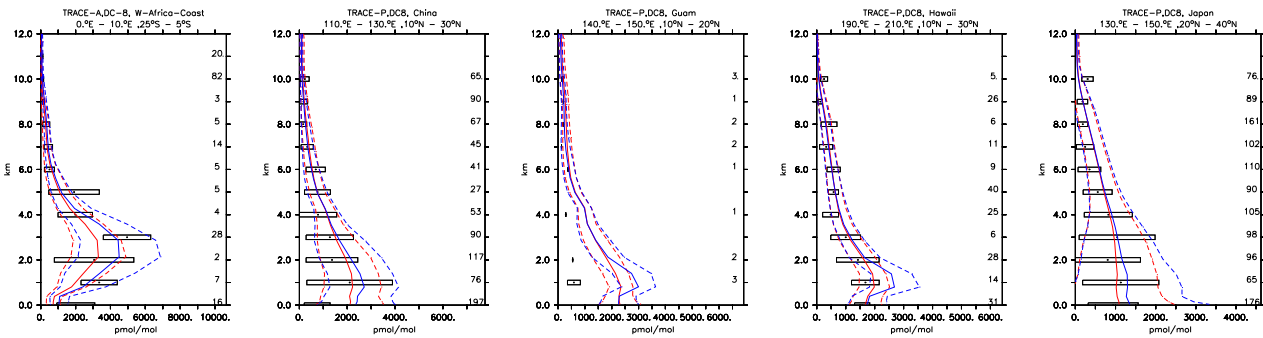


Figure 11: continued

3.9 HCHO

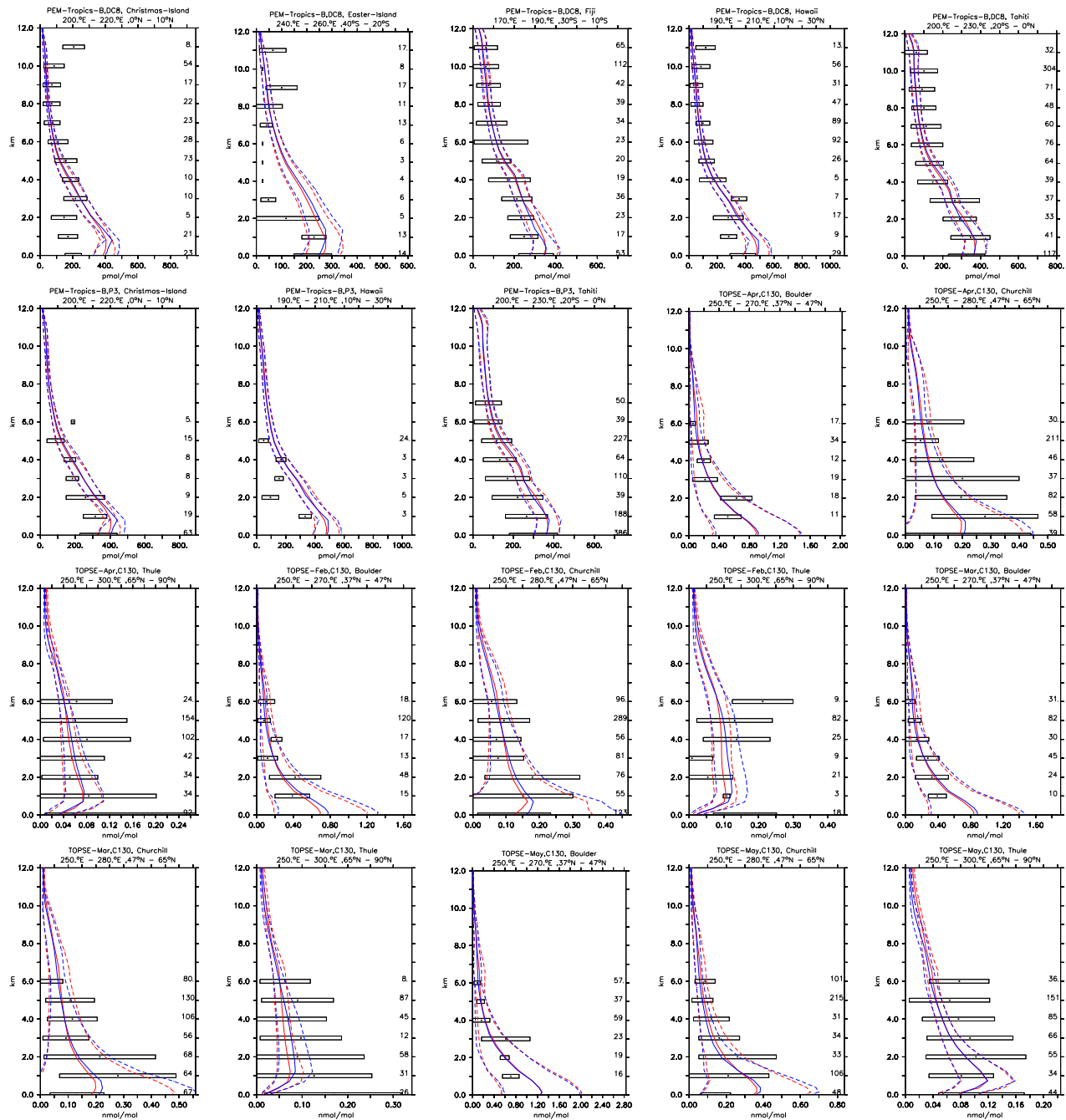


Figure 12:

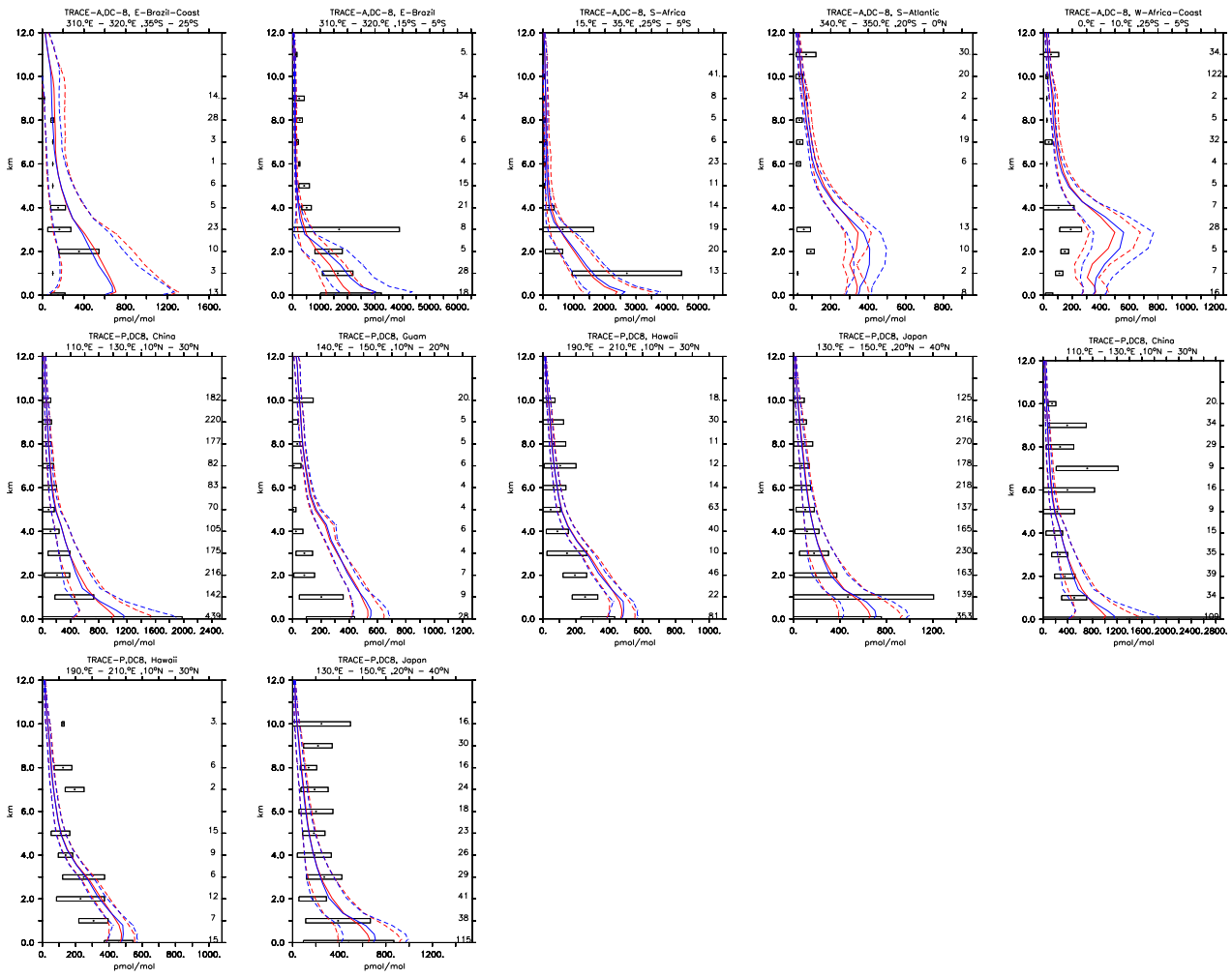


Figure 12: continued

3.10 HNO₃

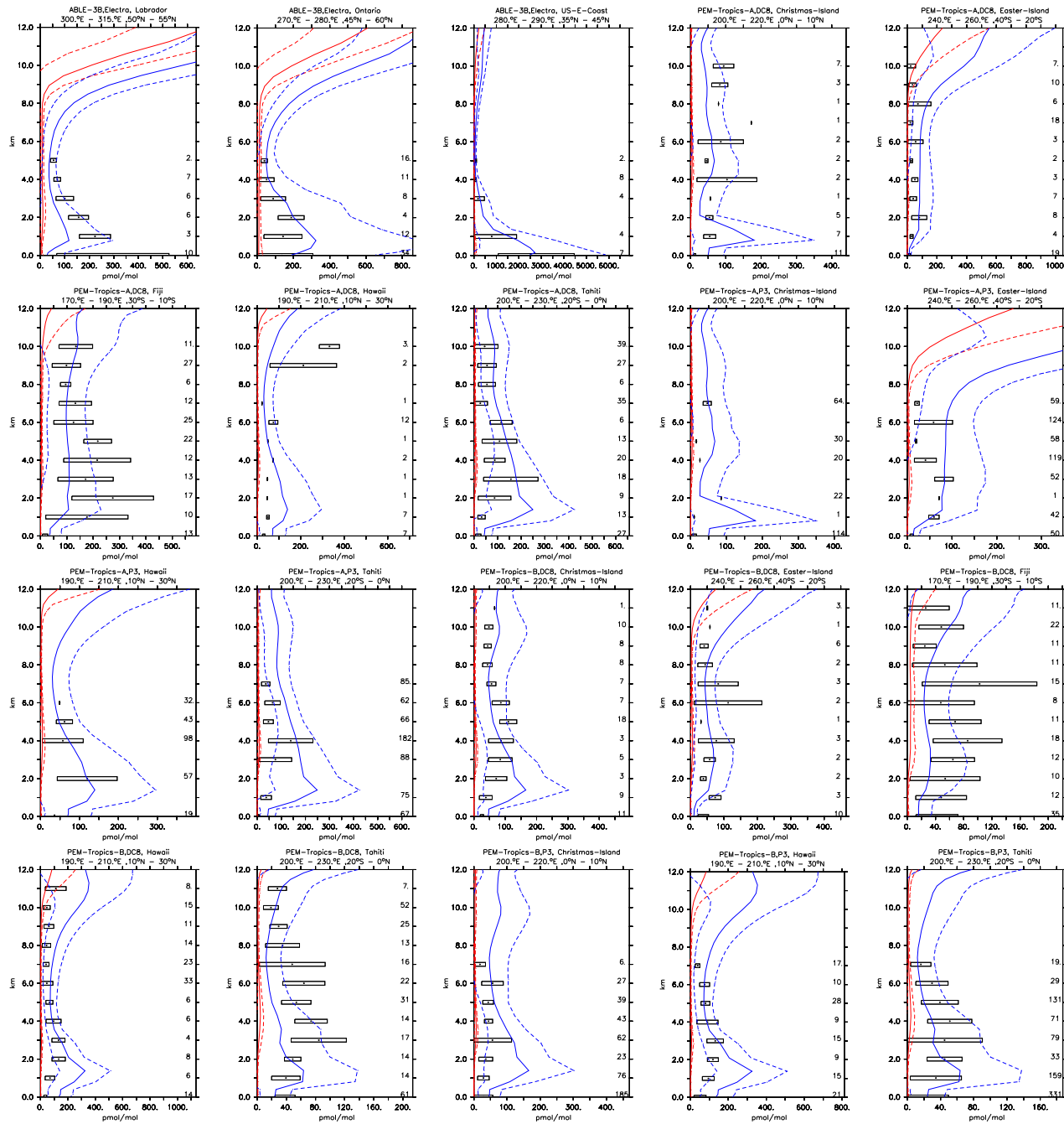


Figure 13:

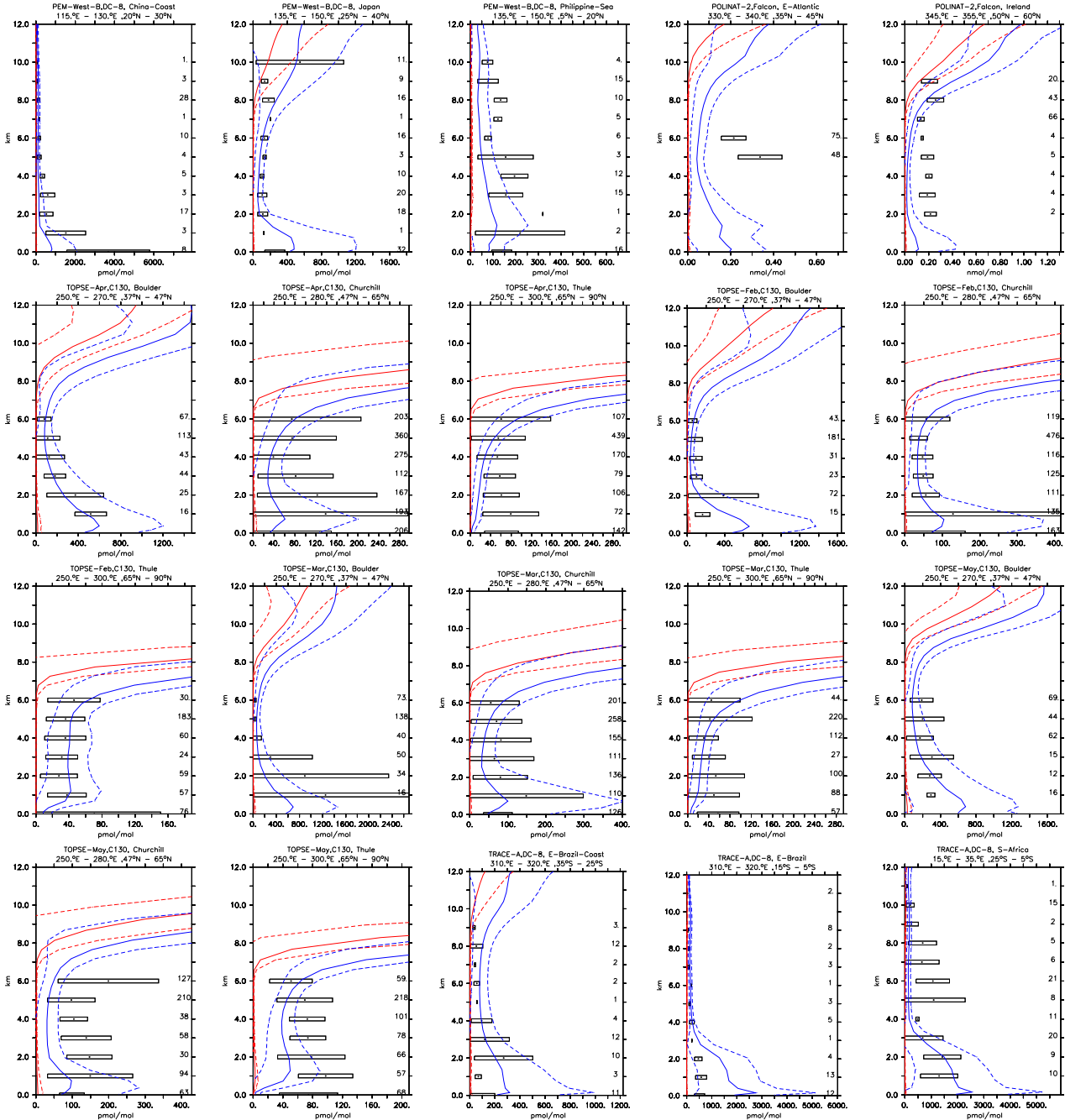


Figure 13: continued

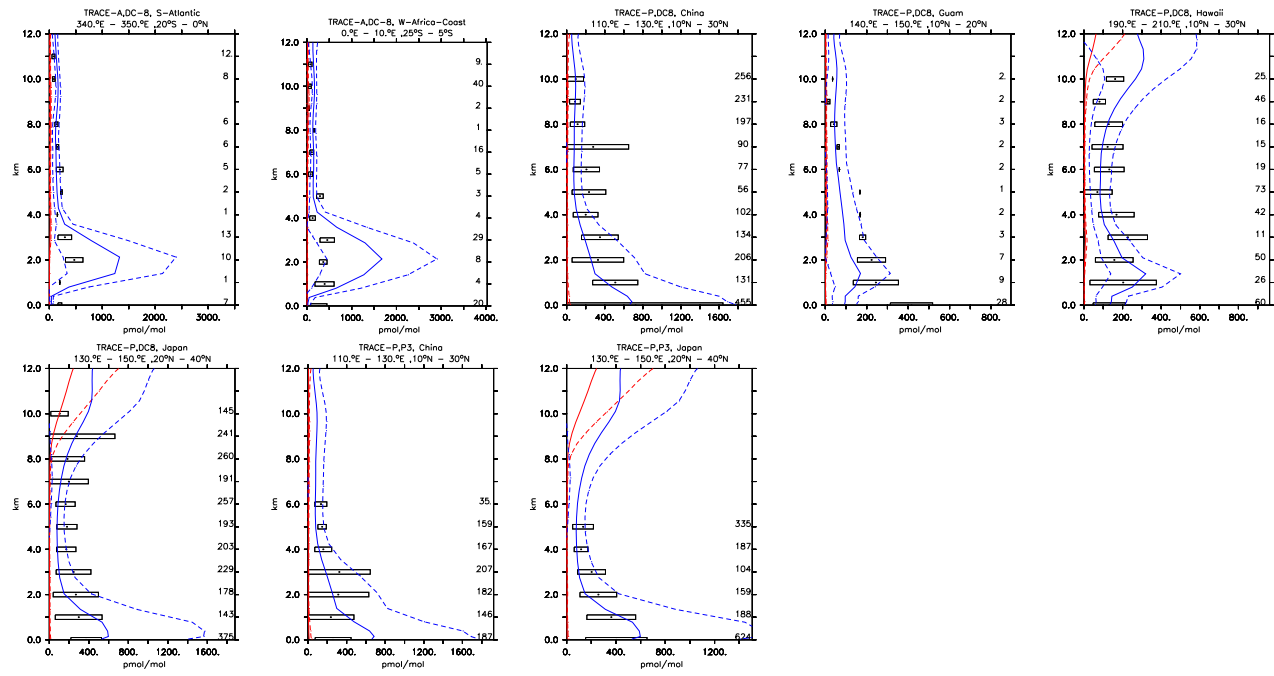


Figure 13: continued

3.11 $\text{HNO}_3 + \text{NO}_3^-(\text{cs})$

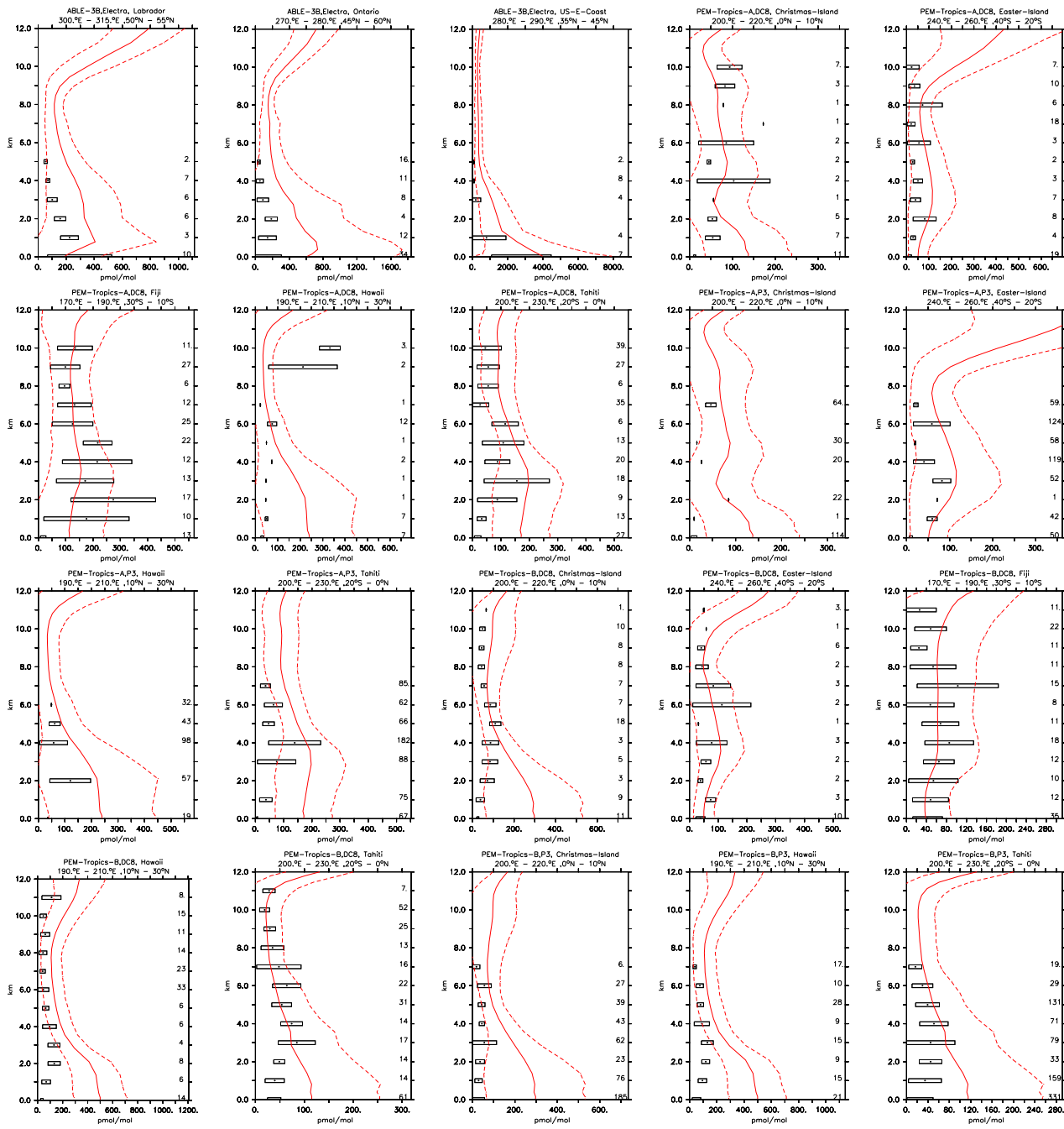


Figure 14:

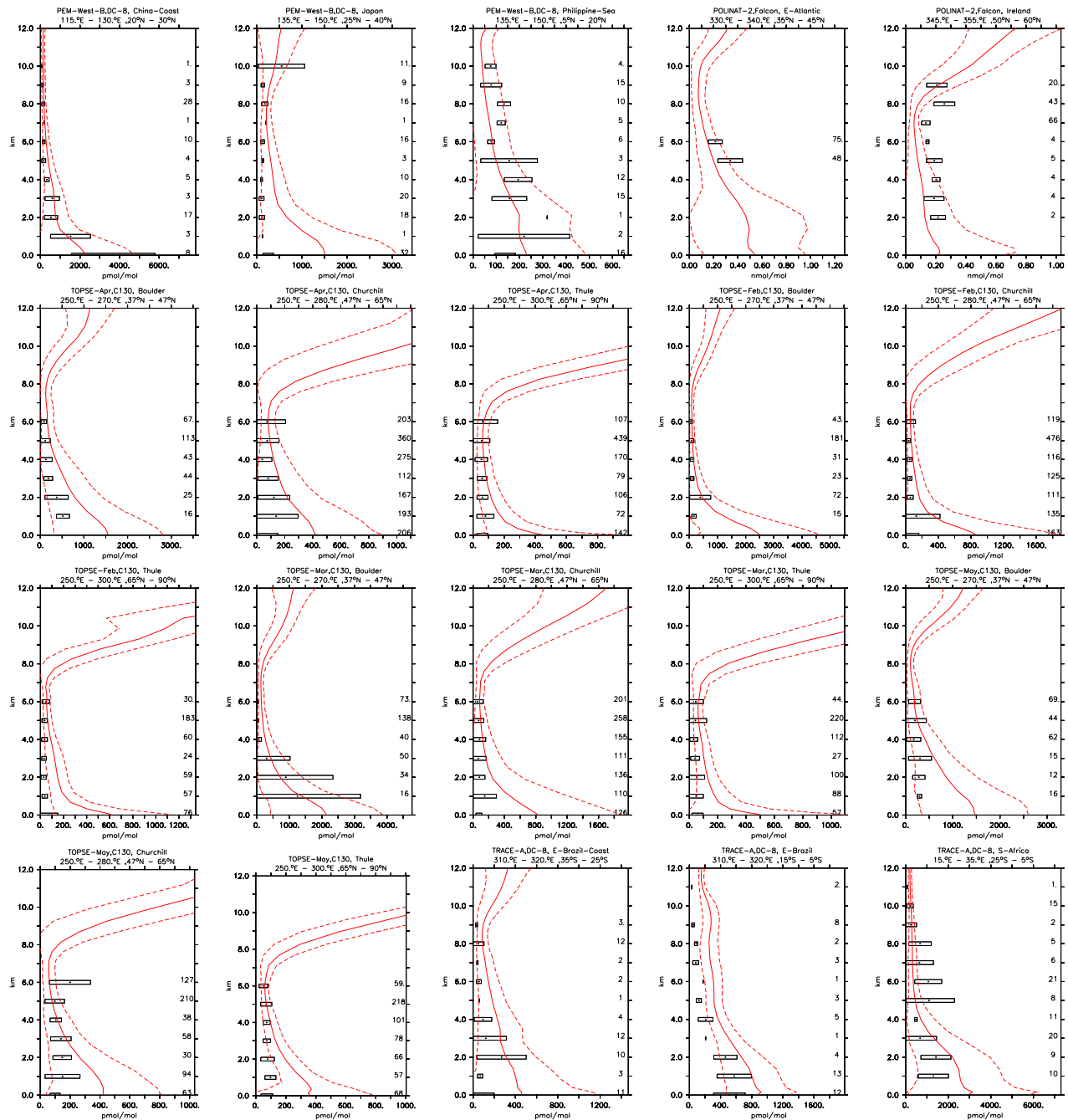


Figure 14: continued

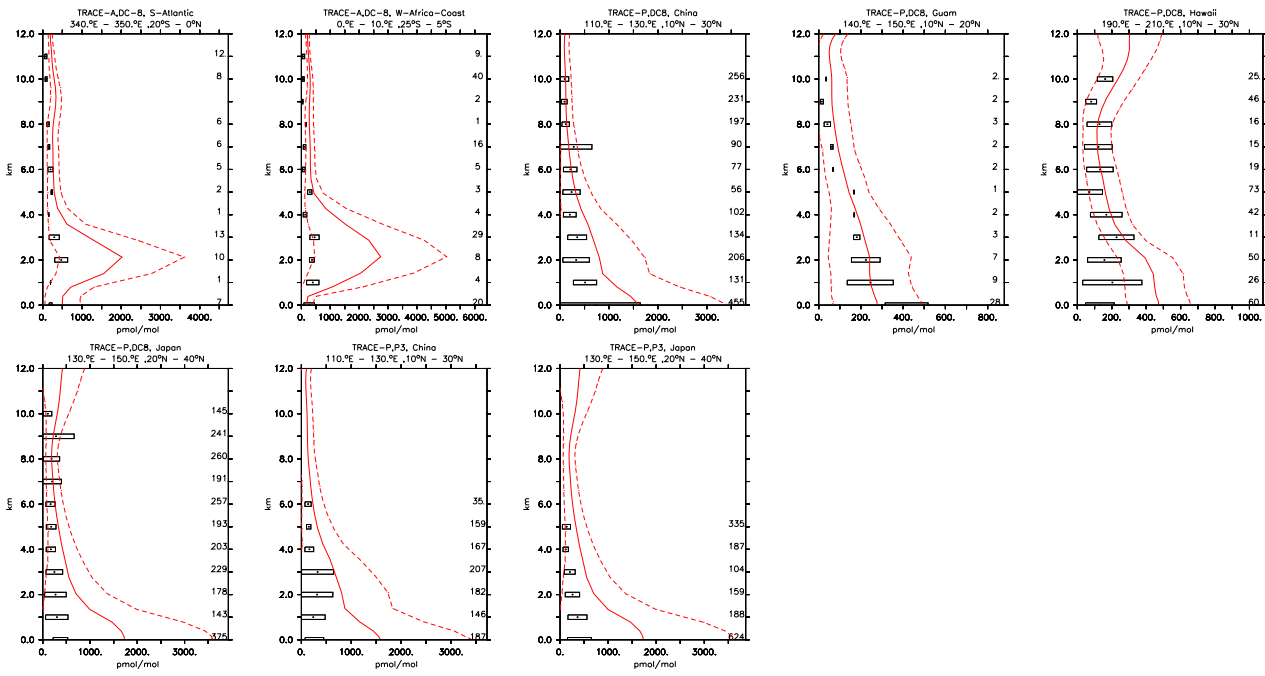


Figure 14: continued

3.12 O₃

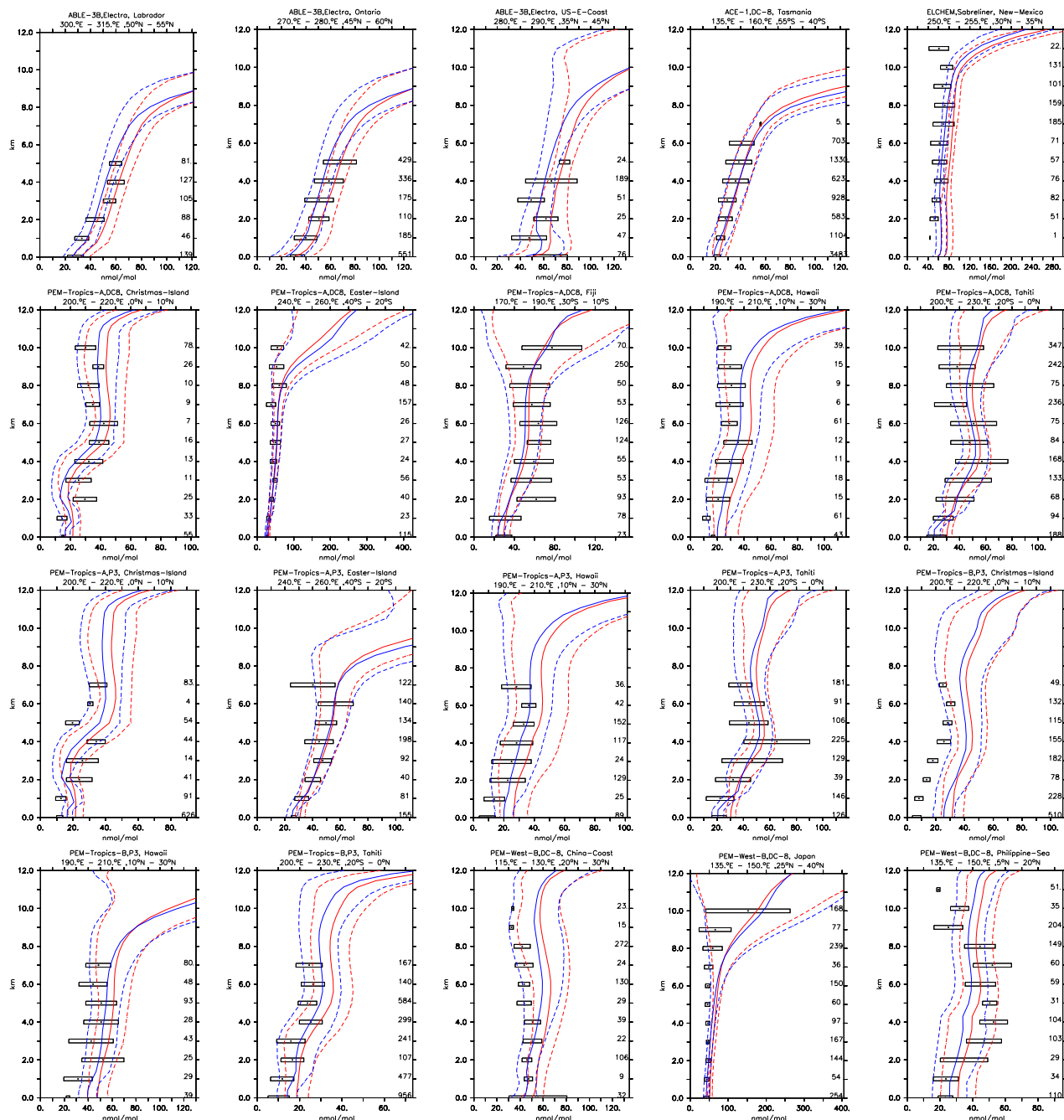


Figure 15:

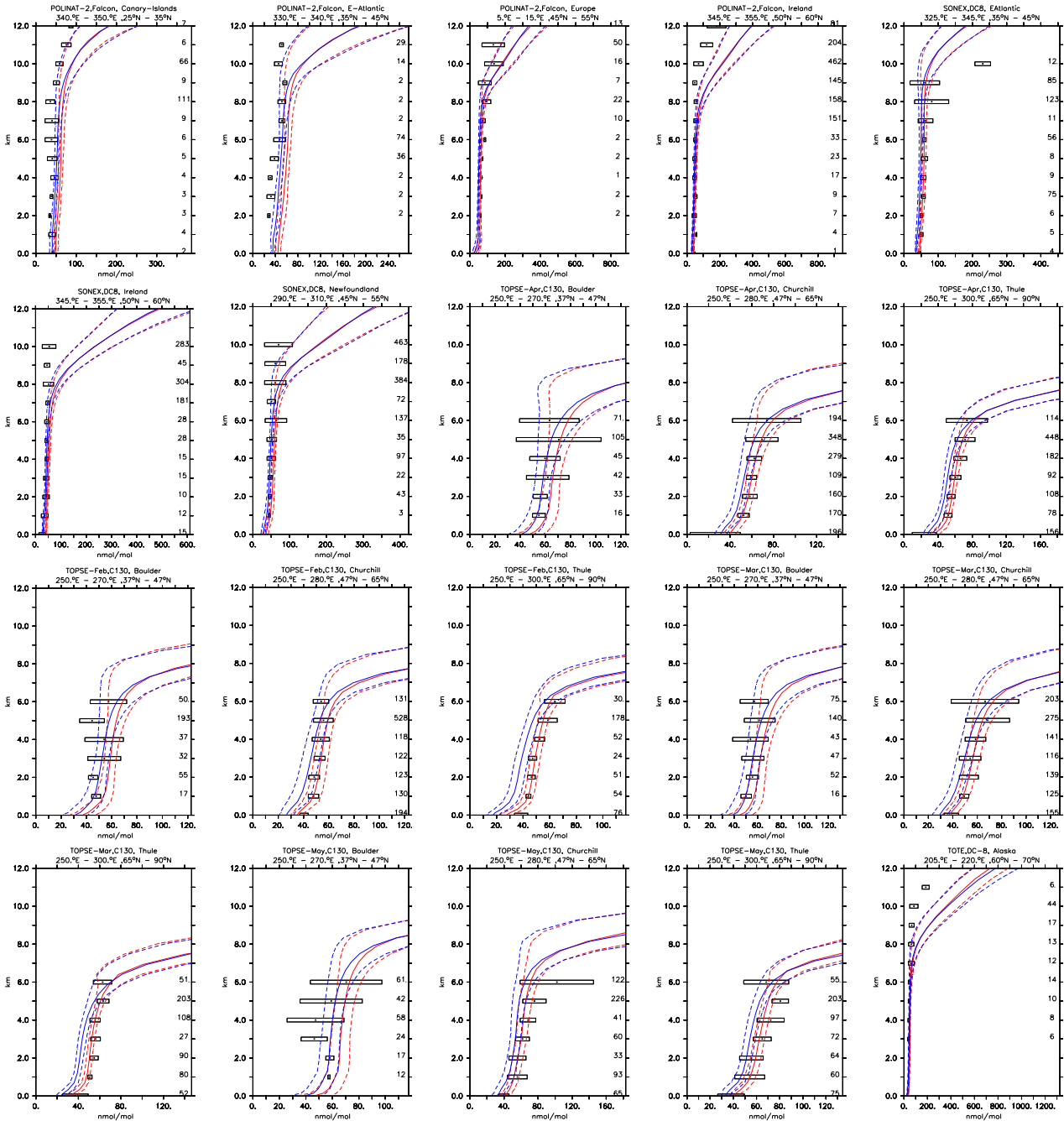


Figure 15: continued

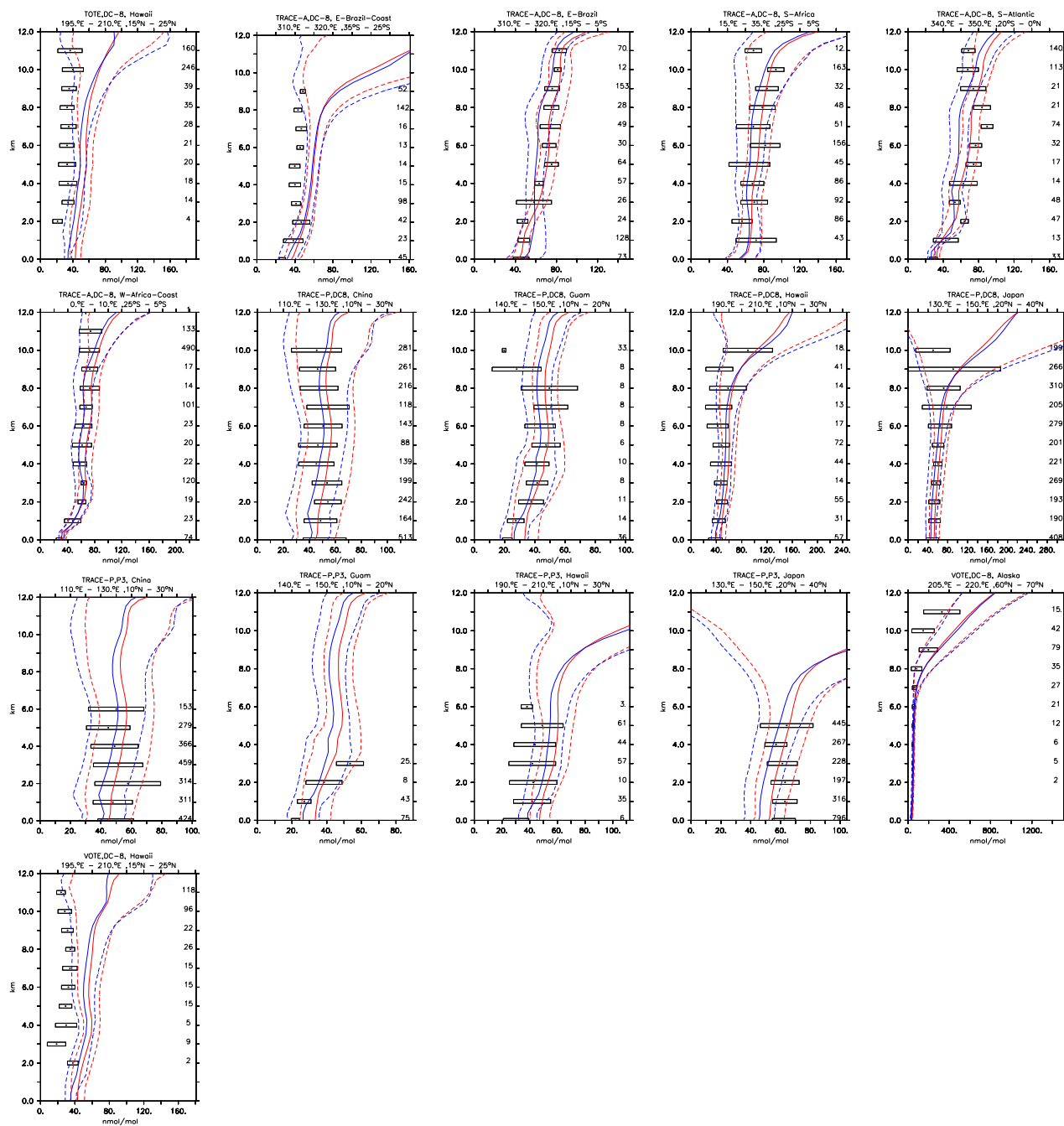


Figure 15: continued

3.13 ^{210}Pb

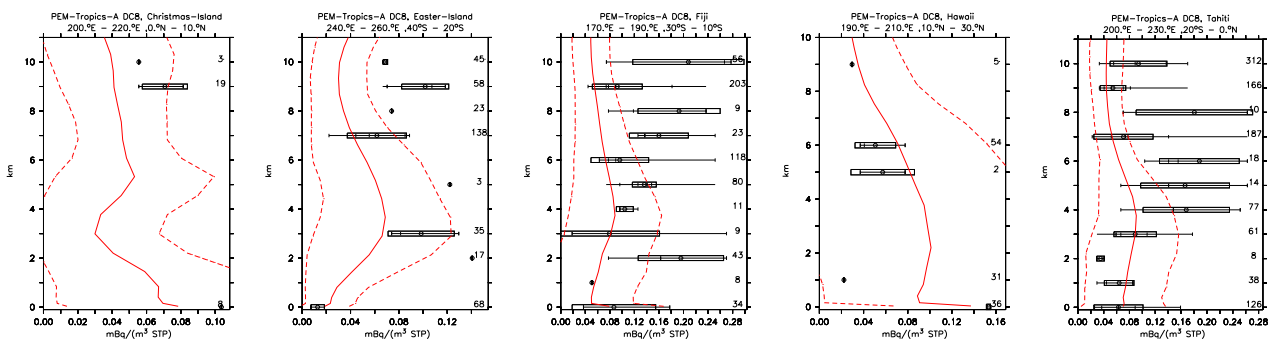


Figure 16:

4 Time series

4.1 CO

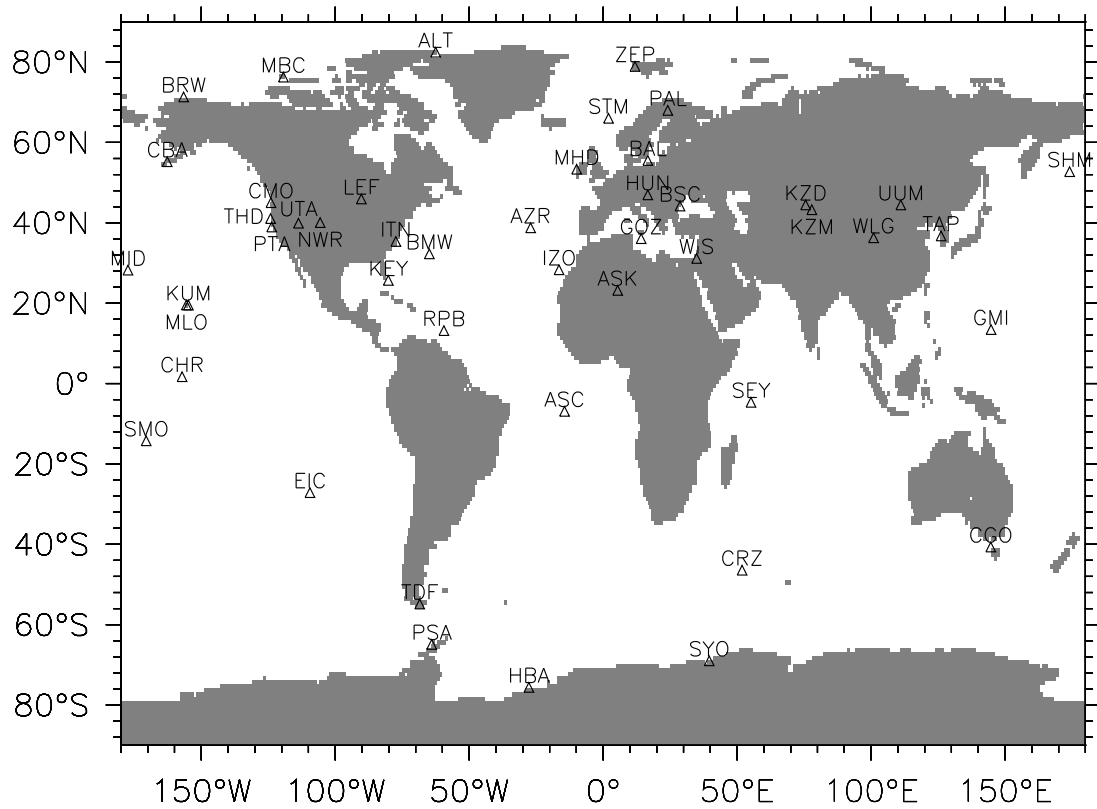


Figure 17: Stations of the National Oceanic and Atmospheric Administration Earth System Research Laboratory (NOAA/ESRL) network (Novelli et al., 1998).

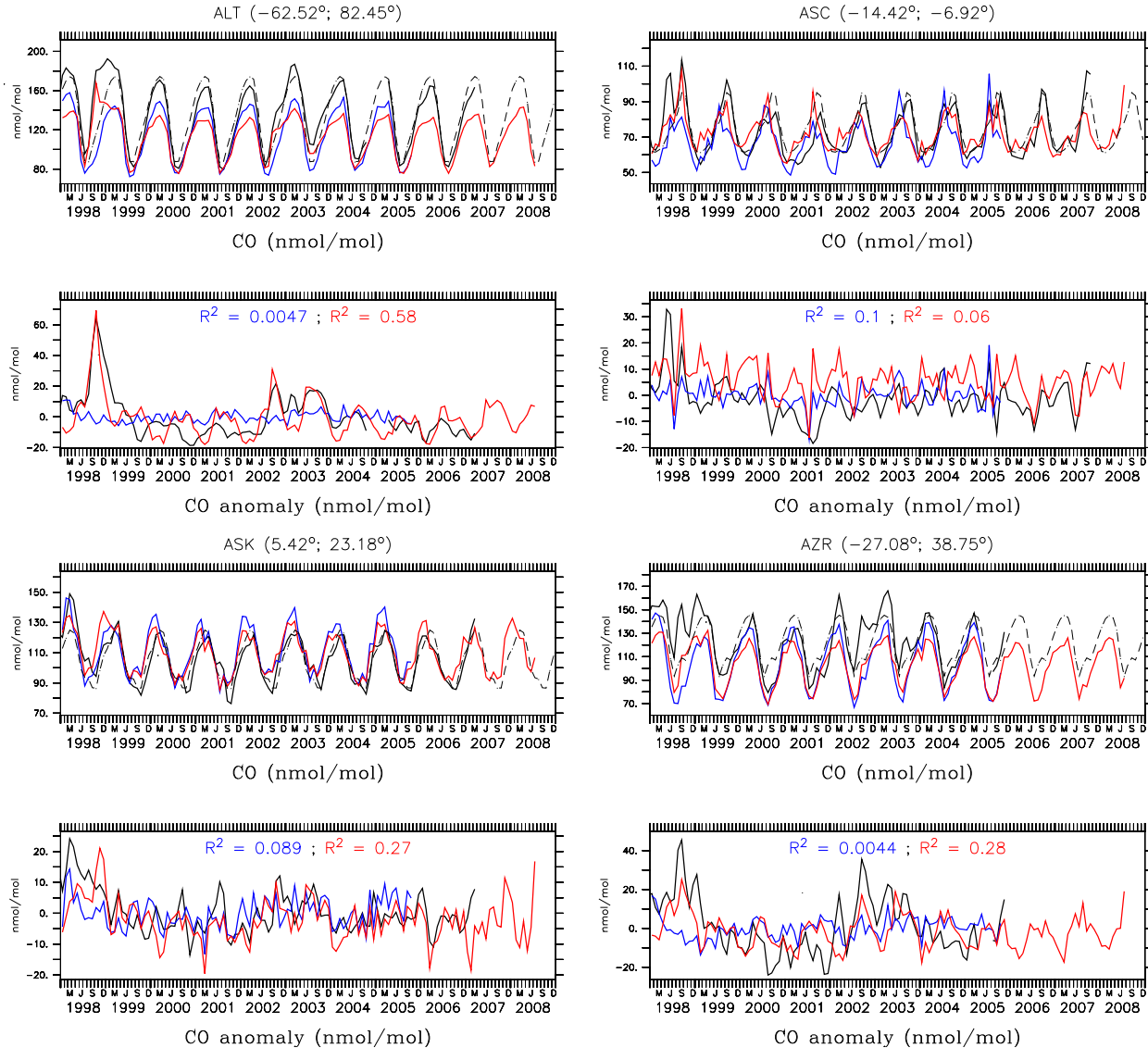


Figure 18: Comparison of simulated monthly average CO mixing ratios with observations (at several surface measurement stations) provided by the National Oceanic and Atmospheric Administration Earth System Research Laboratory (NOAA/ESRL) as originally presented by Novelli et al. (1998). The station identifier and geographical position is indicated at the top of the respective upper panel. The upper panel of each pair shows the absolute values: the black line denotes the observations, the dashed black line the corresponding climatological monthly average, the blue line the results of the simulation S1 (Jöckel et al., 2006) and the red line the results of the new simulation. The lower panel of each pair shows the deviations (anomalies) from the corresponding climatological monthly average in absolute units: black: observations, blue: simulation S1 of Jöckel et al. (2006), red: new simulation. The R^2 are the corresponding Pearson's correlation coefficients between the simulated and observed anomalies.

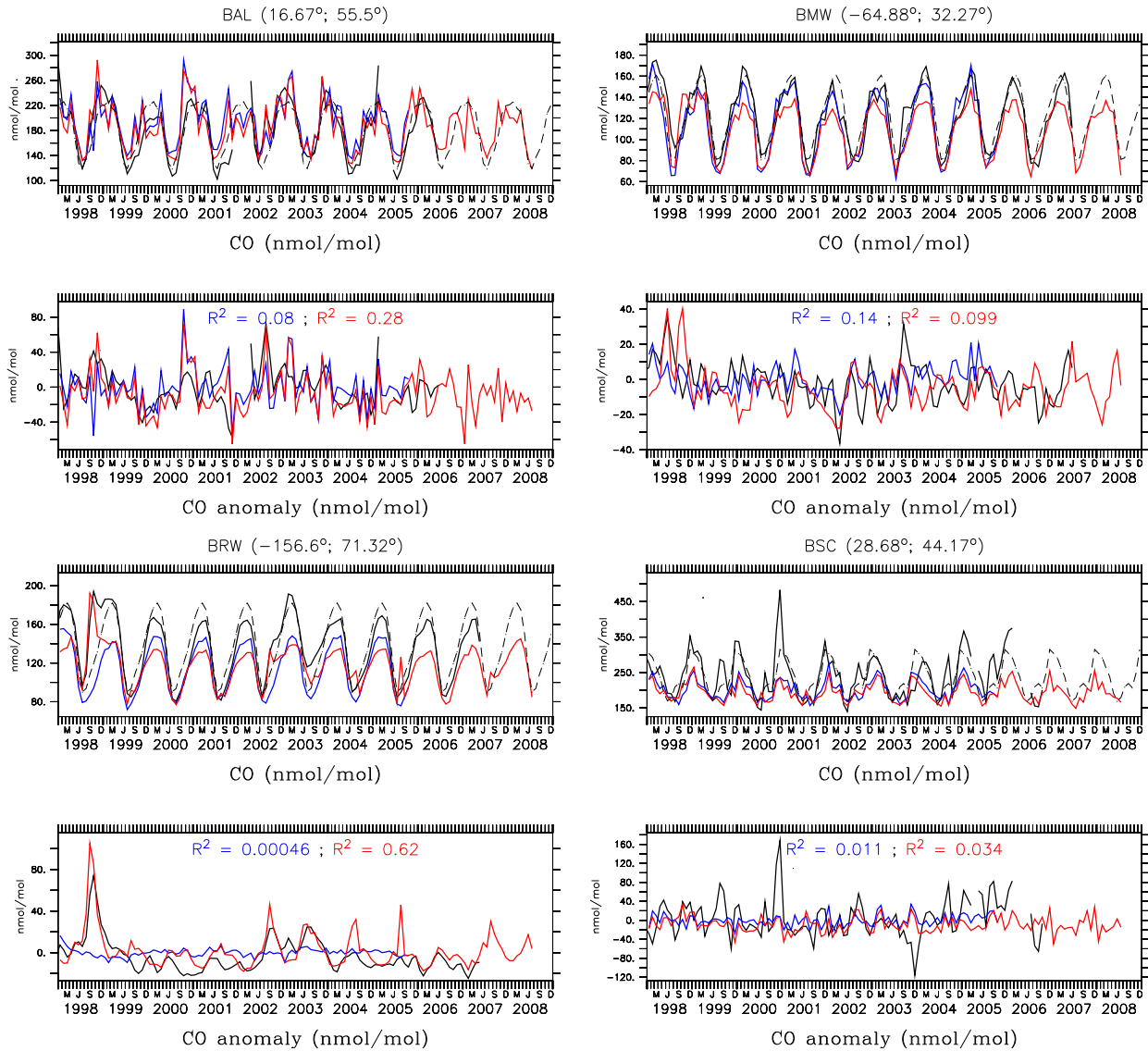


Figure 18: continued

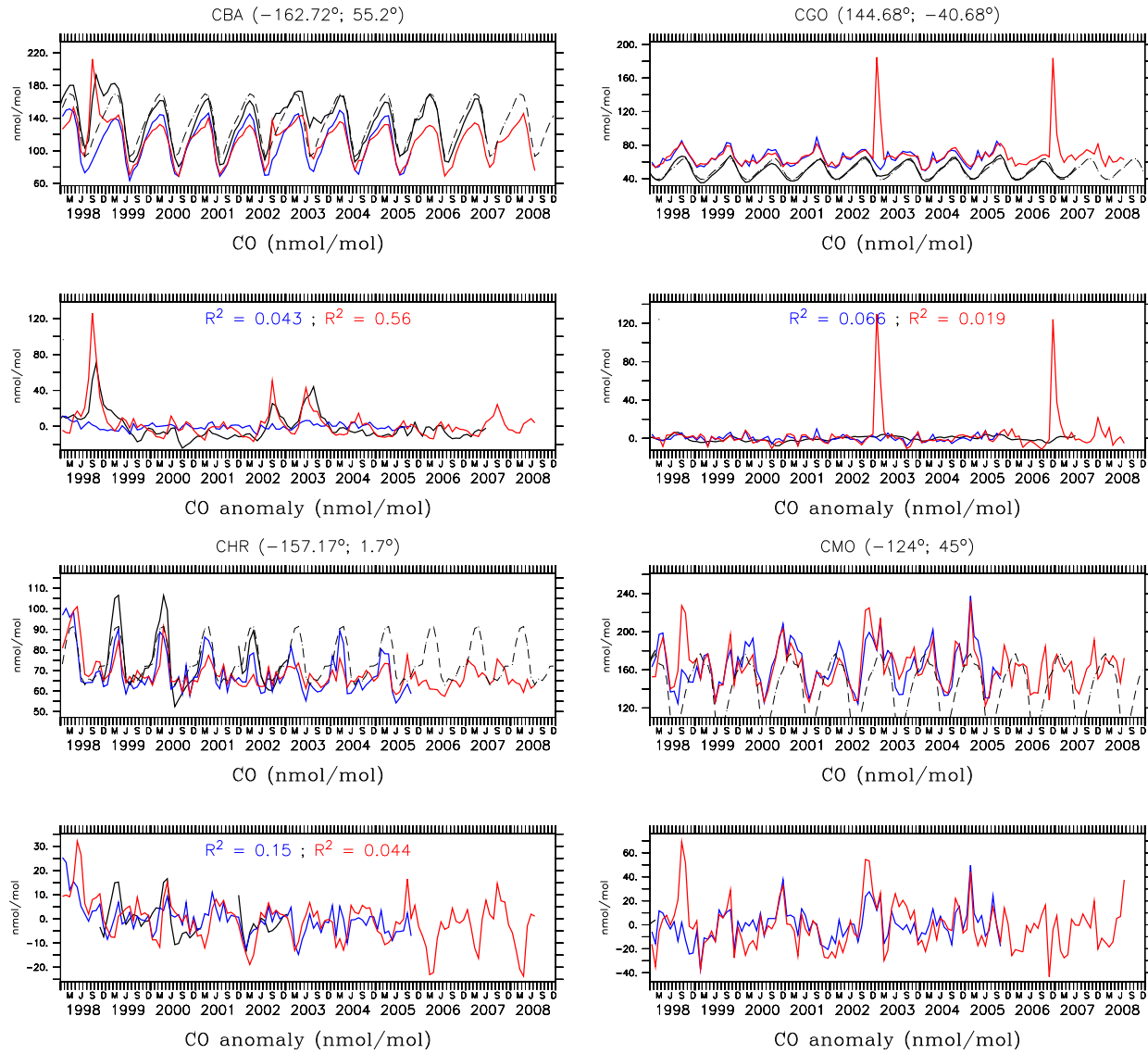


Figure 18: continued

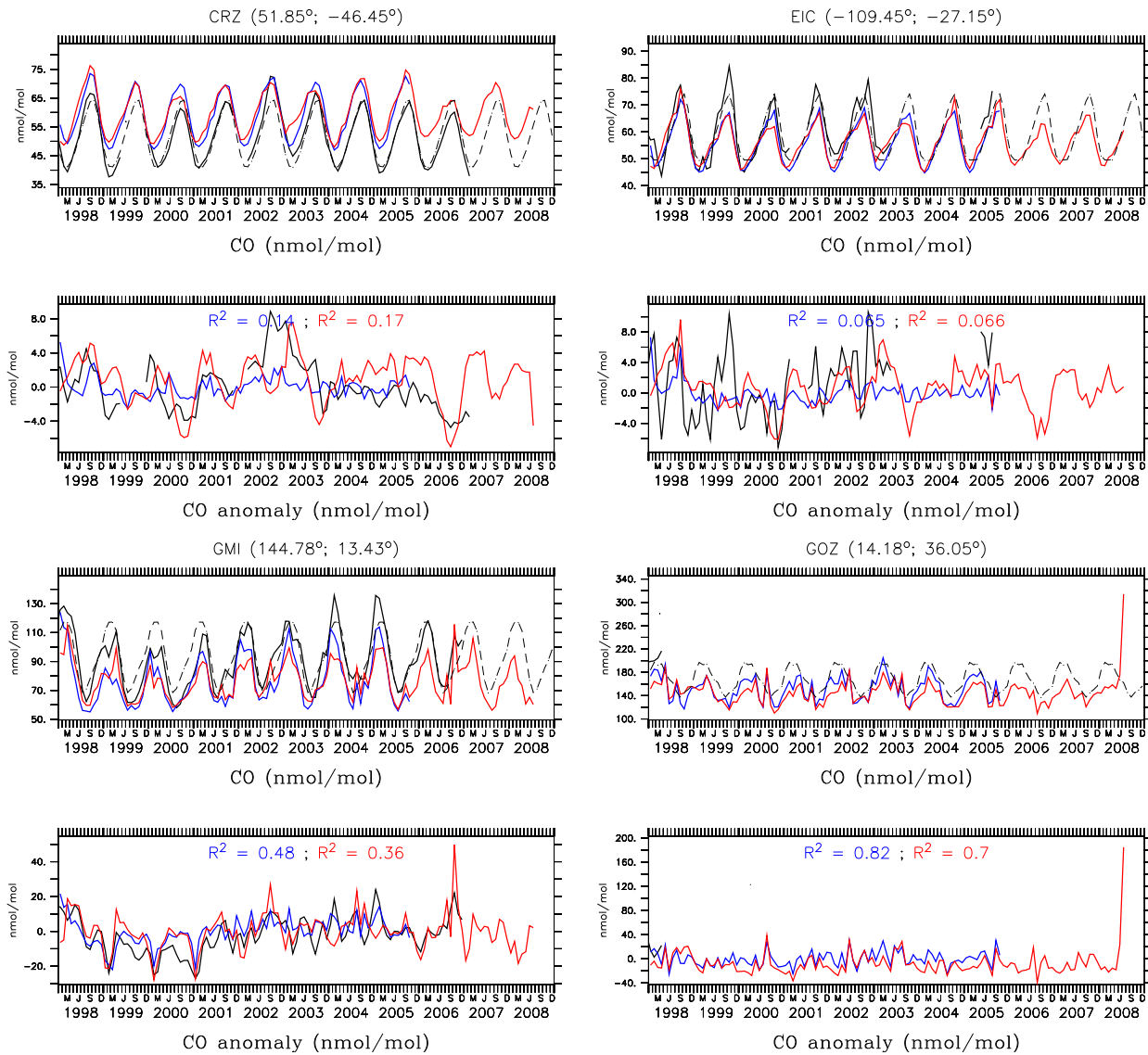


Figure 18: continued

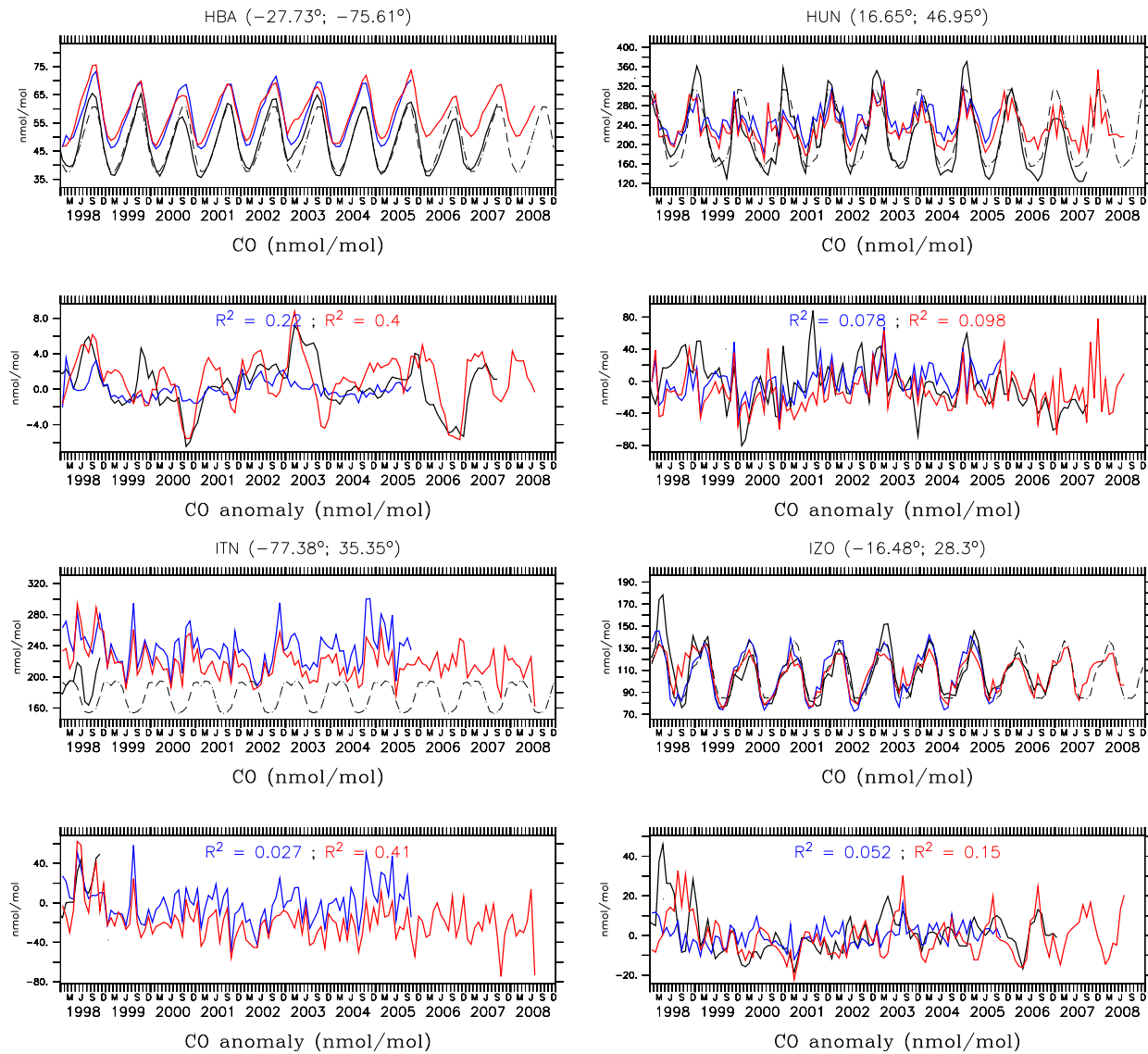


Figure 18: continued

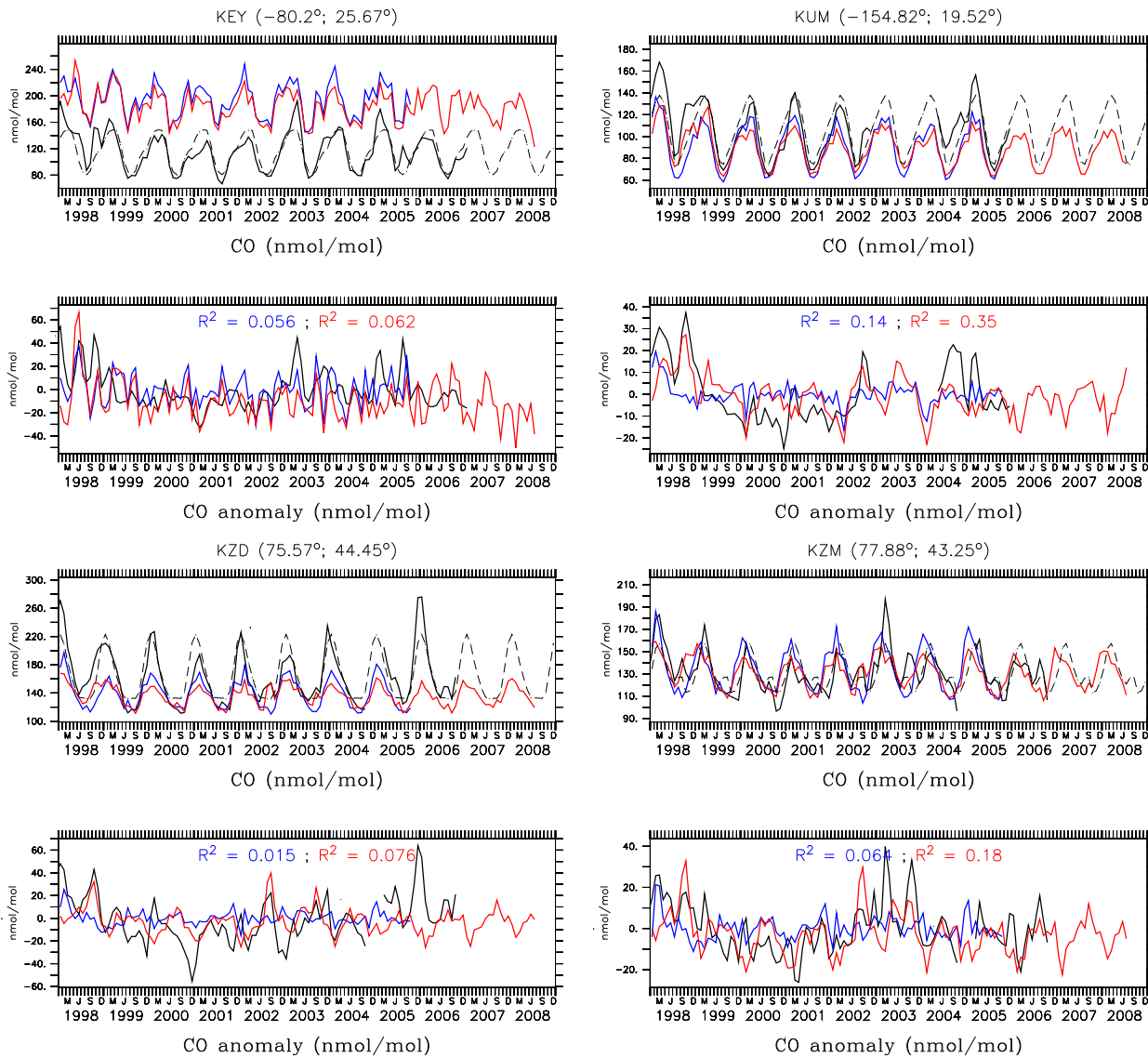


Figure 18: continued

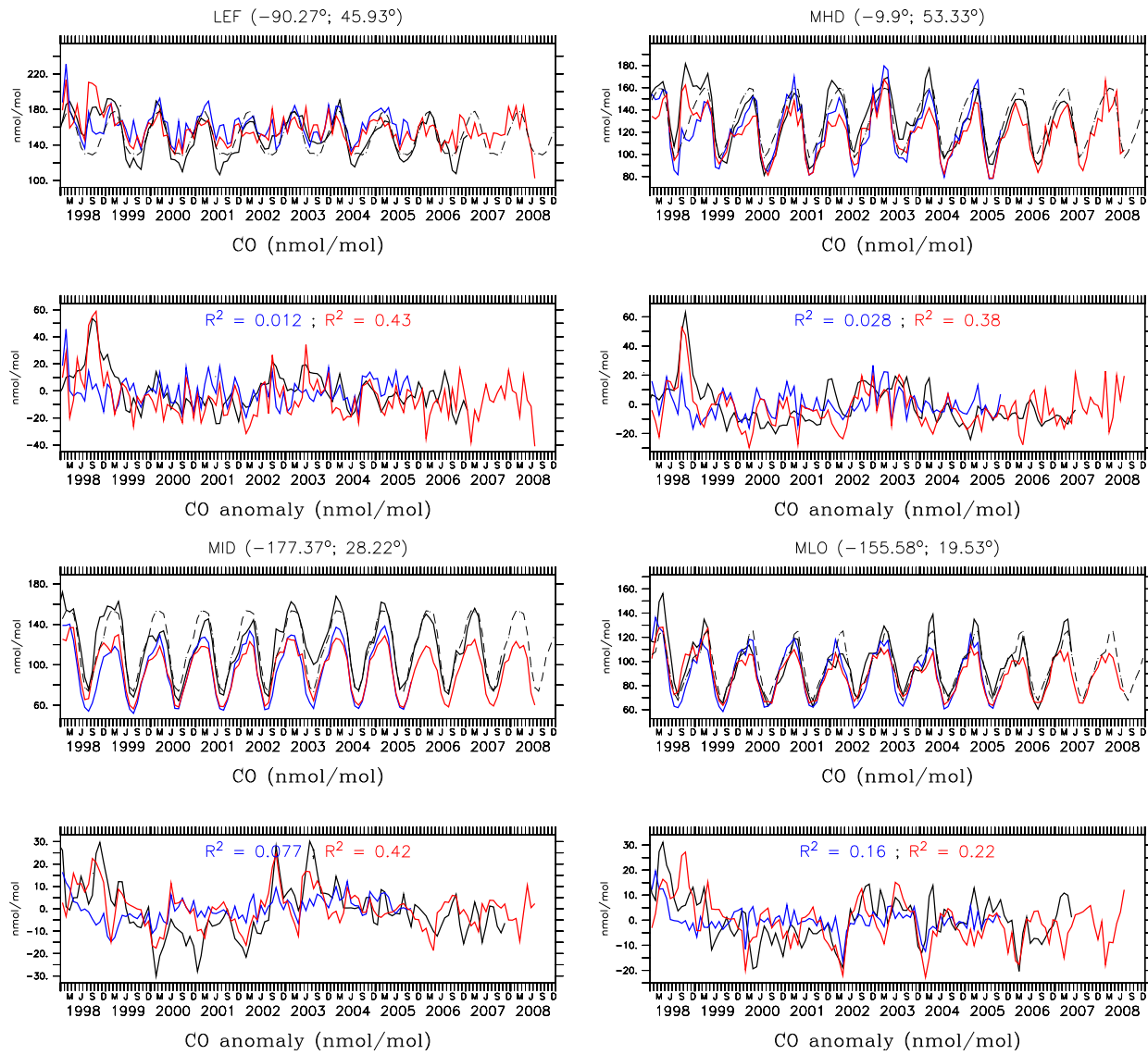


Figure 18: continued

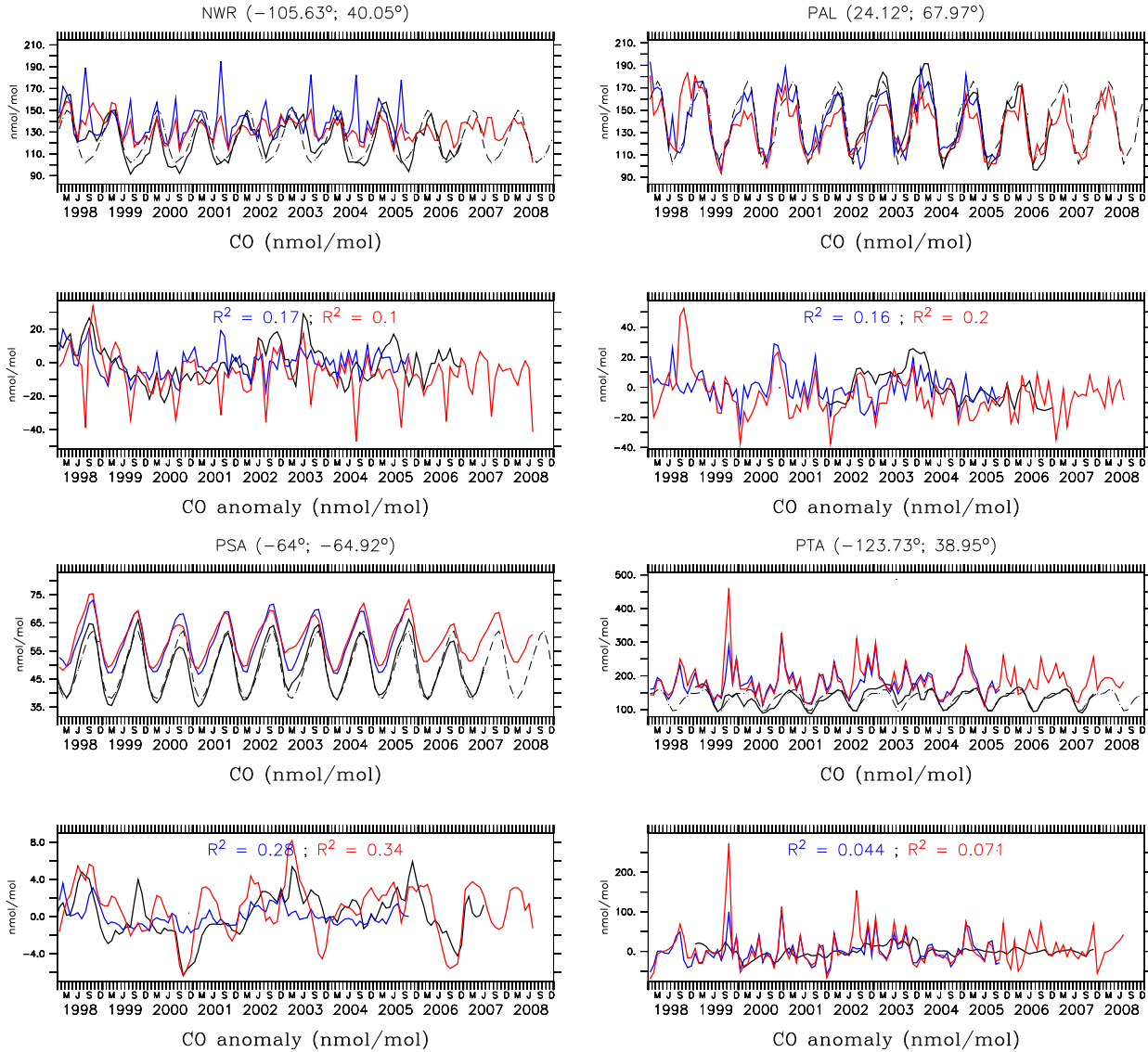


Figure 18: continued

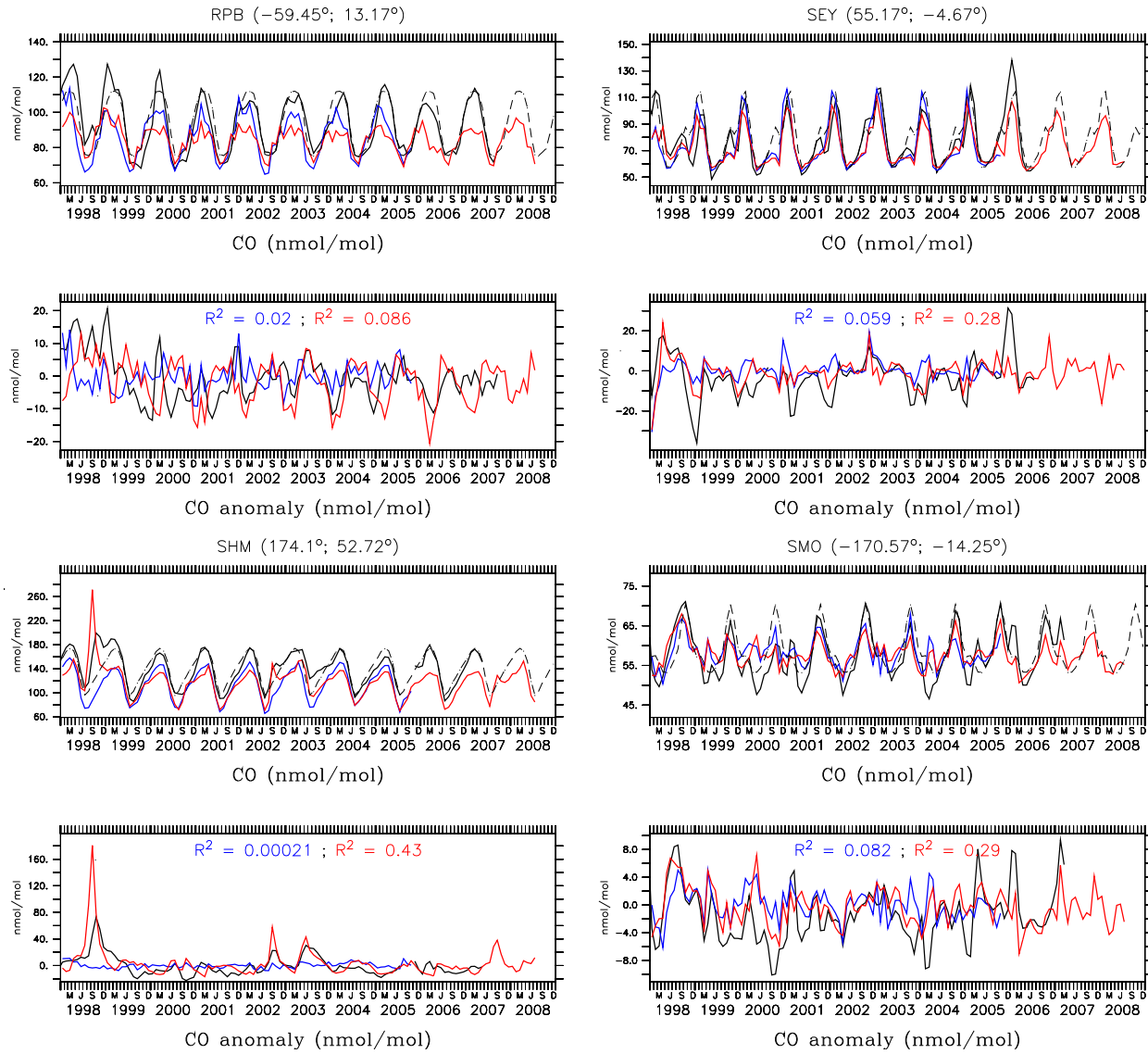


Figure 18: continued

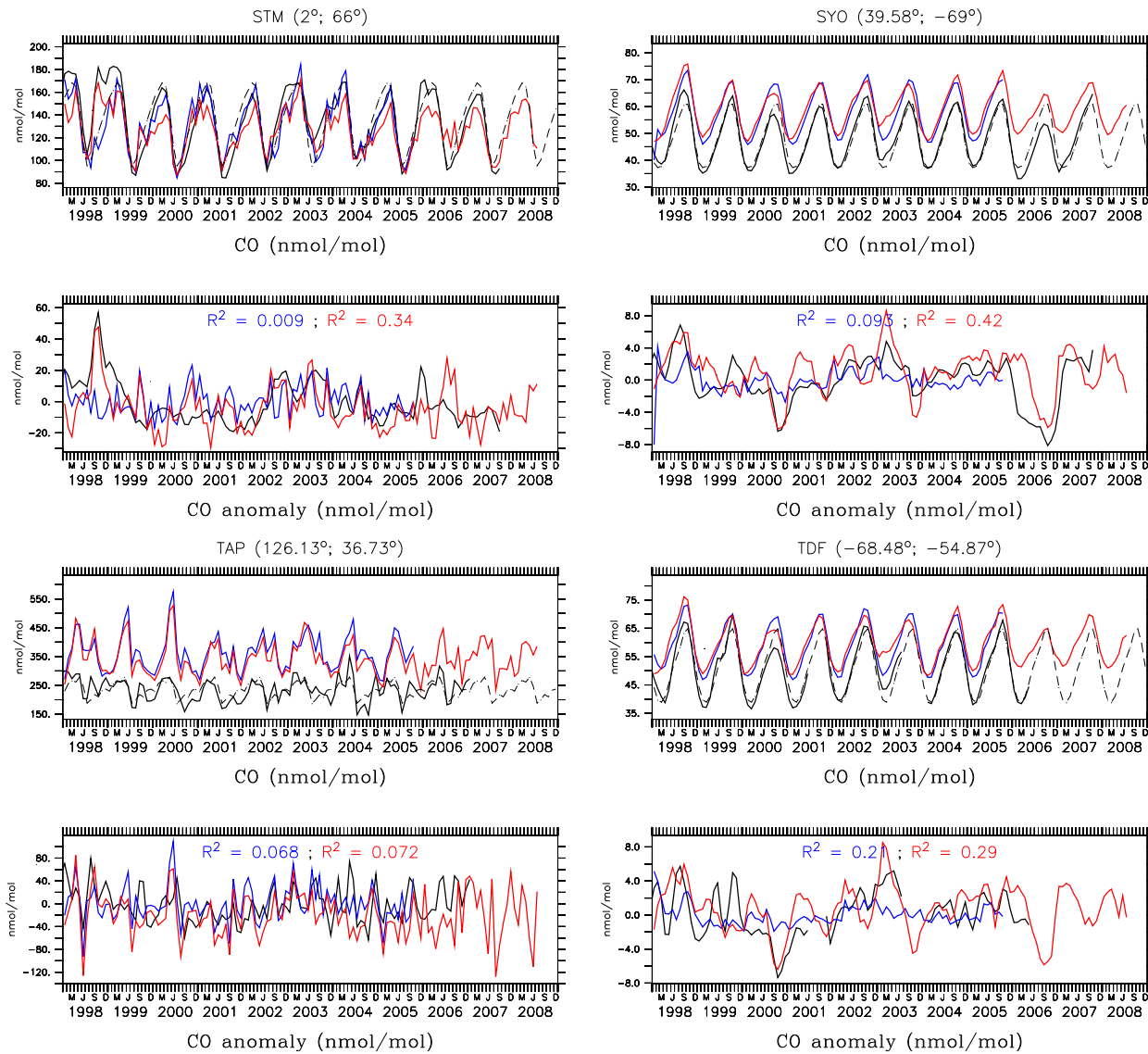


Figure 18: continued

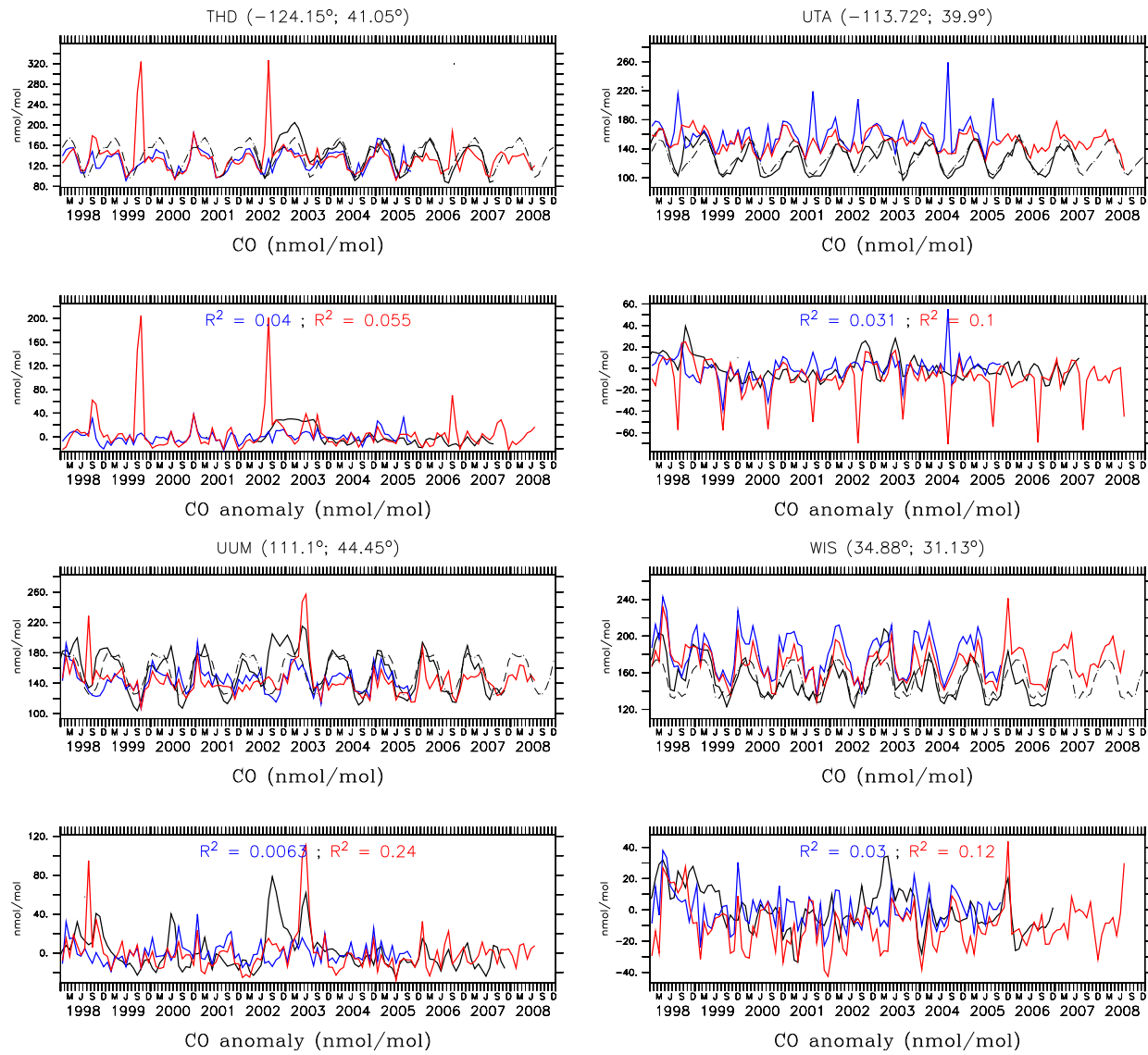


Figure 18: continued

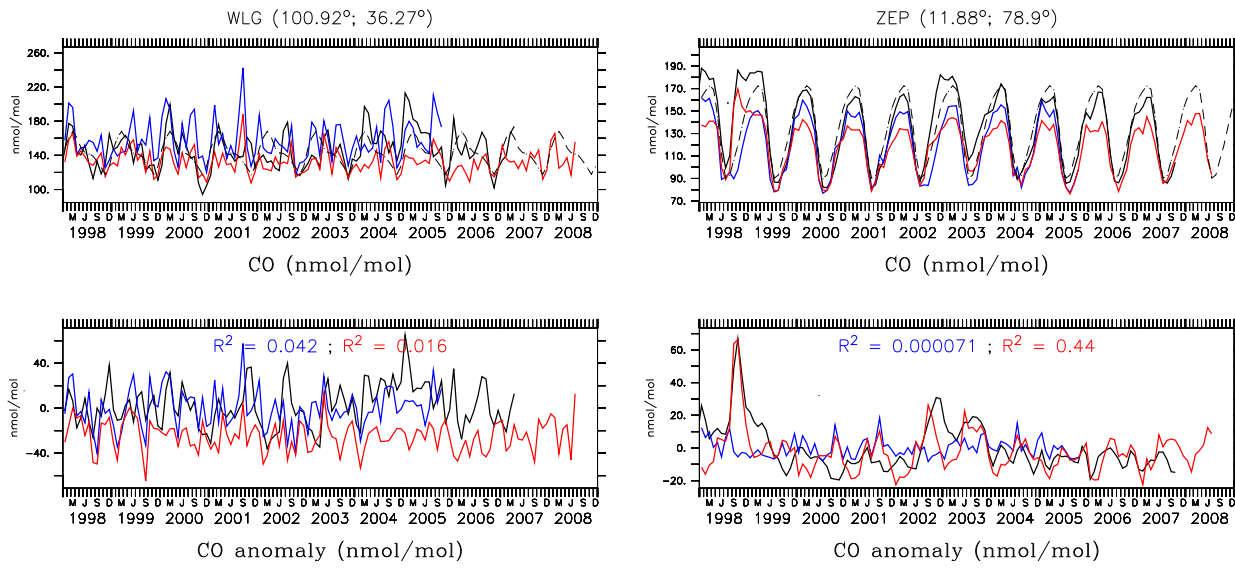


Figure 18: continued

4.2 ^{210}Pb

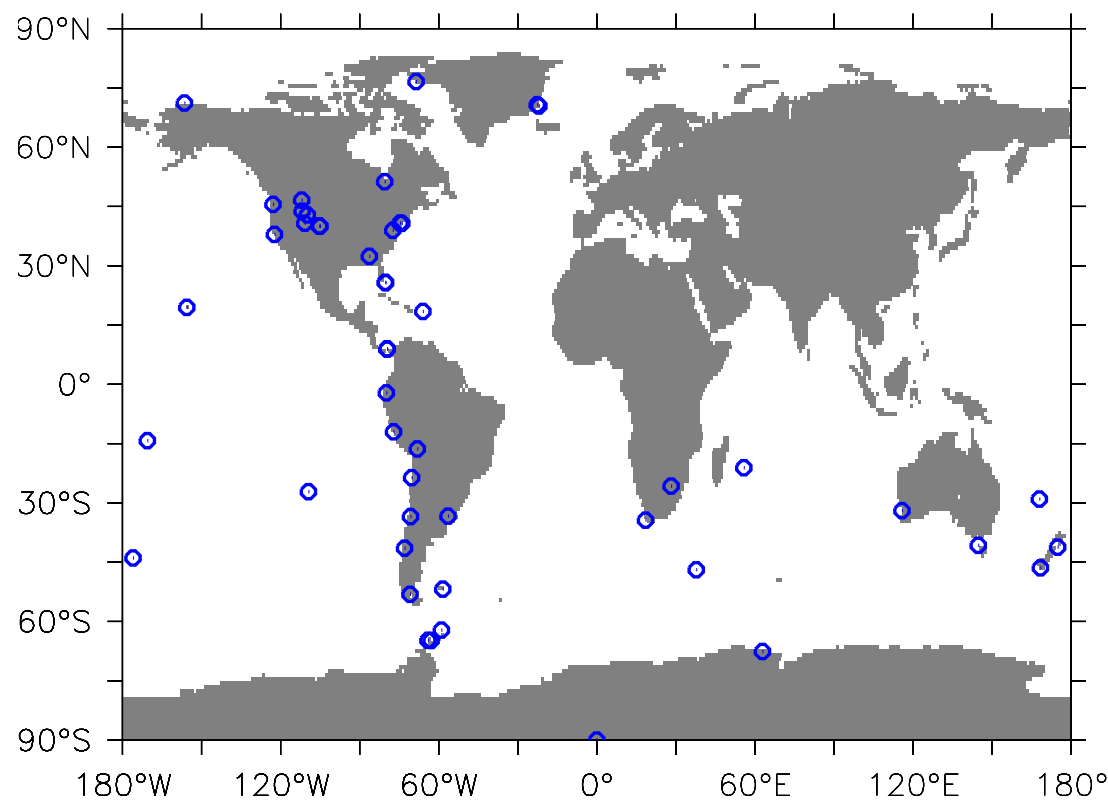


Figure 19: Positions of measurement sites with observations of ^{210}Pb provided by the National Urban Security Technology Laboratory Surface Air Sampling Program (NUSTL/SASP)².

²<http://www.eml.st.dhs.gov/databases/sasp/>

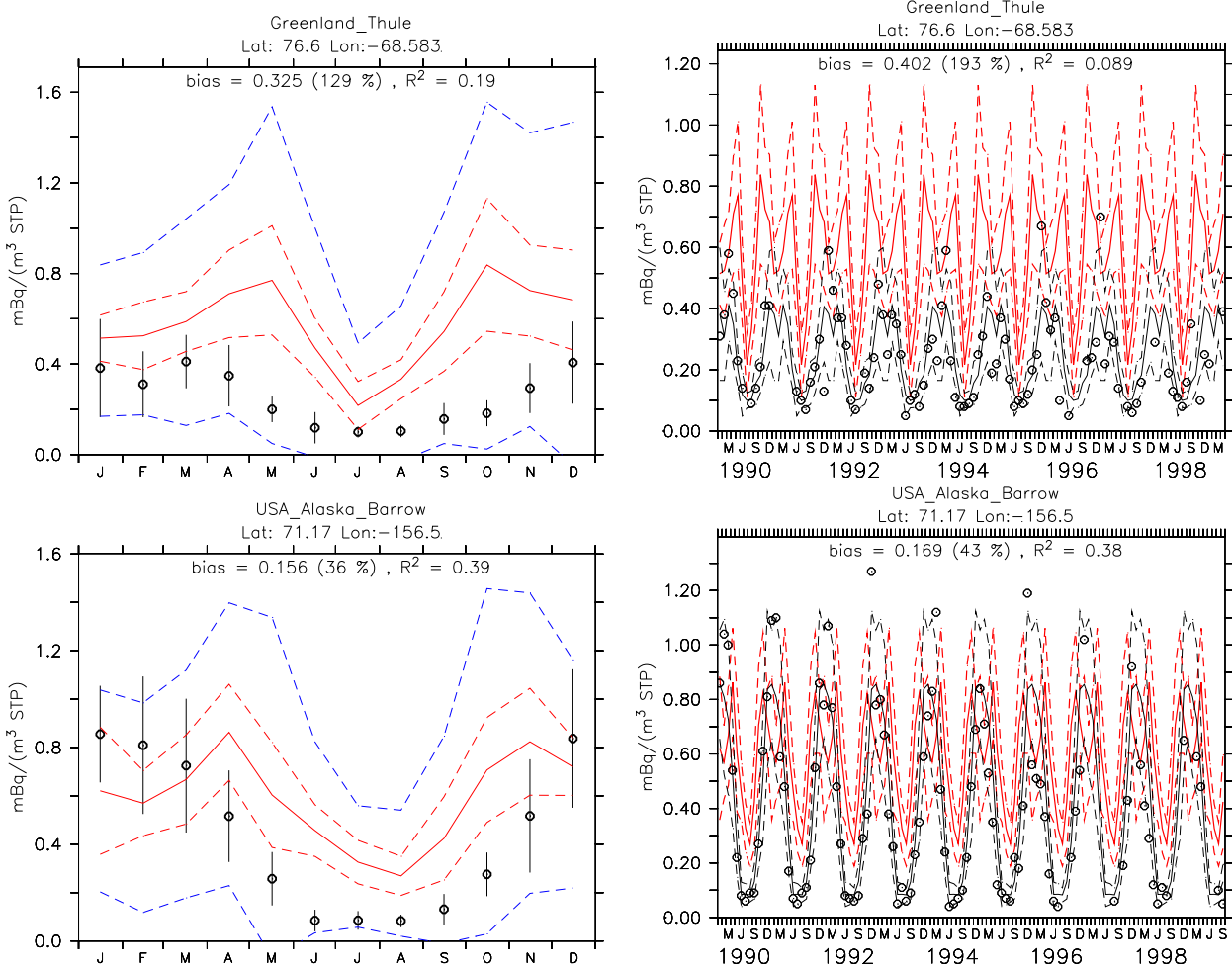


Figure 20: Comparison of simulated ^{210}Pb with surface observations provided by the National Urban Security Technology Laboratory Surface Air Sampling Program (NUSTL/SASP). The name of the sites and the geographical coordinates are listed at the top of each panel. The left panels show the multi-annual average of monthly averages (black symbols) with corresponding standard deviation (black error bars), i.e., the interannual variation of the monthly averages. If more than 10 years of data after 1990 are available, the calculation of the average is limited to the period starting January 1990. The red line denotes the simulated multi-annual (2000-2007) average of monthly averages, the dashed red lines indicate the interval of the corresponding standard deviation, i.e., the interannual variation of the monthly averages. The dashed blue lines show the interval of the full standard deviation (w.r.t. time) based on the 5-hourly model output. The bias is given as the average (12 months) difference between the simulated and the observed climatological monthly averages and as relative deviation (in %) of the simulated from the observed climatological average. R^2 is Pearson's coefficient of the correlation between the simulated and observed multi-annual monthly averages. The right panels show the individual monthly averages from the observations (open symbols), the corresponding multi-annual climatological monthly average (black lines) plus / minus standard deviation (black dashed lines) and the simulated multi-annual monthly averages (red lines) plus / minus the standard deviation (dashed red lines). Bias and R^2 are calculated between simulated multi-annual monthly averages and individual monthly observations.

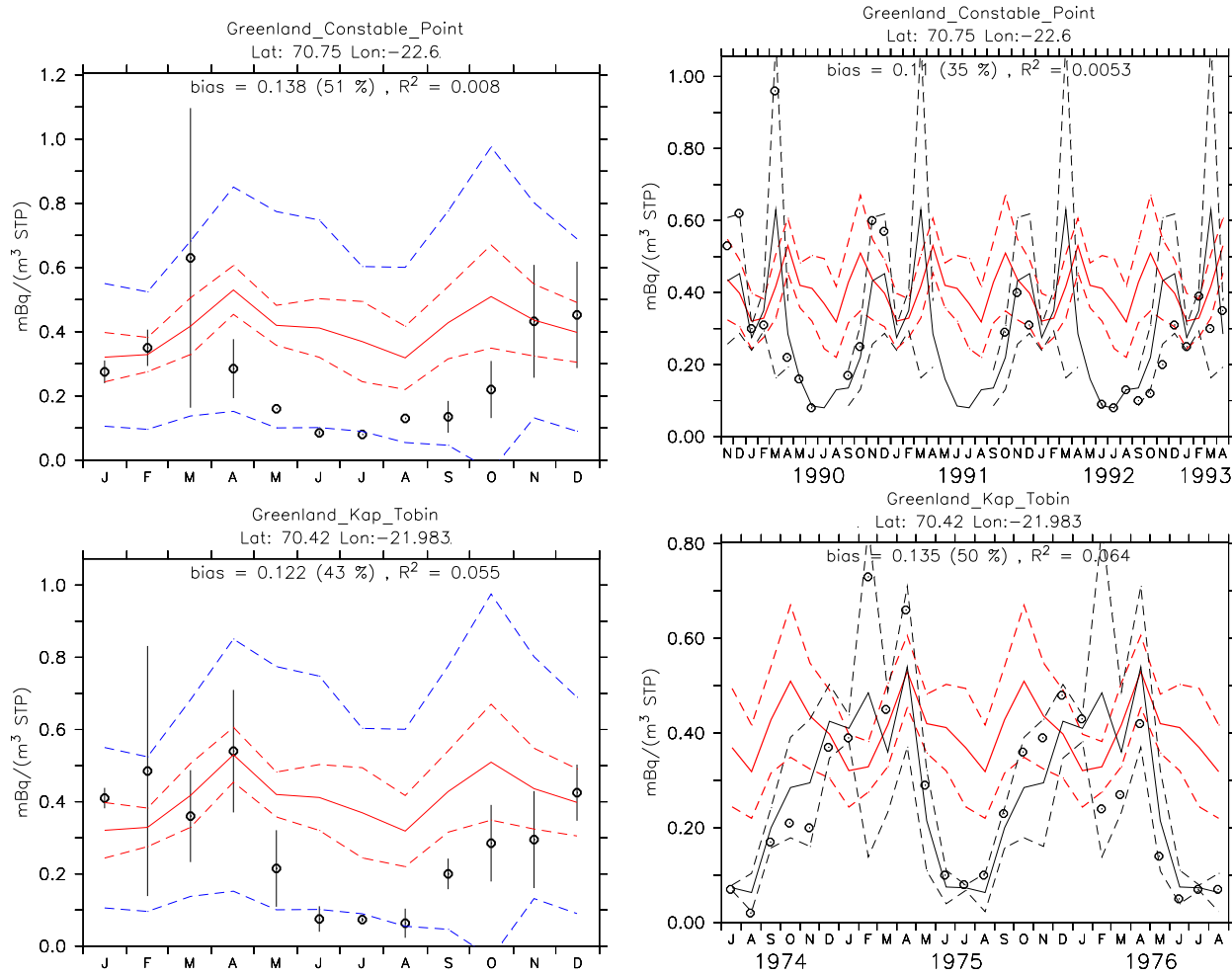


Figure 20: continued

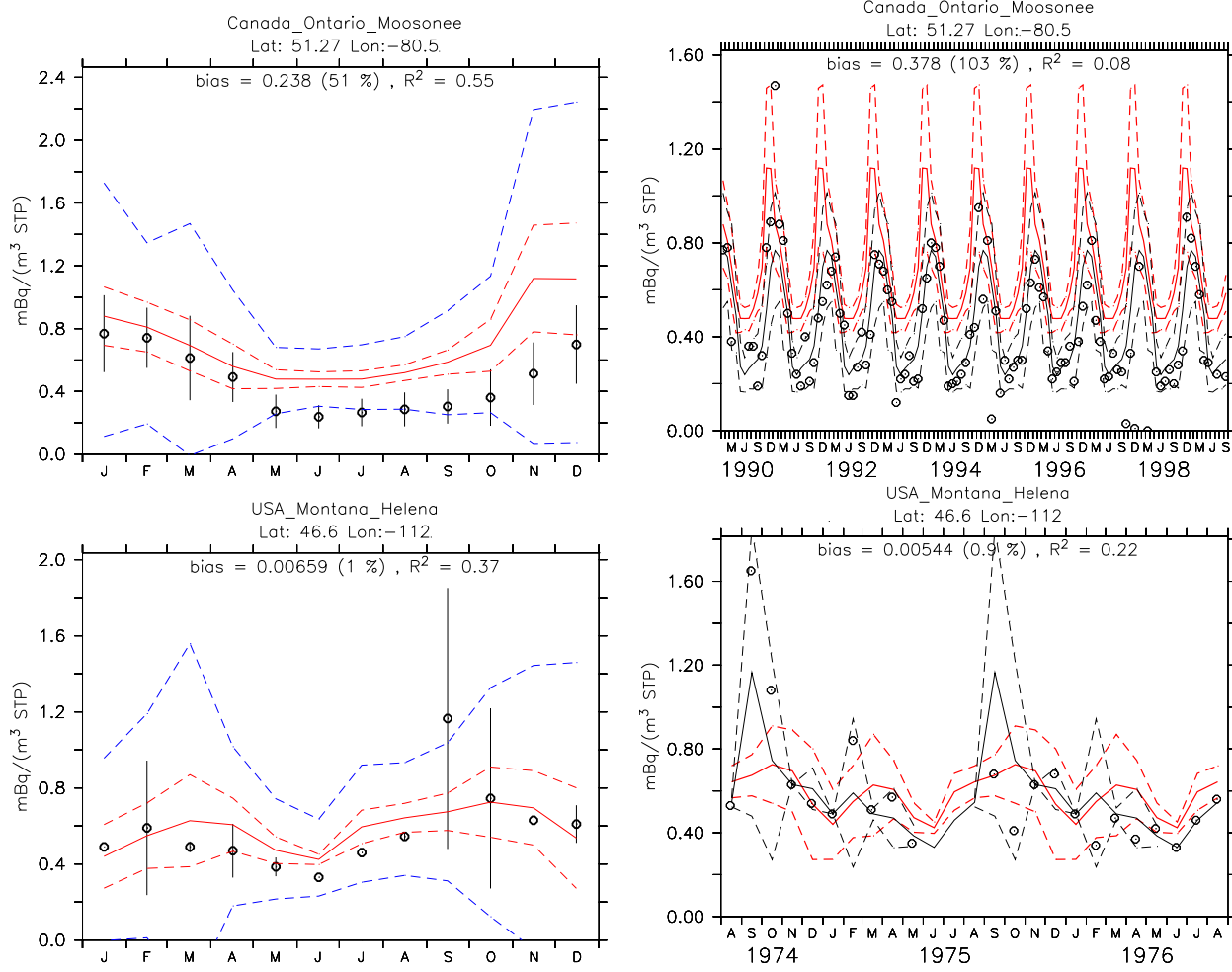


Figure 20: continued

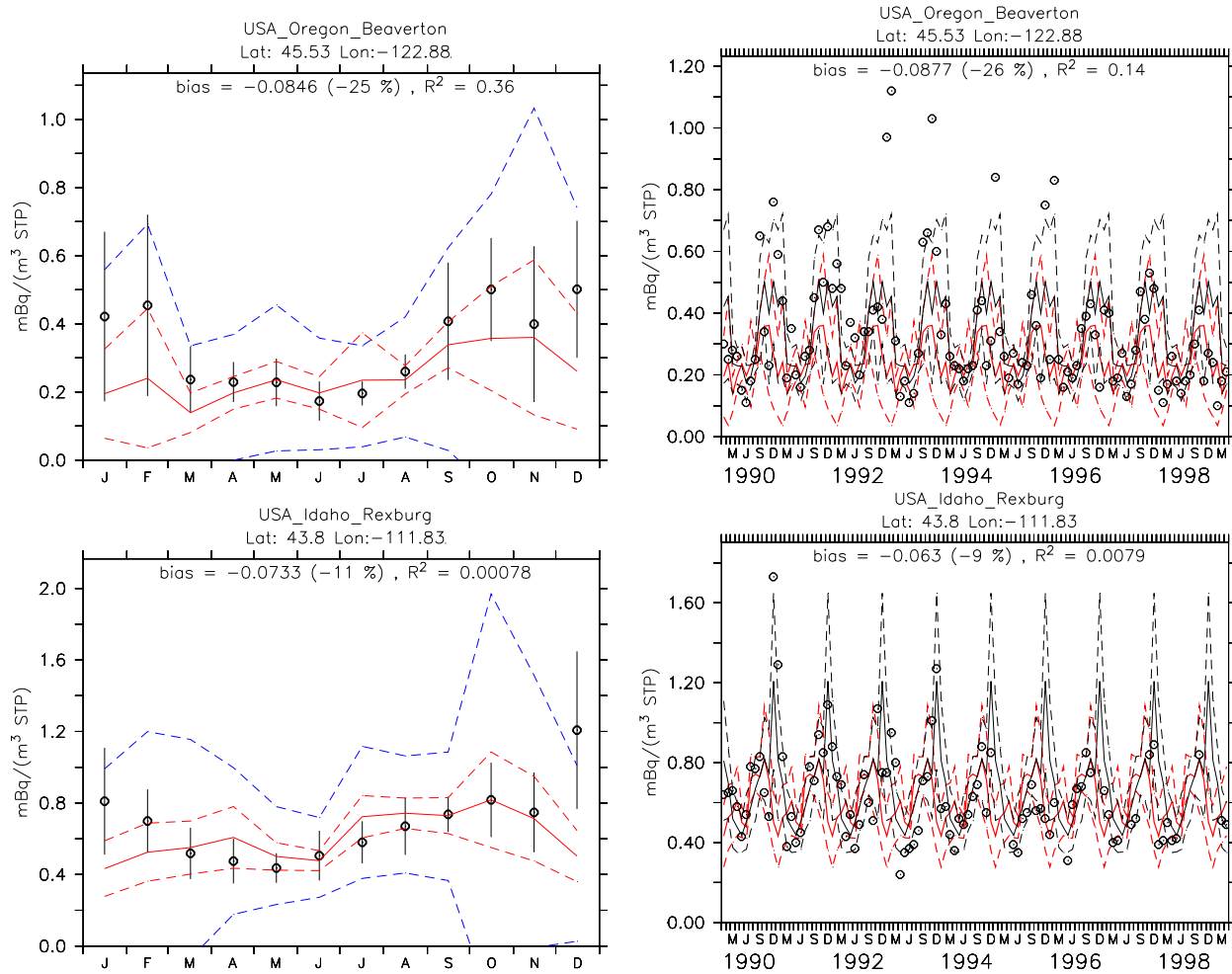


Figure 20: continued

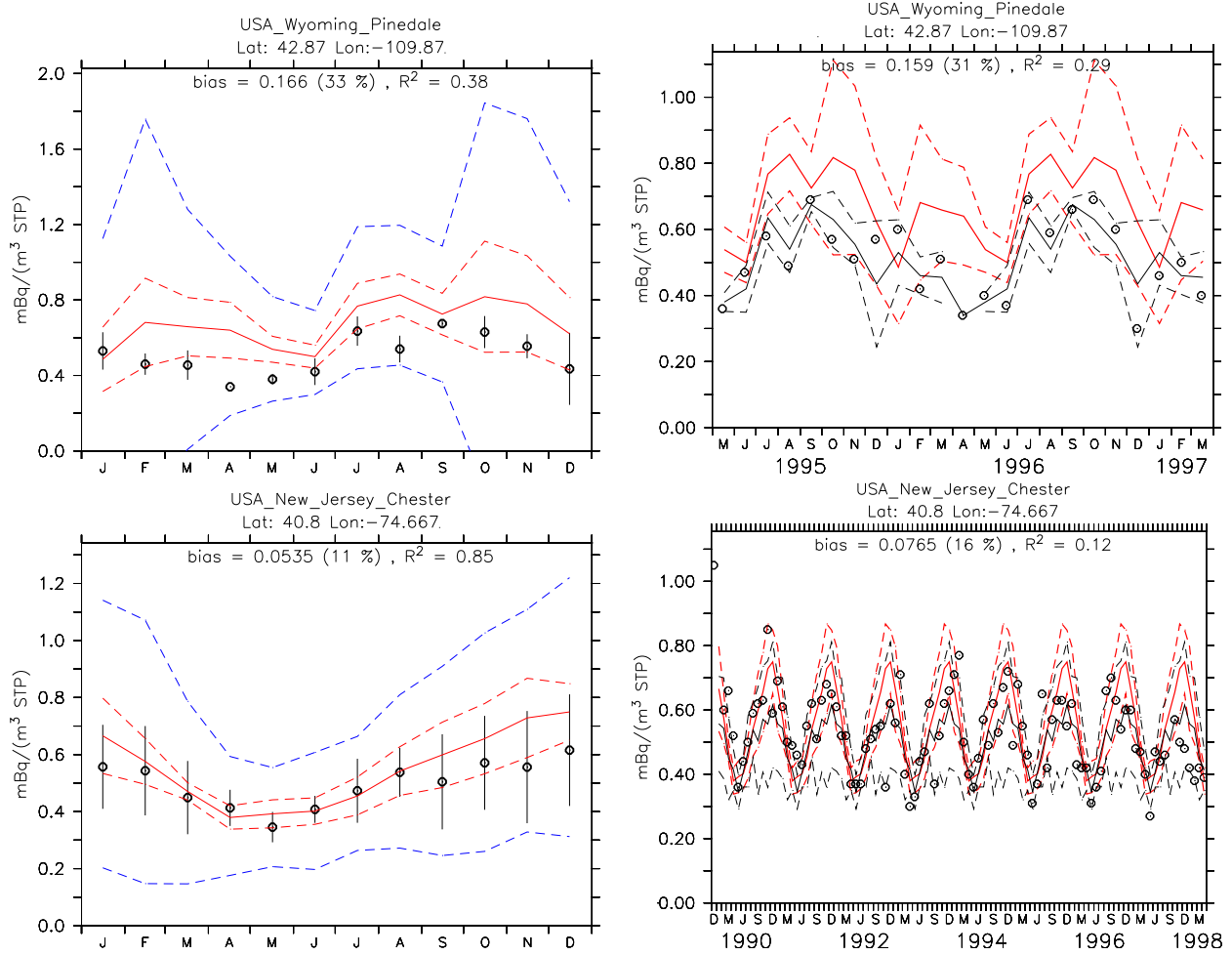


Figure 20: continued

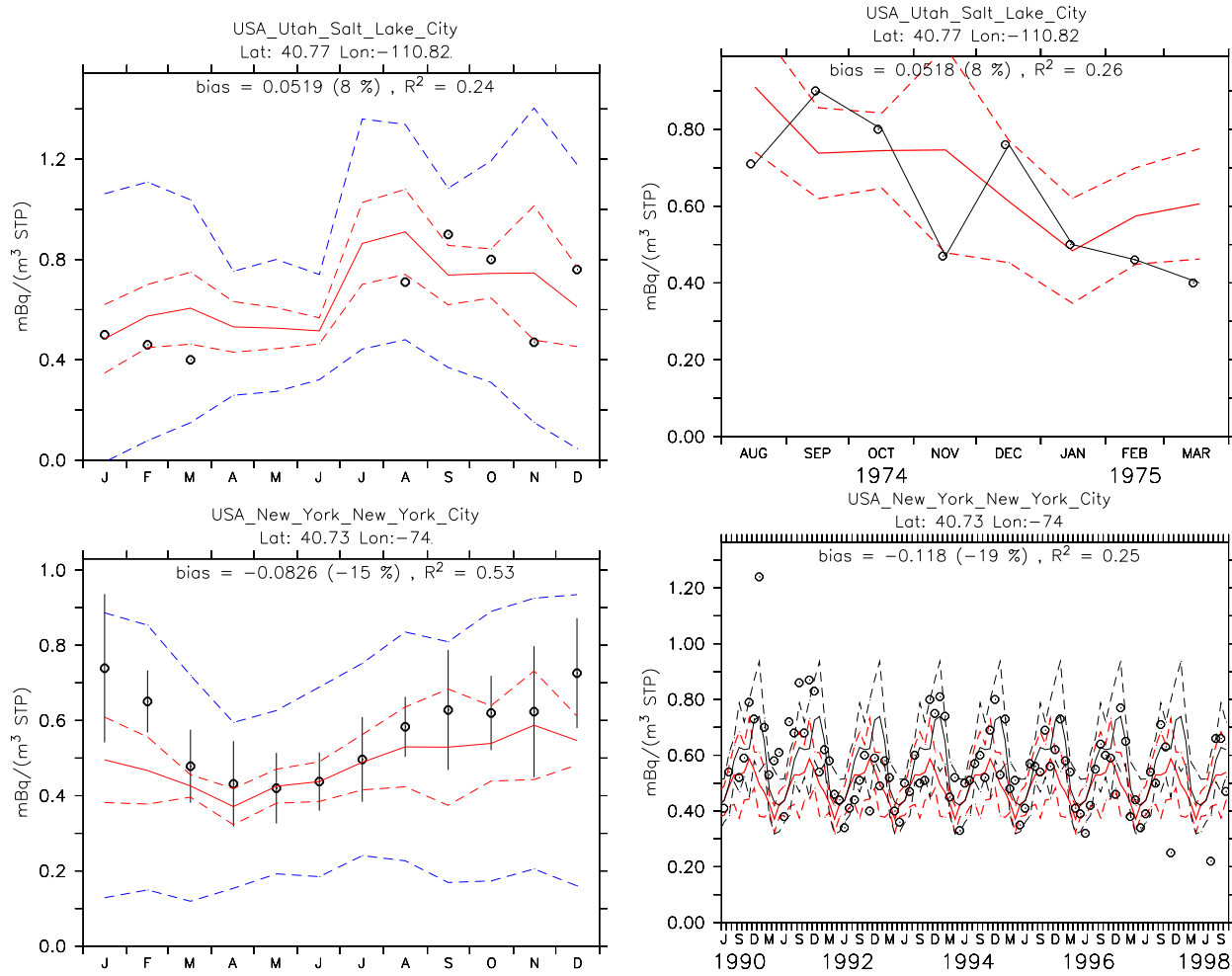


Figure 20: continued

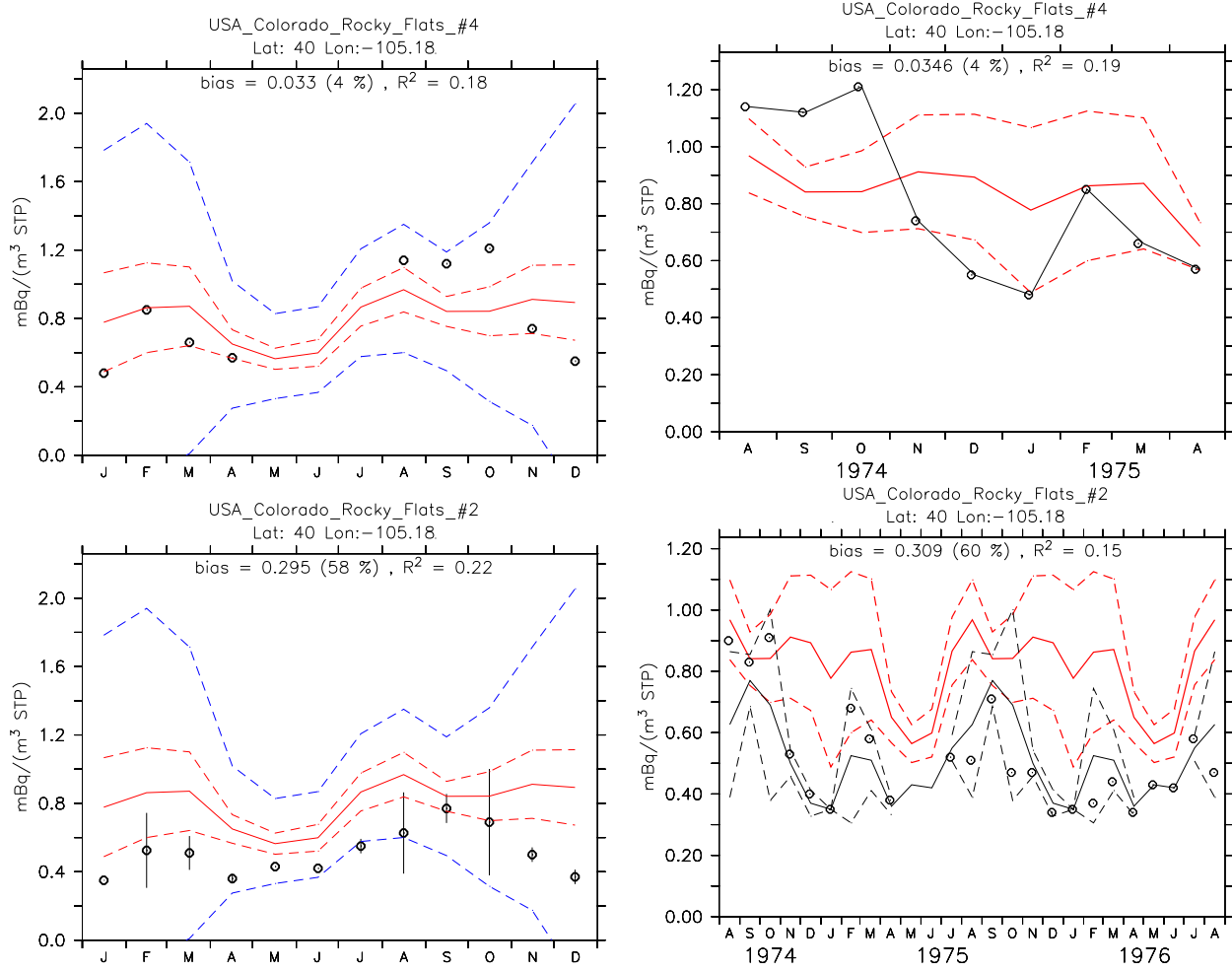


Figure 20: continued

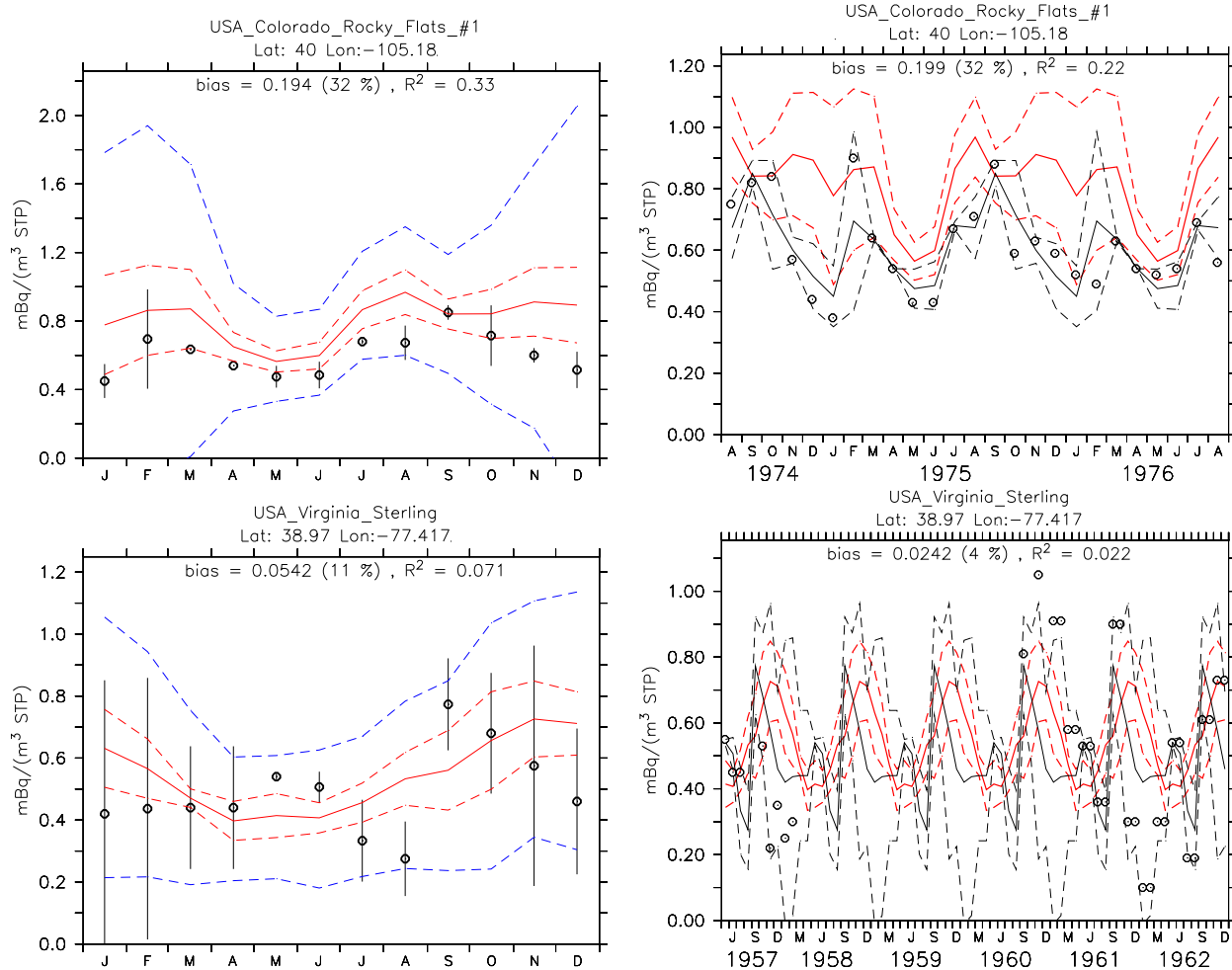


Figure 20: continued

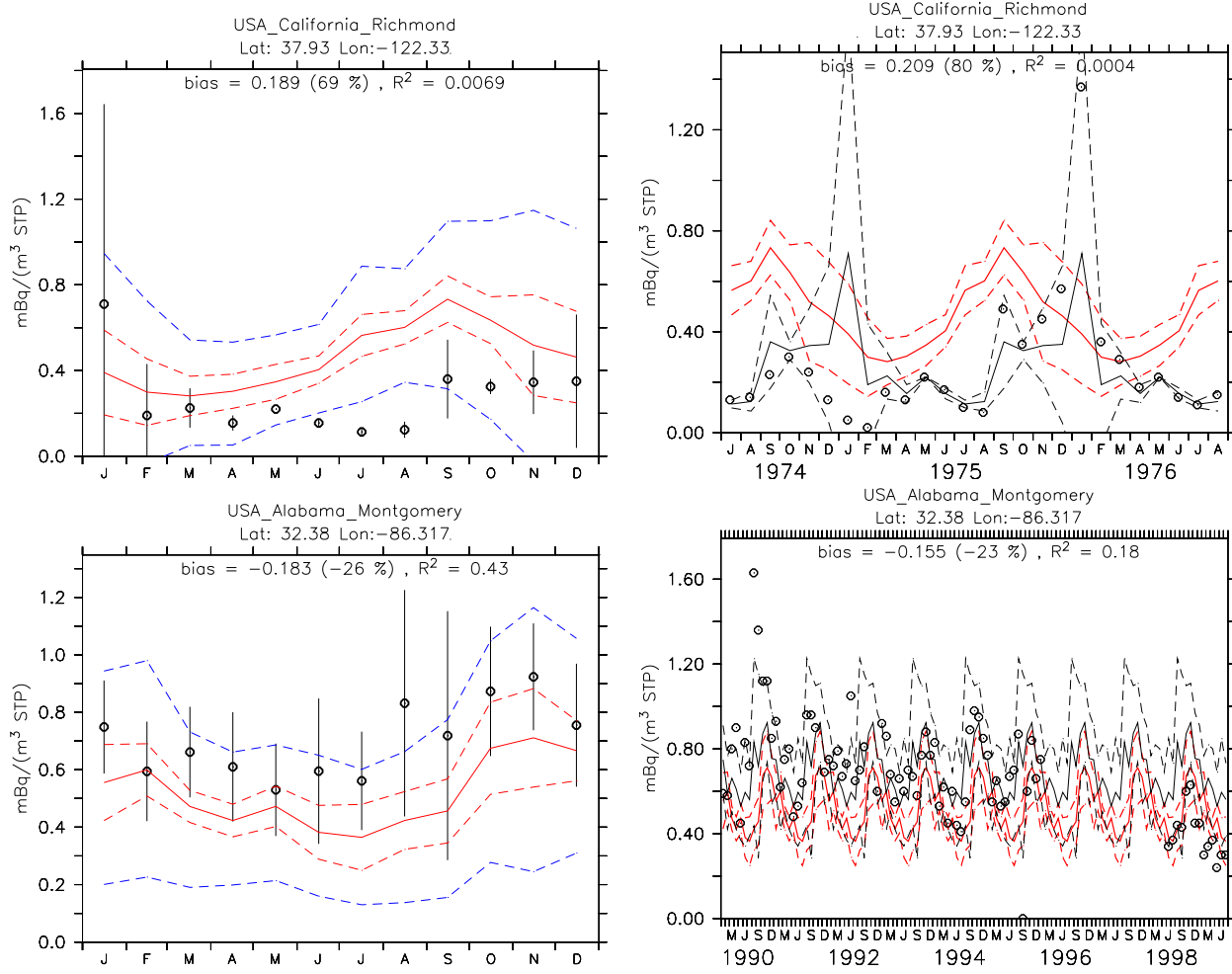


Figure 20: continued

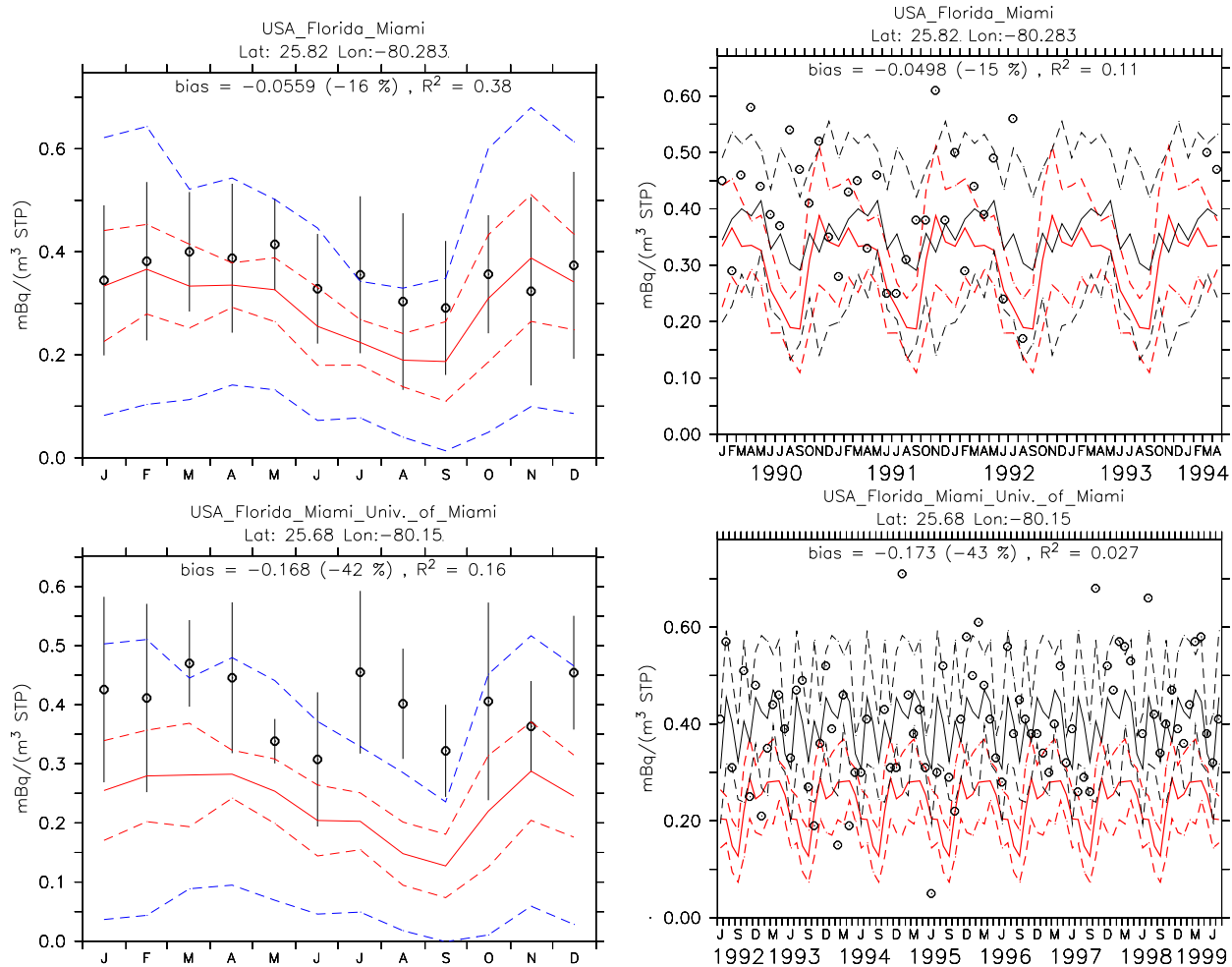


Figure 20: continued

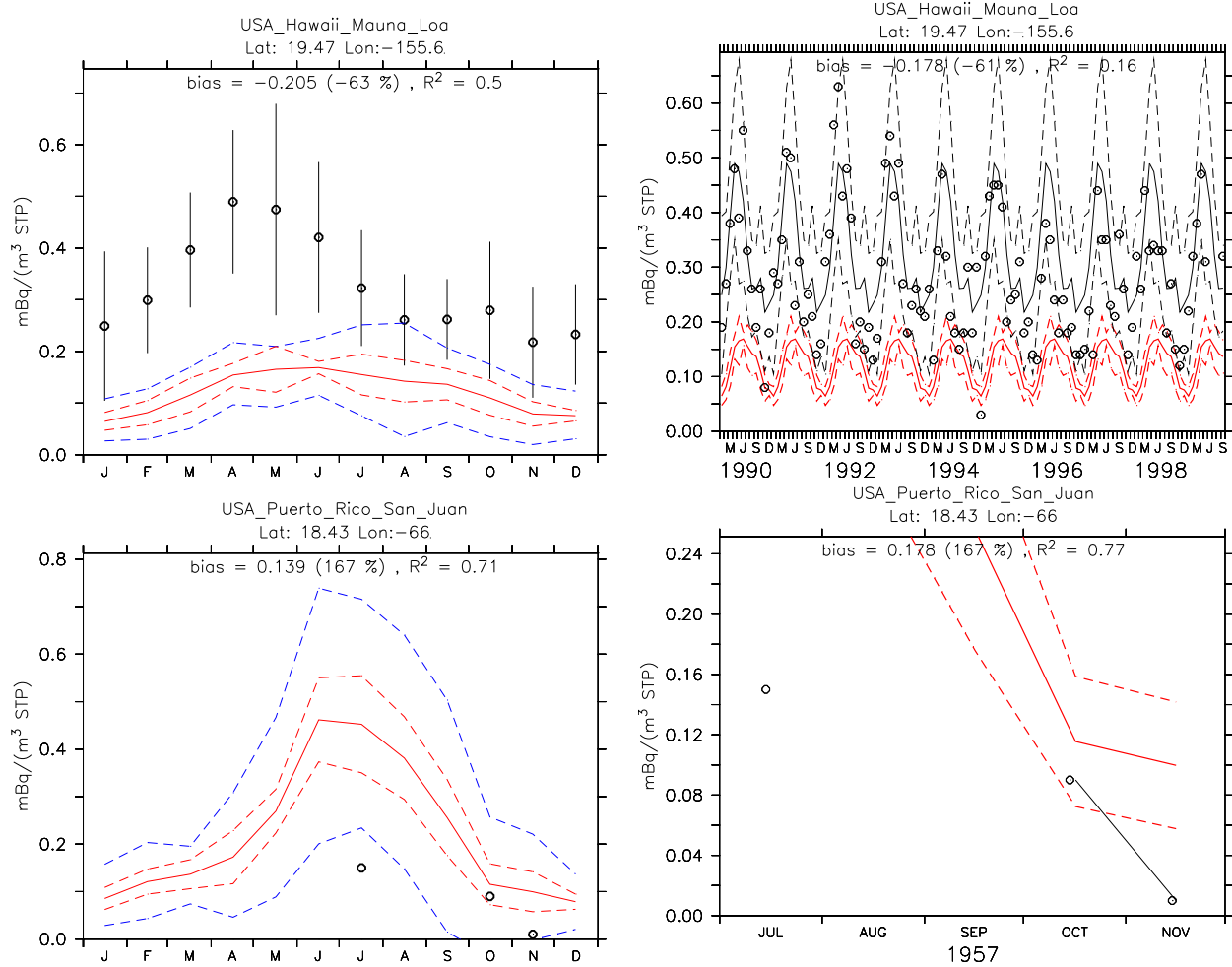


Figure 20: continued

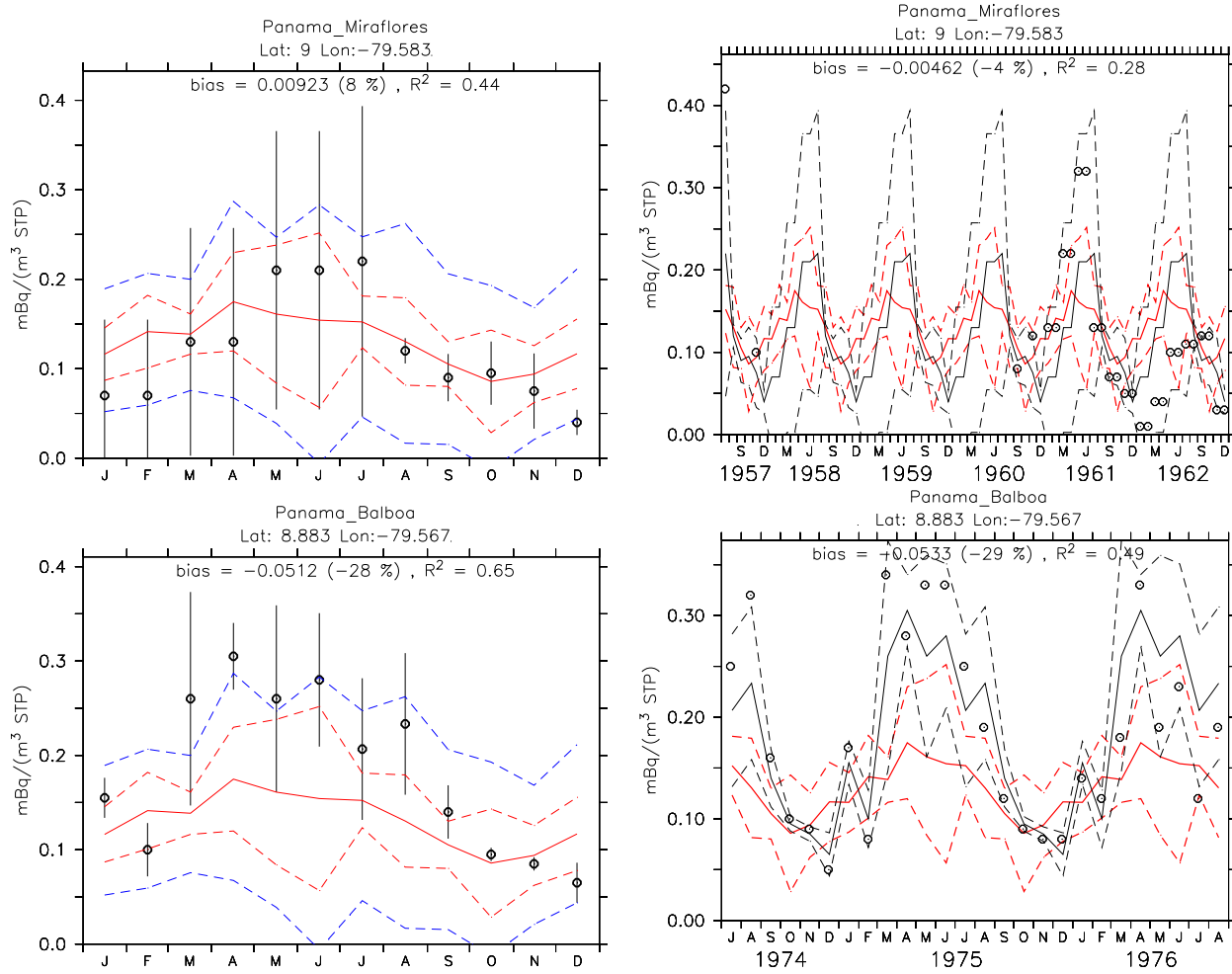


Figure 20: continued

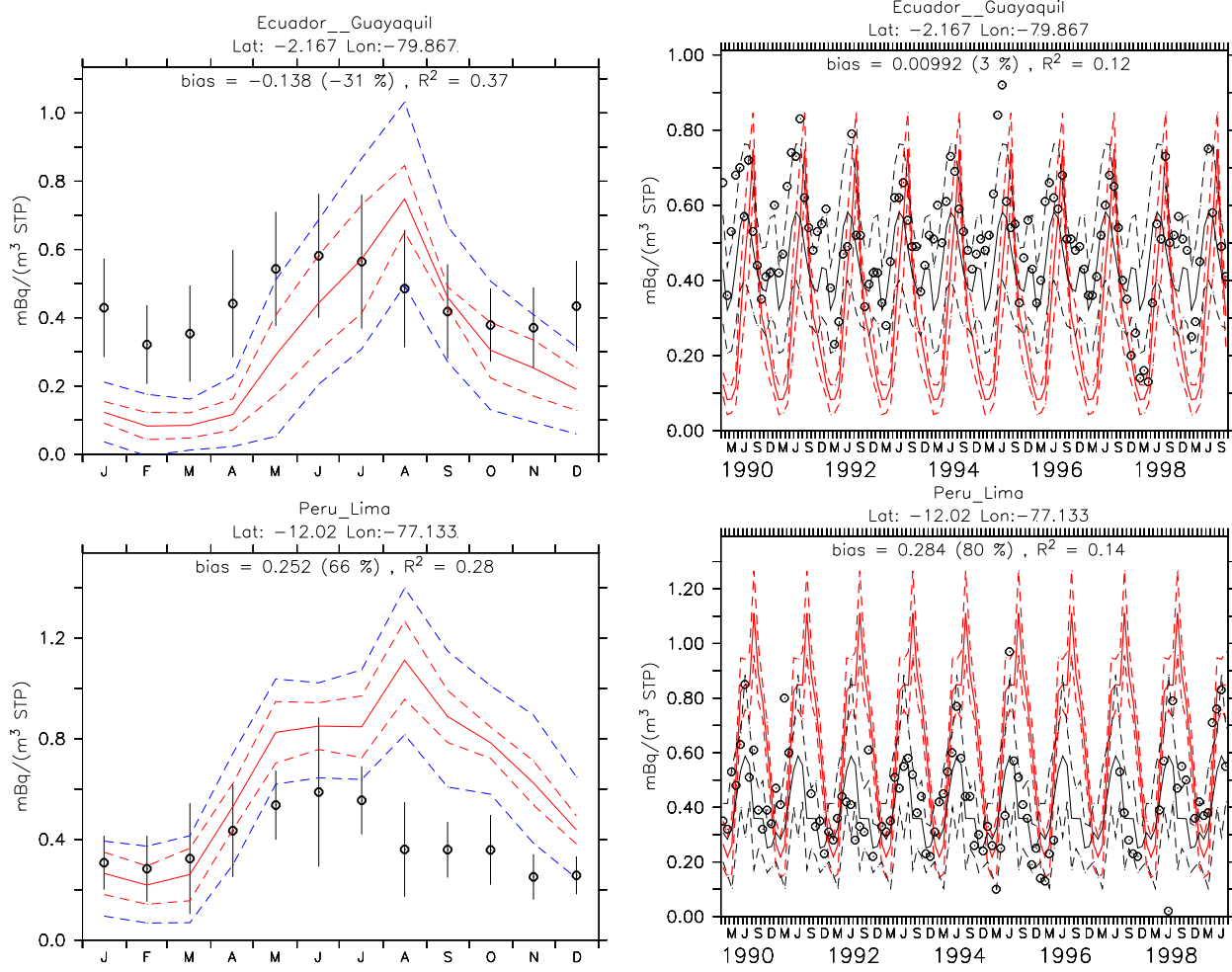


Figure 20: continued

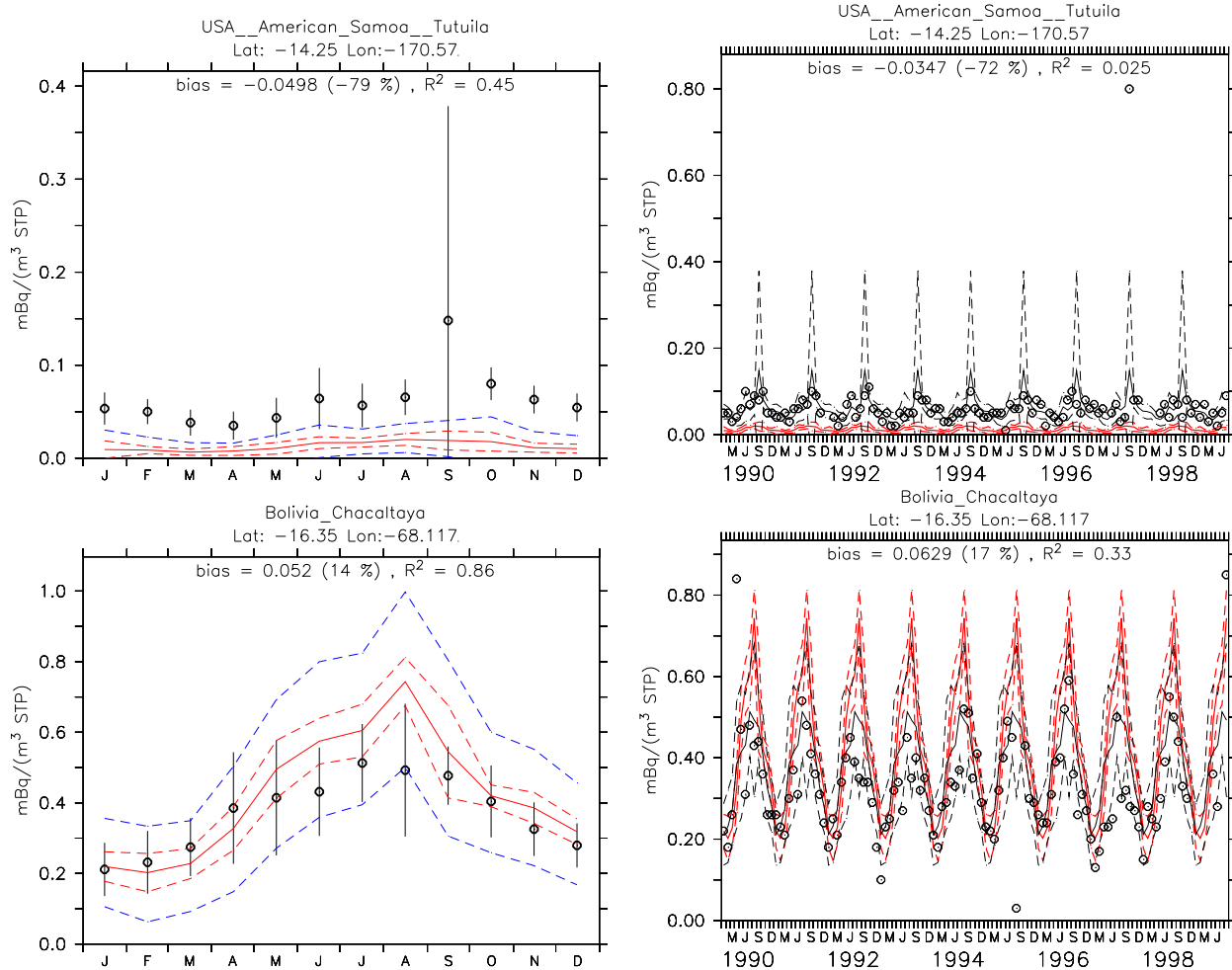


Figure 20: continued

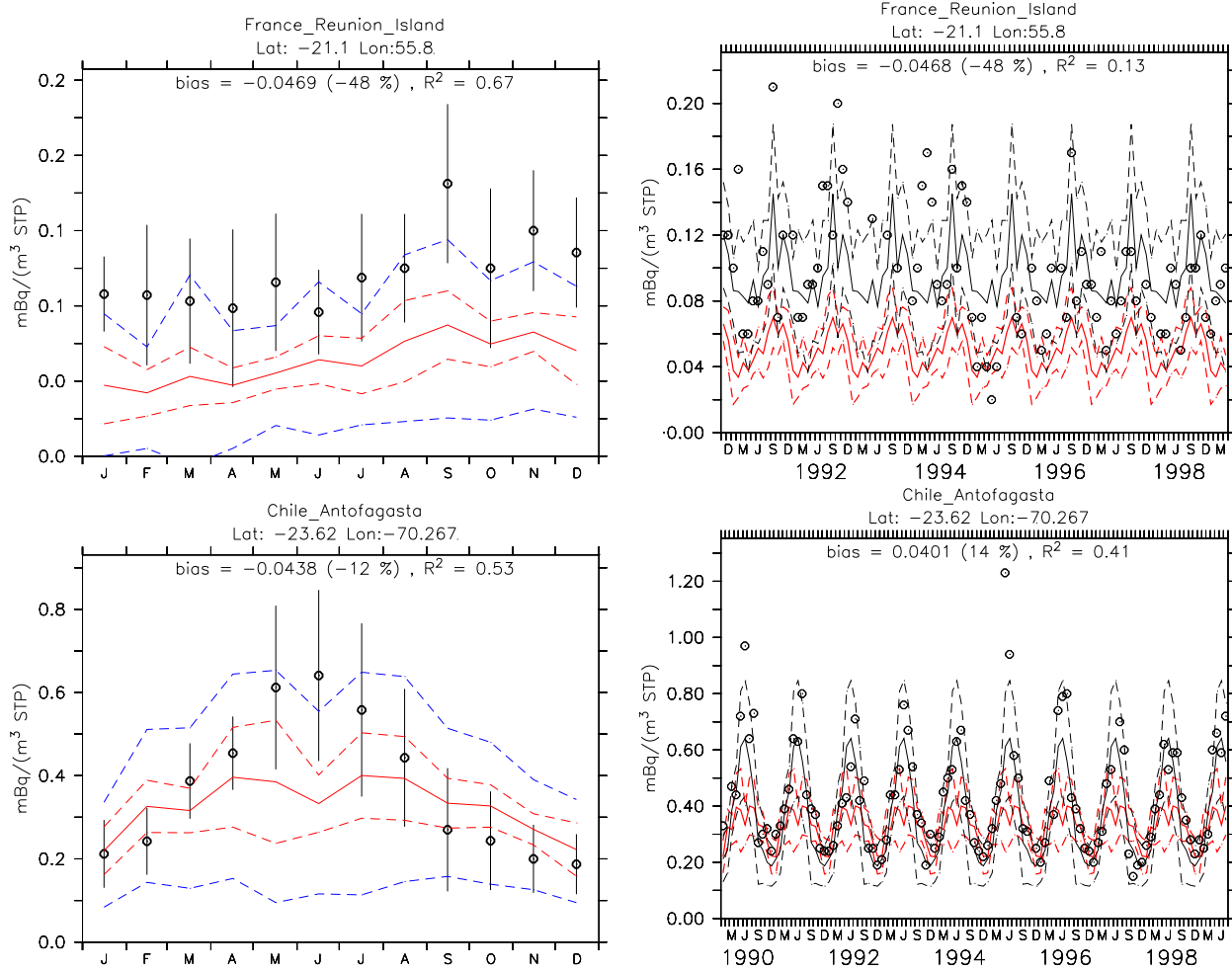


Figure 20: continued

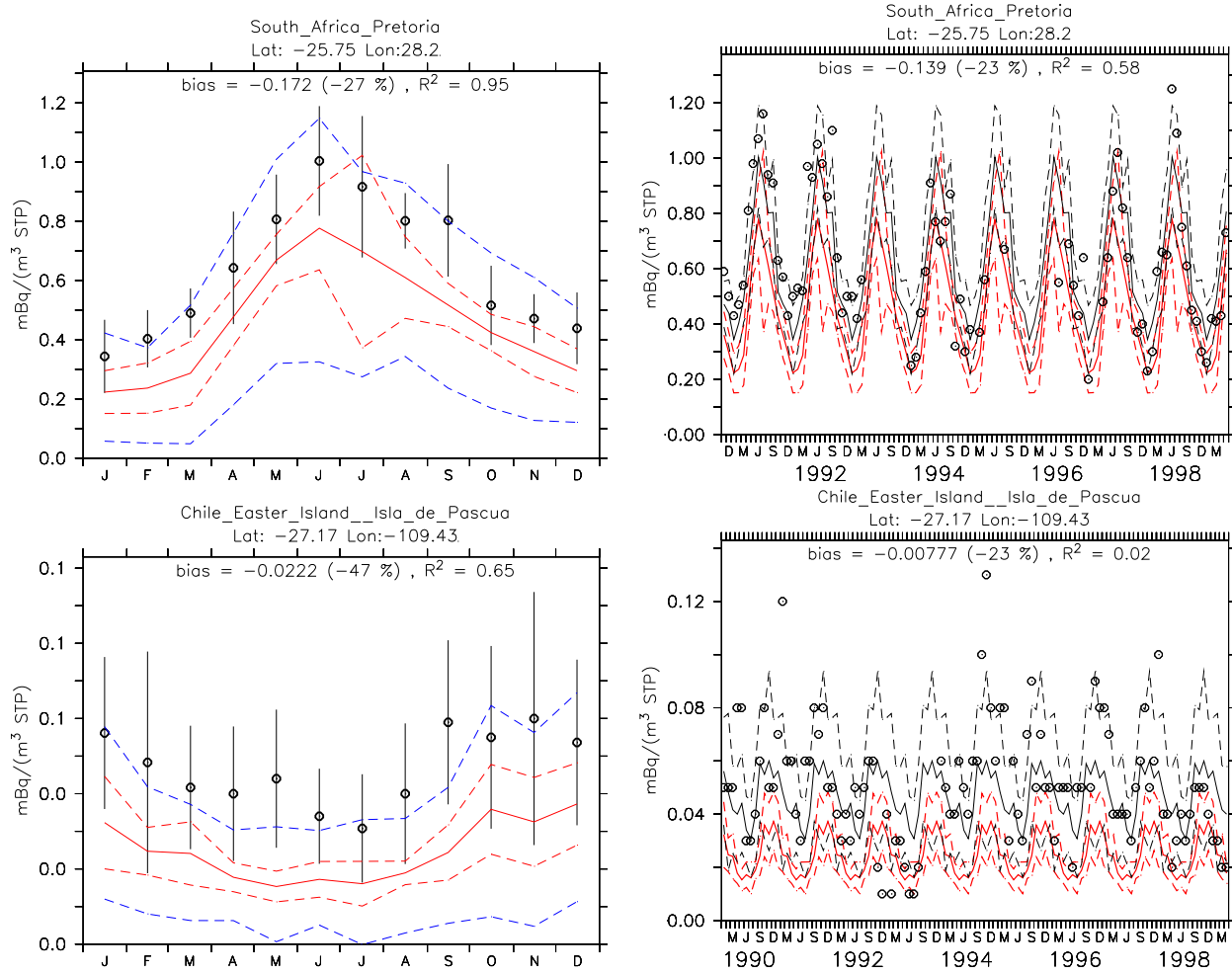


Figure 20: continued

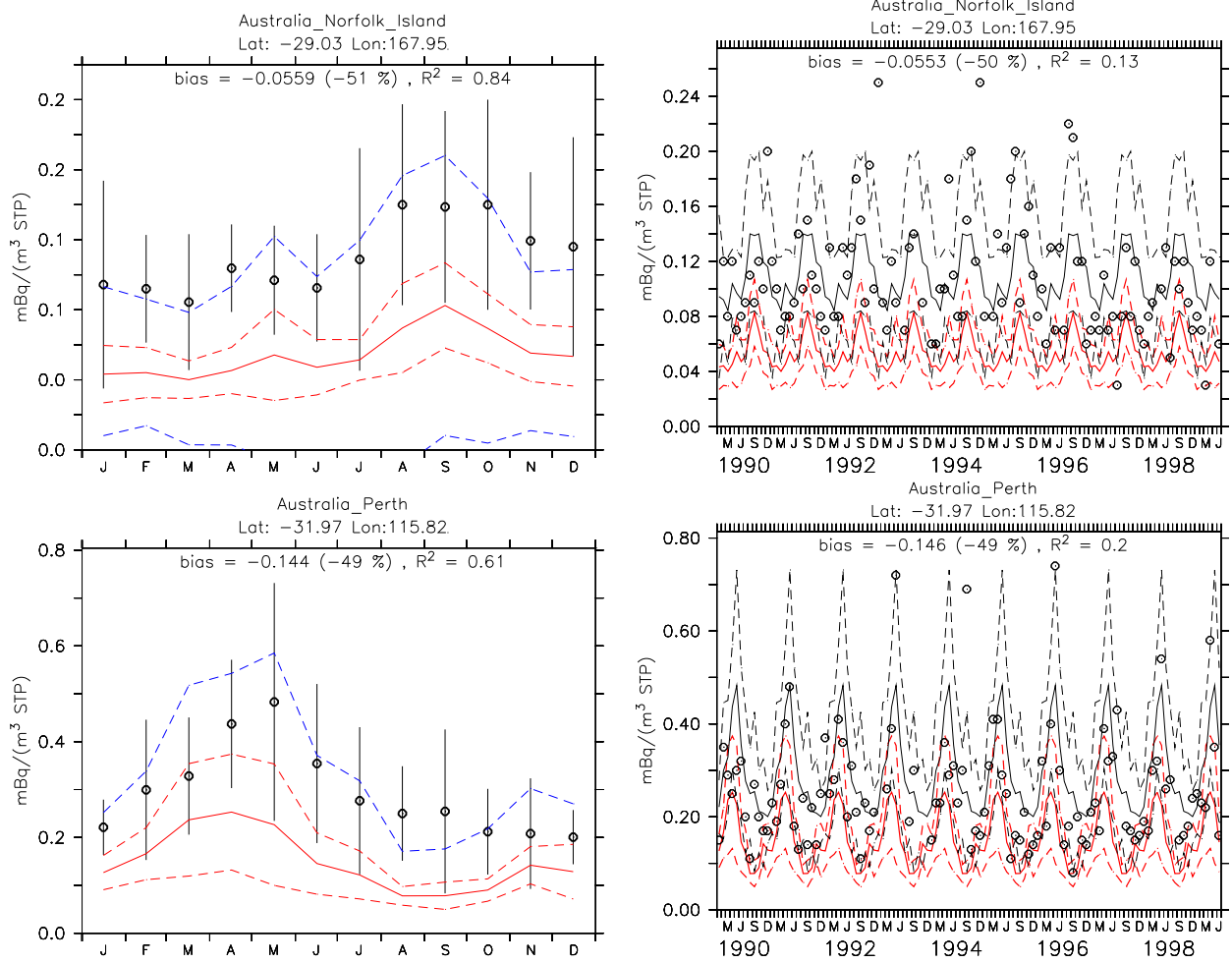


Figure 20: continued

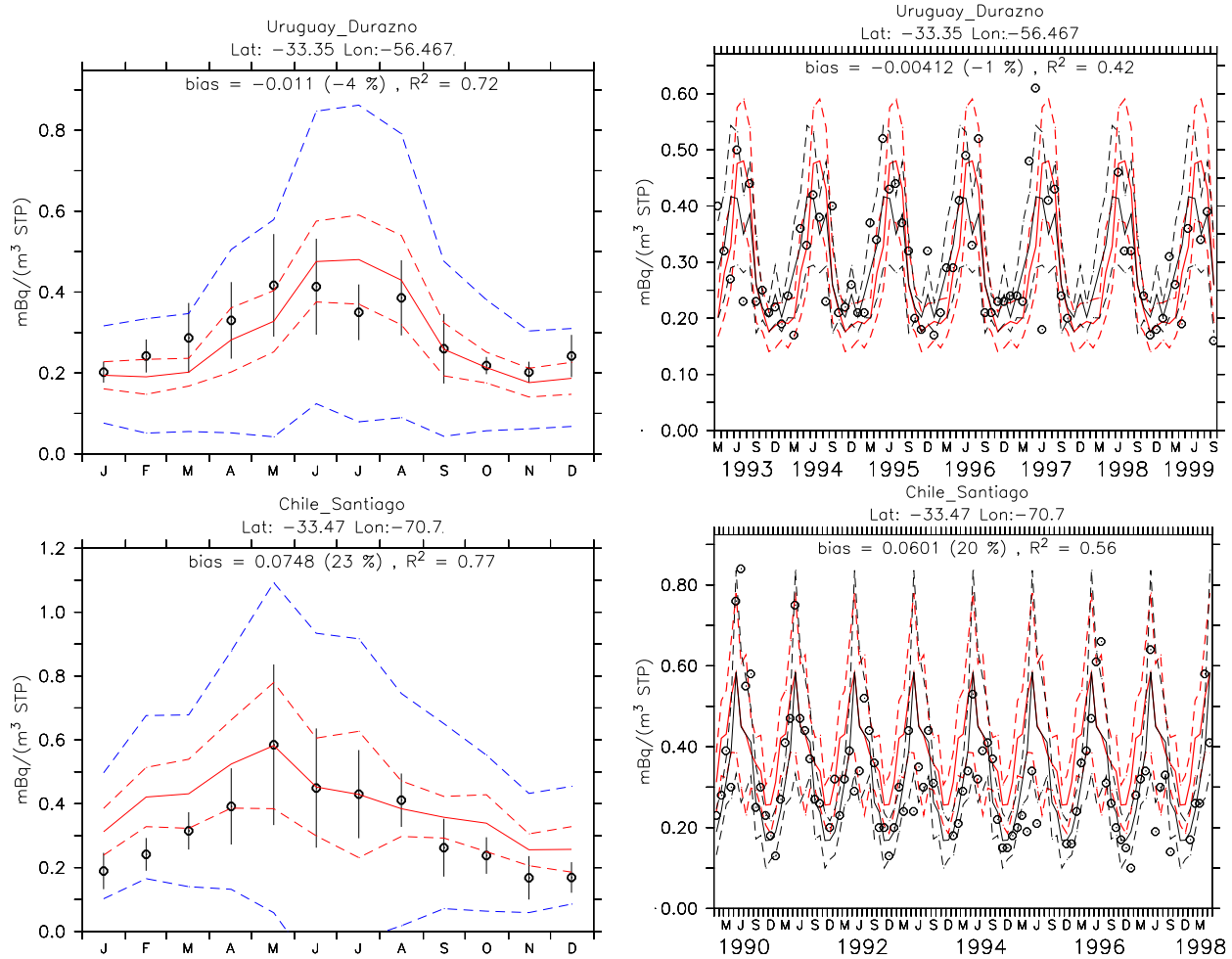


Figure 20: continued

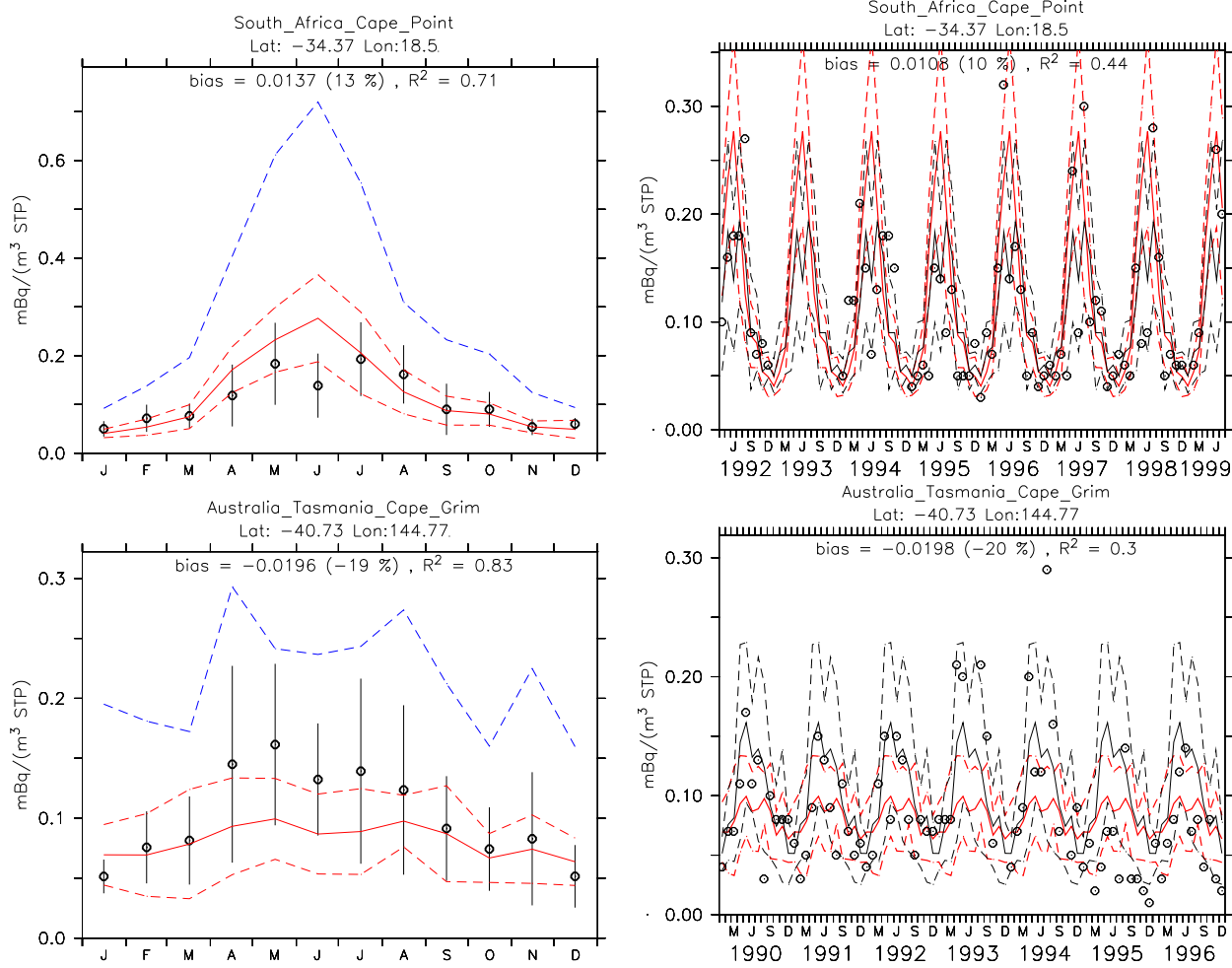


Figure 20: continued

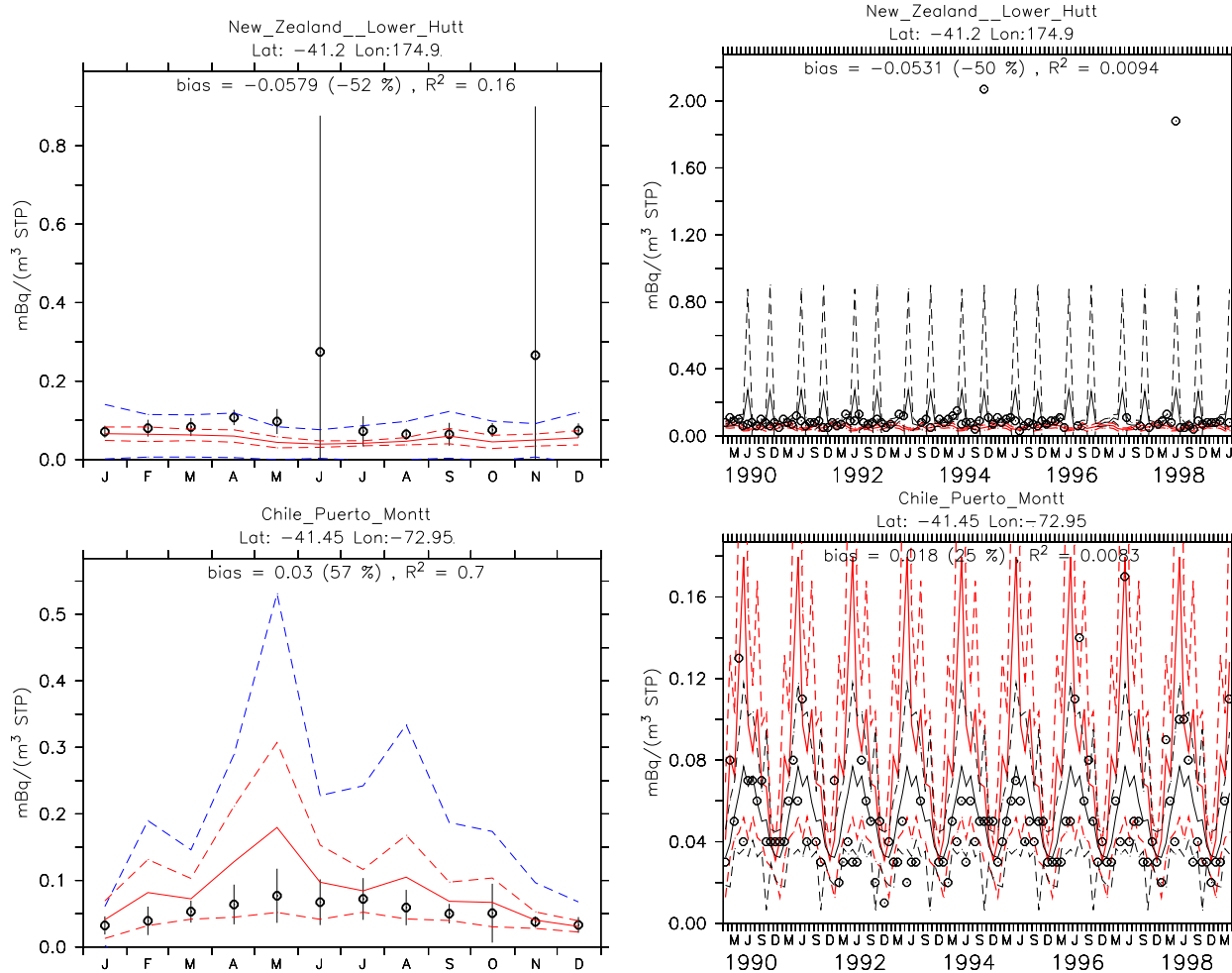


Figure 20: continued

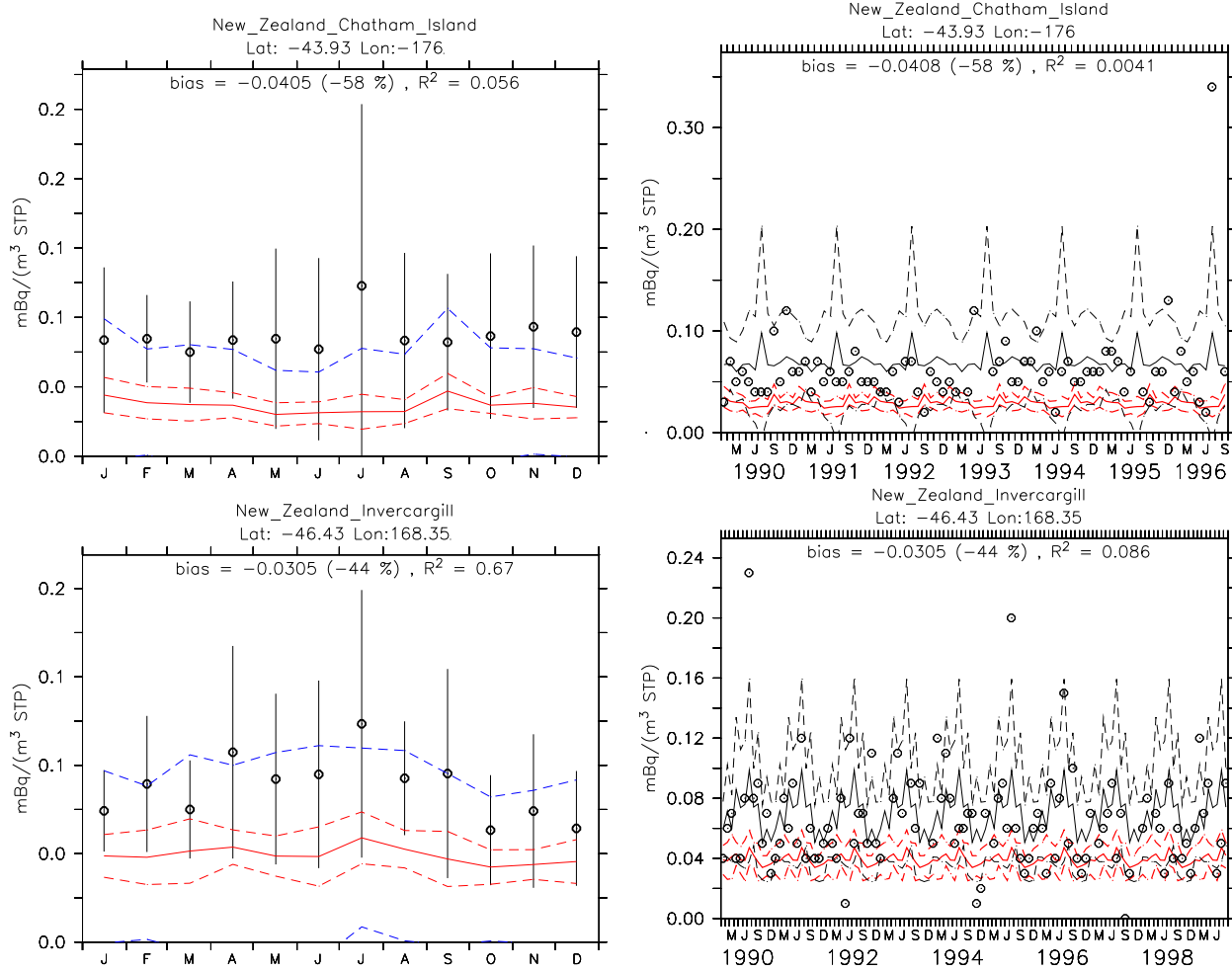


Figure 20: continued

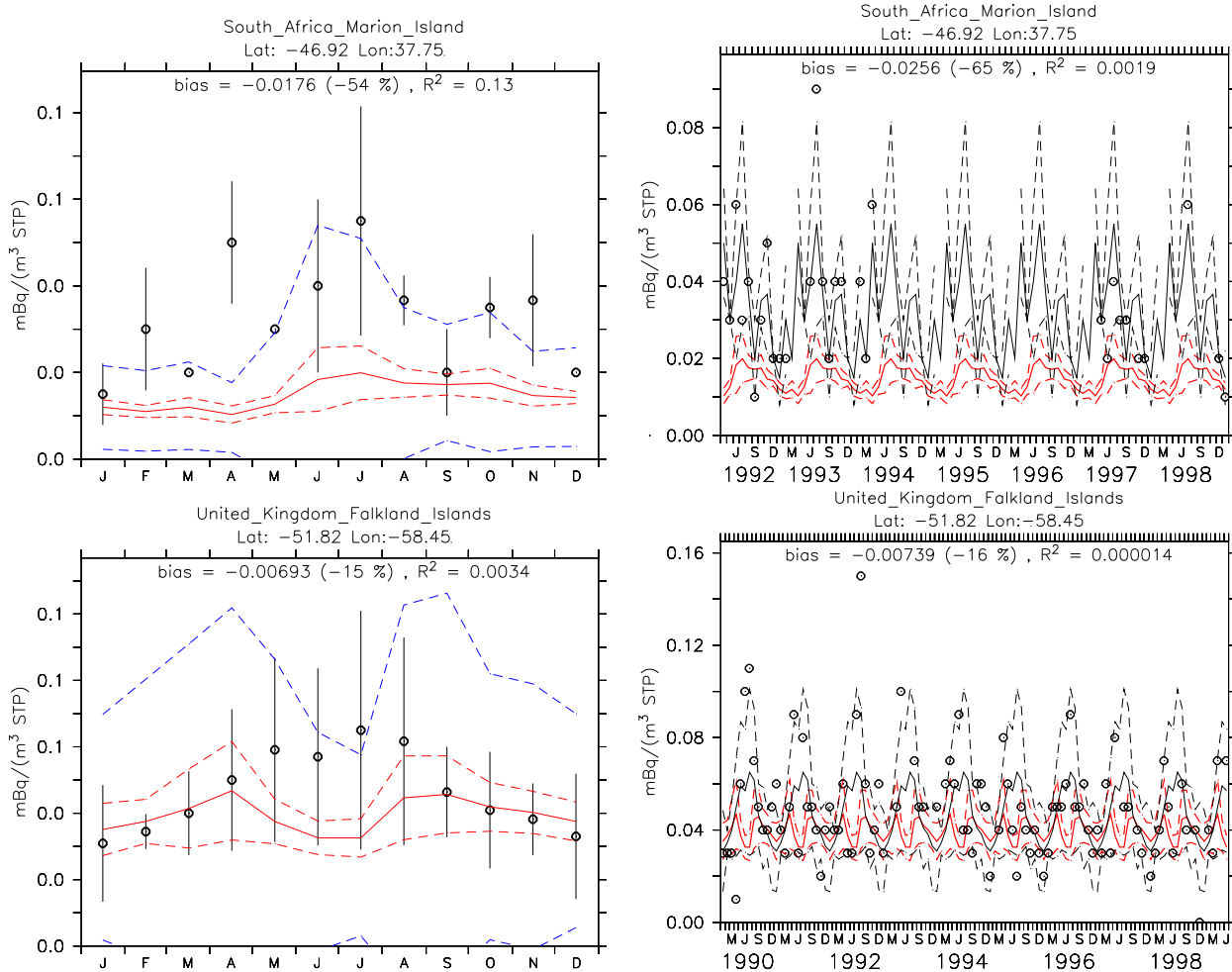


Figure 20: continued

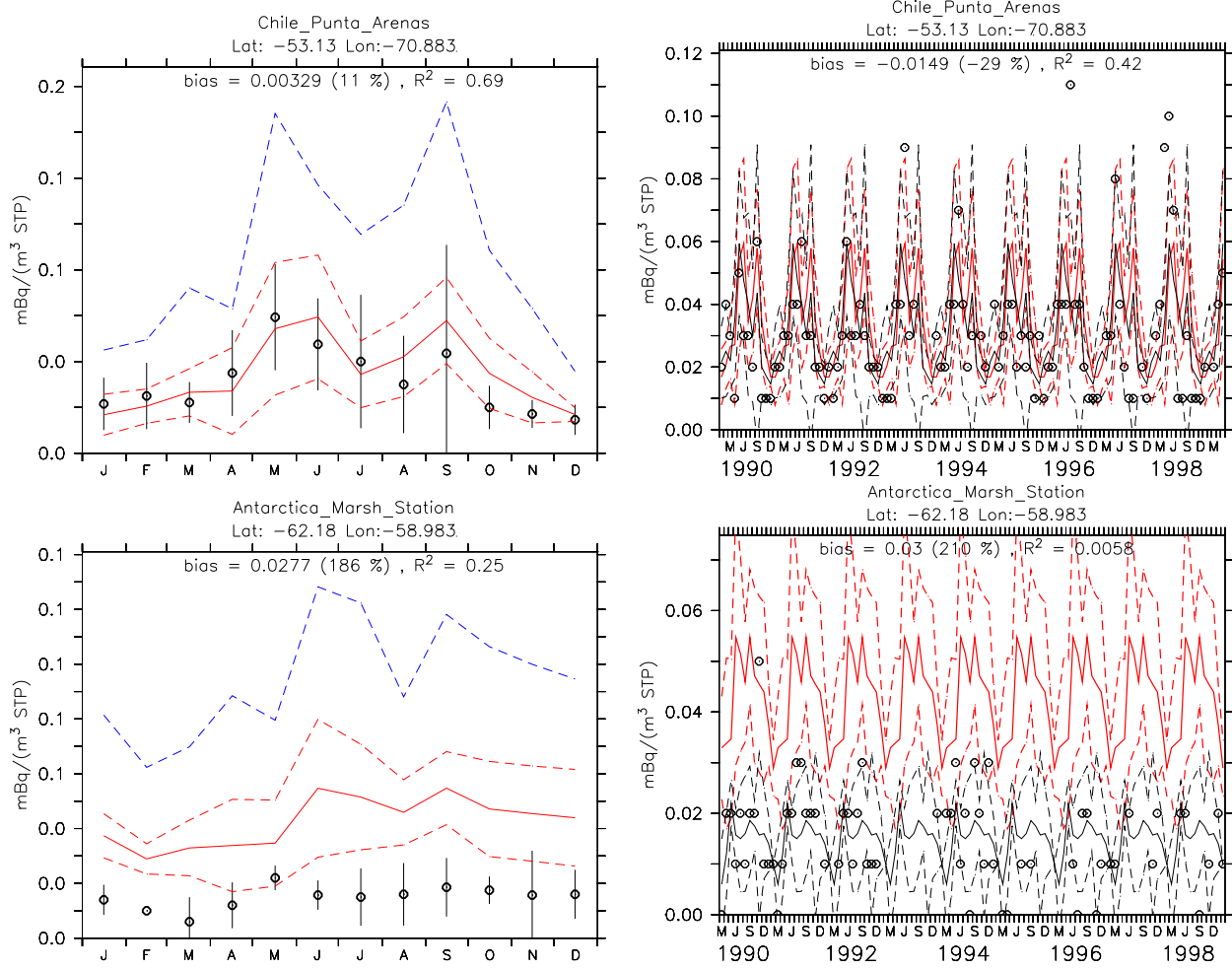


Figure 20: continued

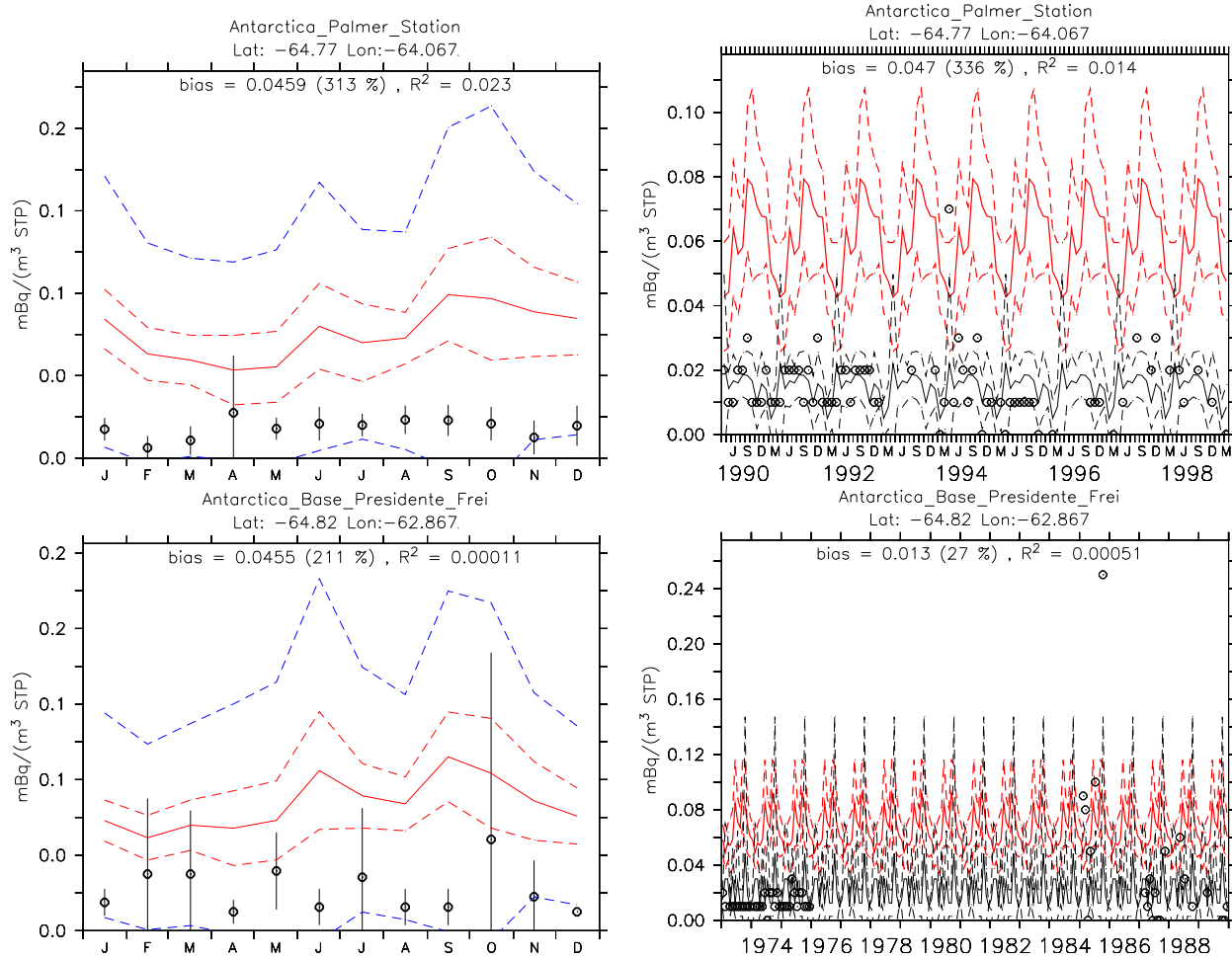


Figure 20: continued

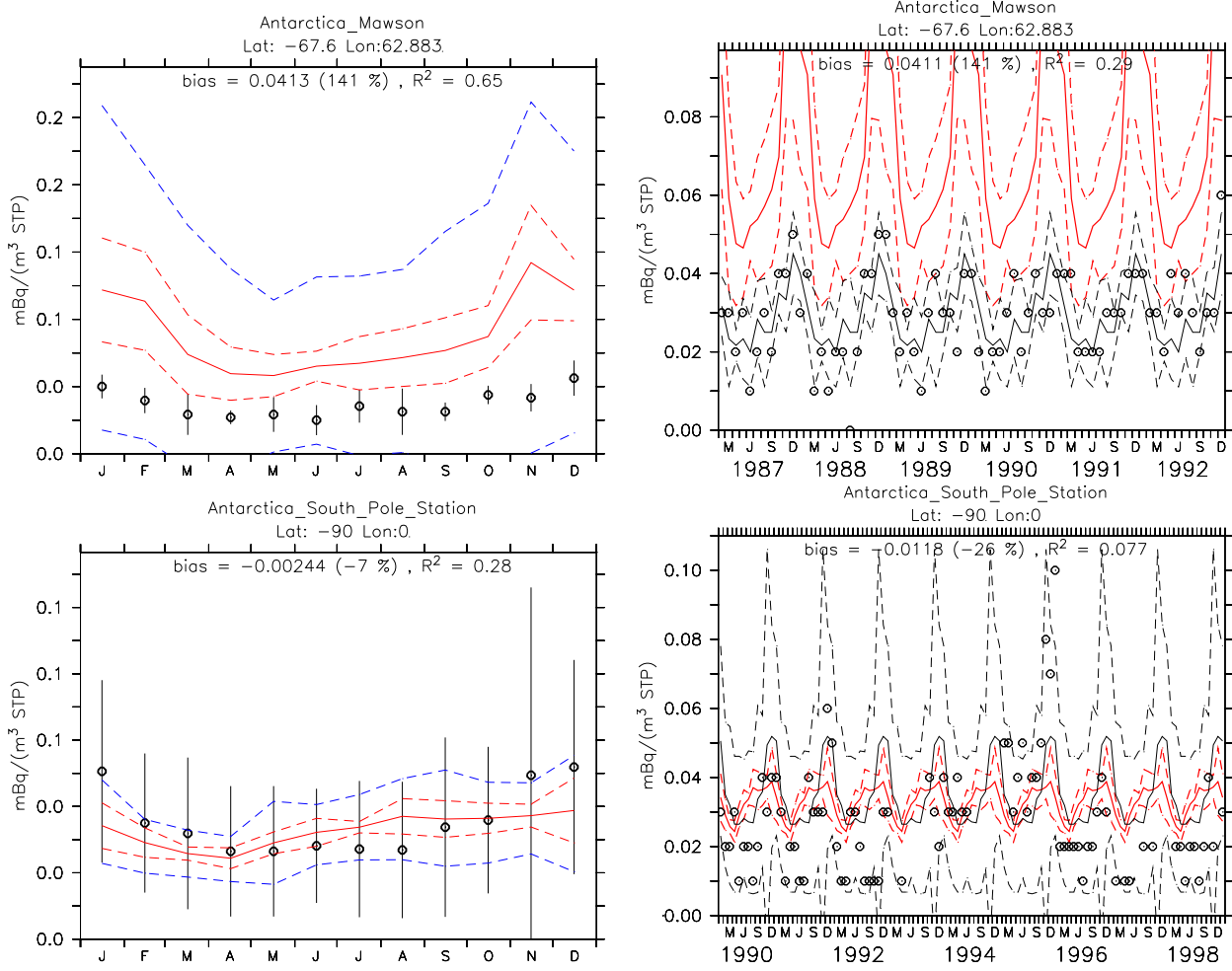


Figure 20: continued

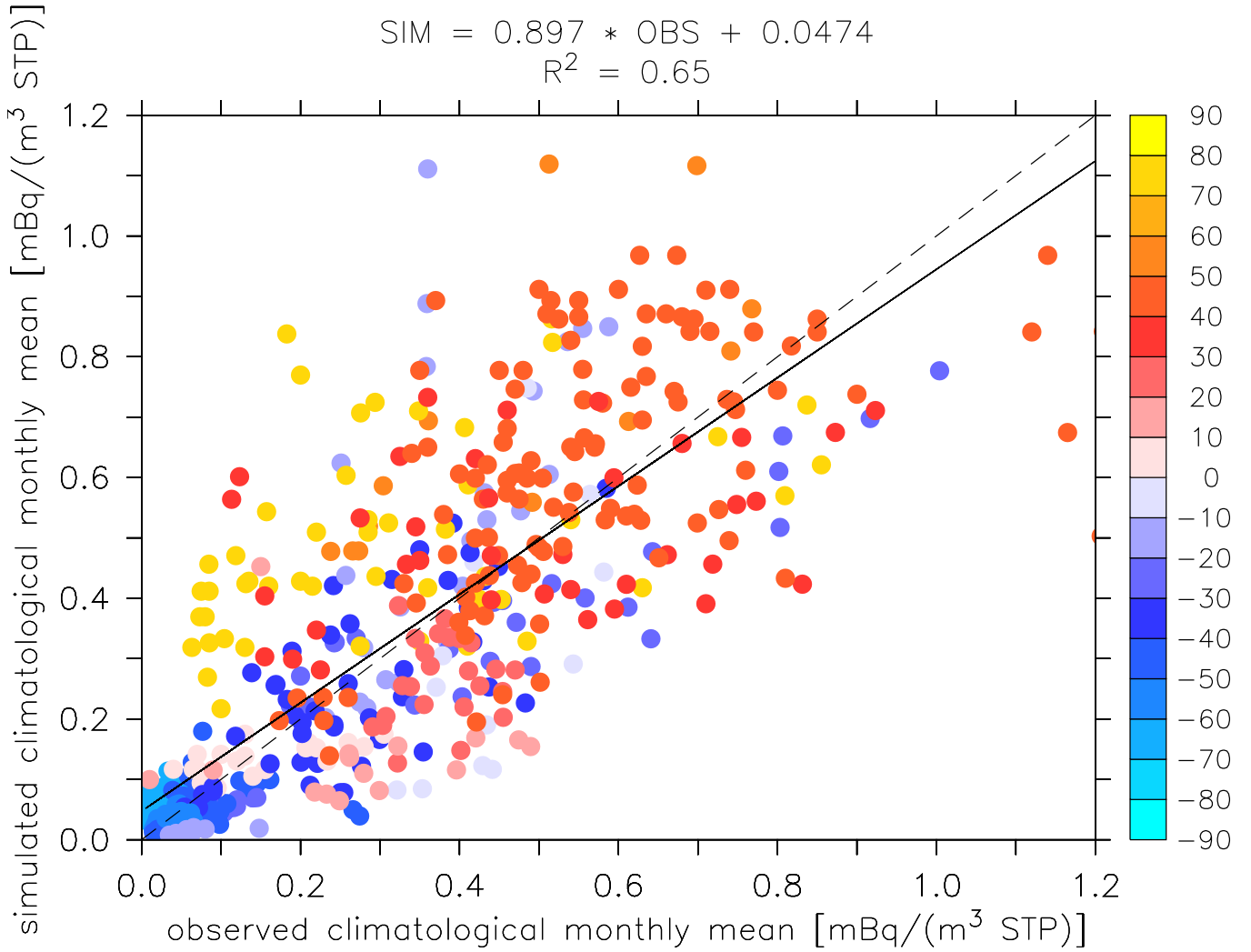


Figure 21: Simulated versus observed monthly climatological averages of ^{210}Pb (see Fig.20). The observations are from the National Urban Security Technology Laboratory Surface Air Sampling Program (NUSTL/SASP), the model results are from the years 2000-2007. The color denotes the geographical latitude, the dashed black line indicates the perfect correspondence. The black line shows the result of the linear regression analysis (as indicated in the top of the panel). R^2 is Pearson's correlation coefficient.

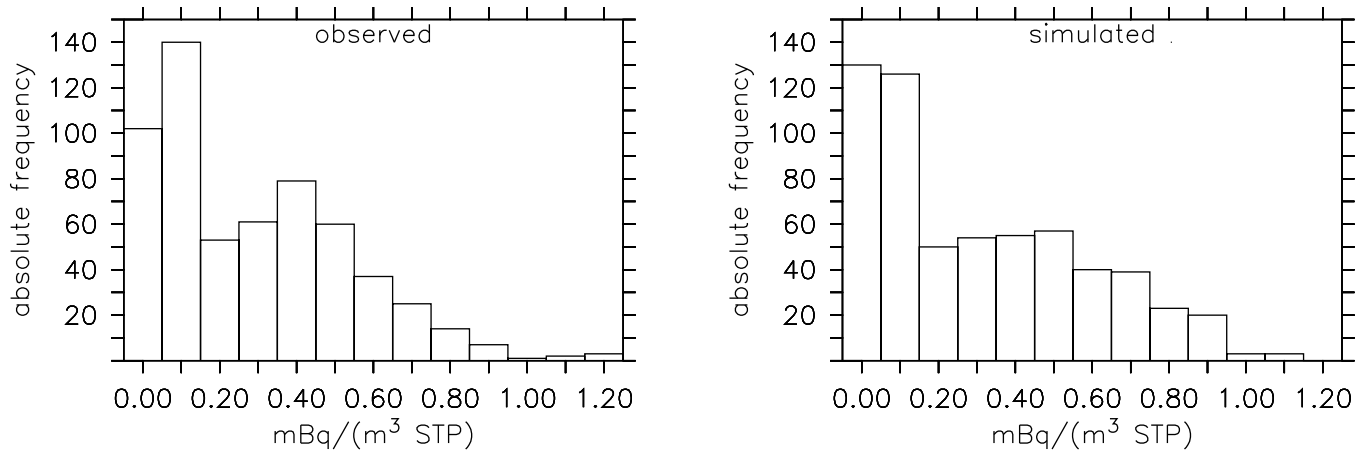


Figure 22: Frequency histograms of observed (left) and simulated (right) monthly climatological averages of ^{210}Pb (see Fig.20). The observations are from the National Urban Security Technology Laboratory Surface Air Sampling Program (NUSTL/SASP), the model results are from the years 2000-2007.

4.3 ^{222}Rn

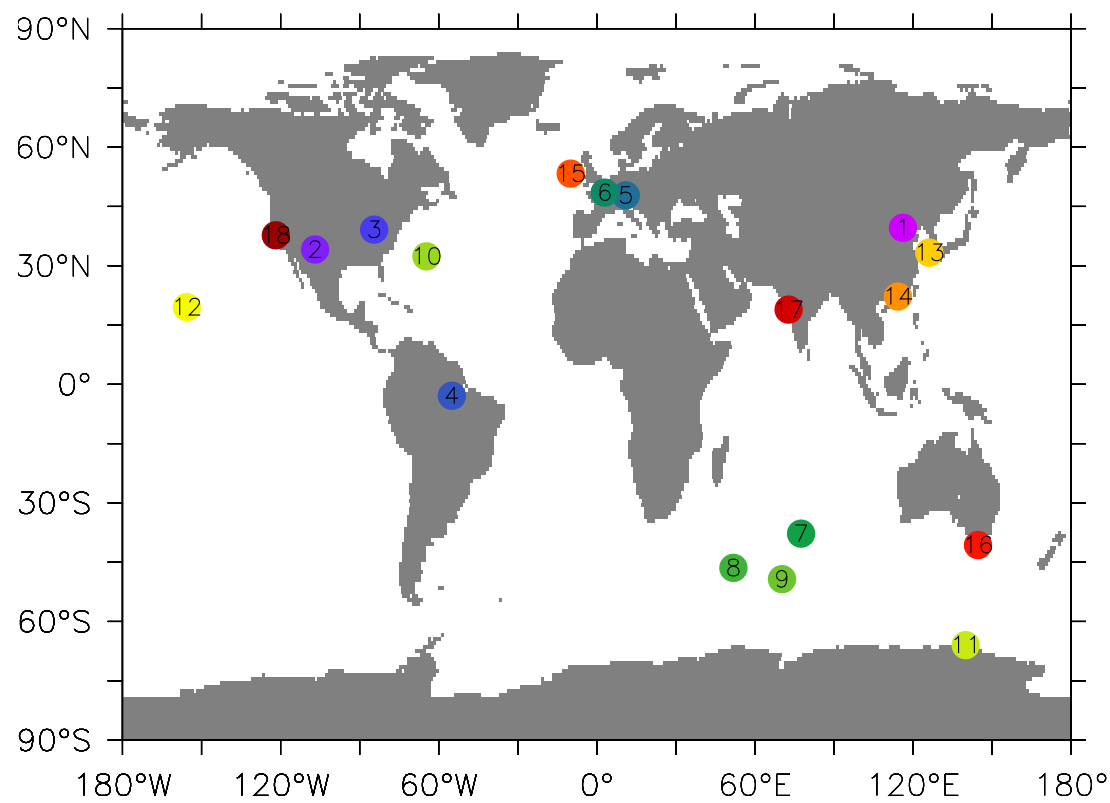


Figure 23: Geographical location of ^{222}Rn surface observations as used by Zhang et al. (2008, and references therein).

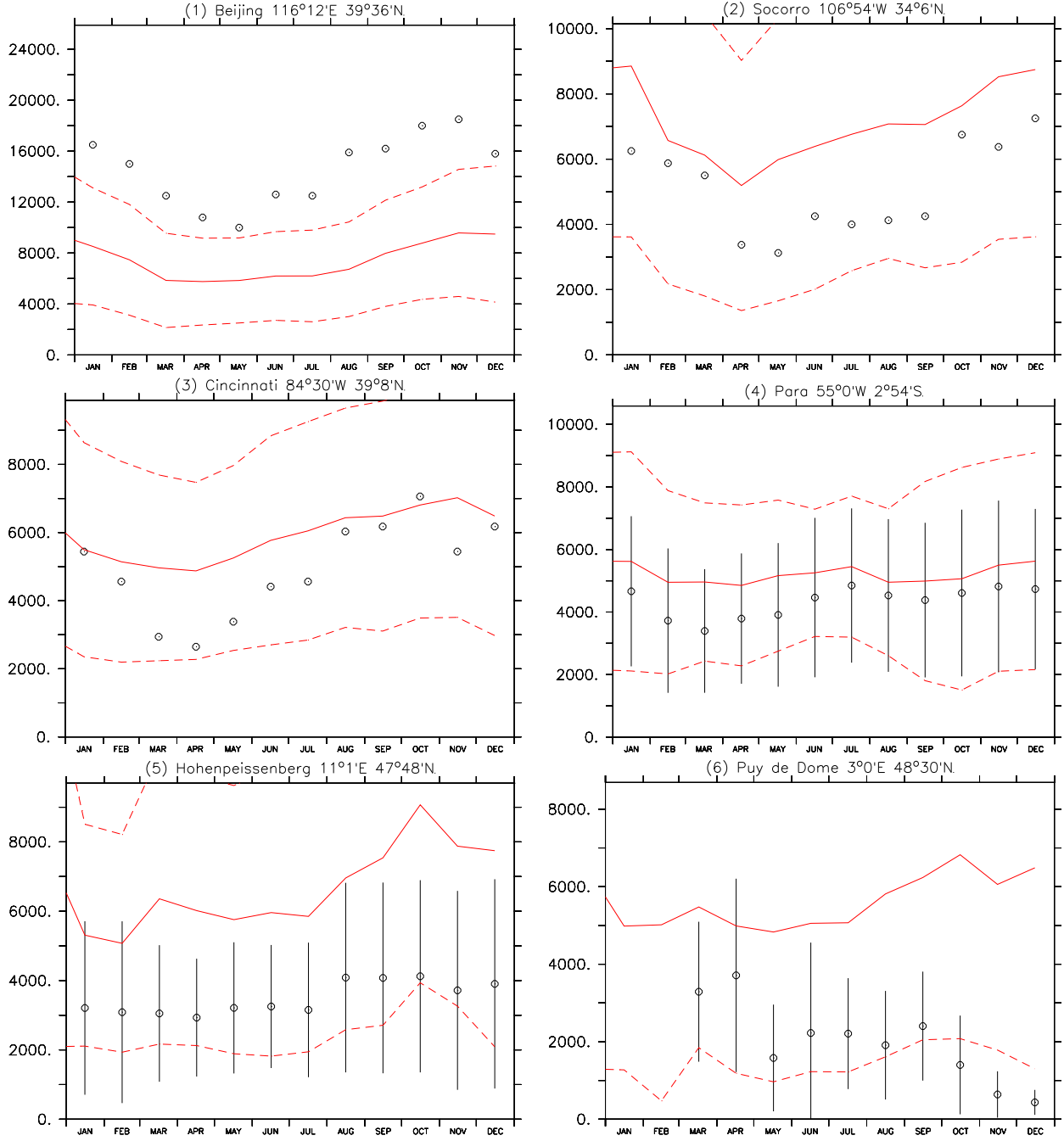


Figure 24: Observed (black symbols) and simulated (red lines) monthly average ^{222}Rn activity (in mBq/m³ STP) at ground level. The observations are the same as used by Zhang et al. (2008, and references therein), the model results are climatological monthly averages of the years 2000 - 2007. The black bars (if available) show the multi-annual standard deviation of the observations, the dashed red lines indicate the corresponding simulated standard deviations (plus / minus). The numbers in the titles correspond to the location labels in Fig. 23, the name of the sites and the geographical coordinates are listed in addition.

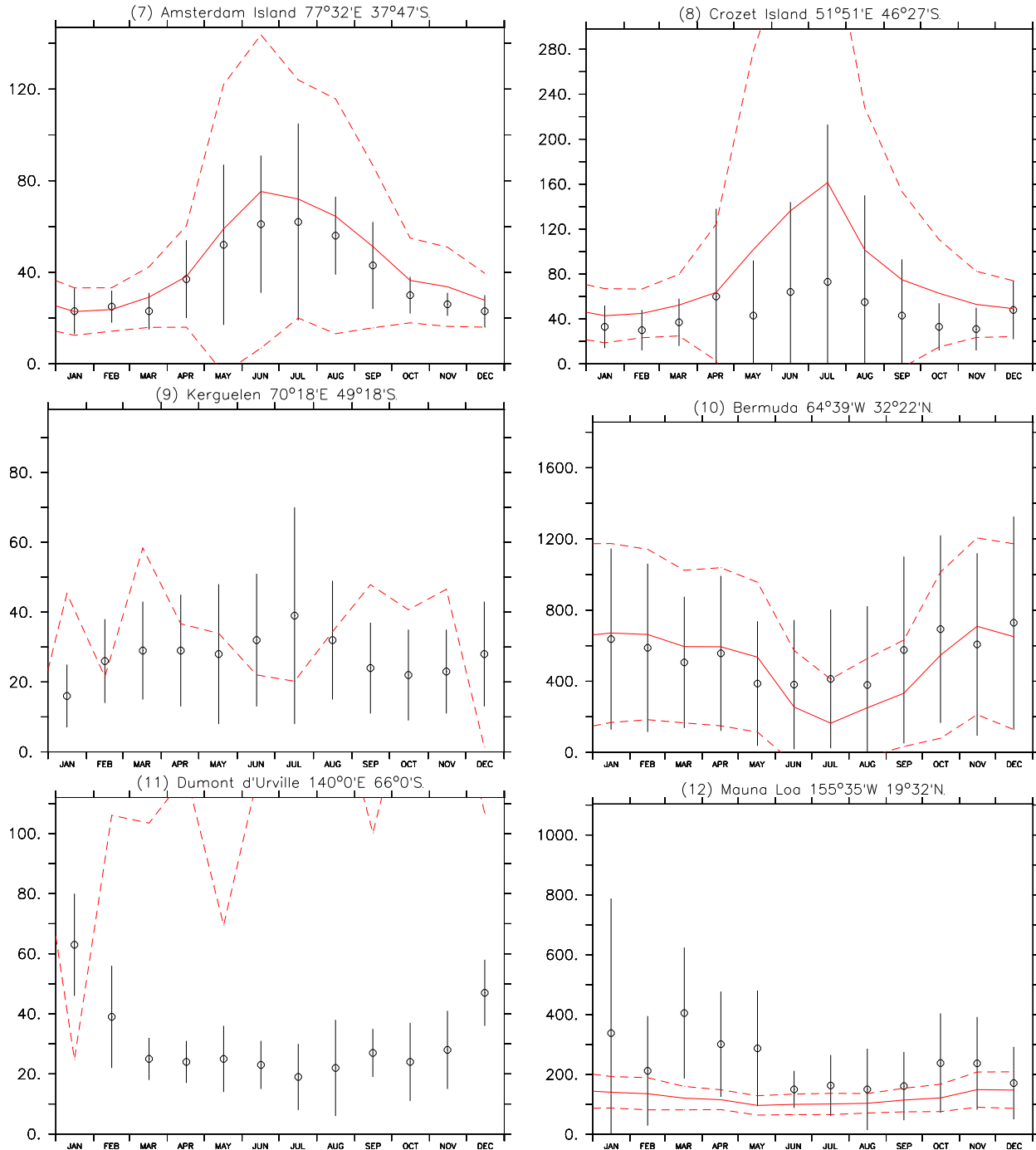


Figure 24: continued

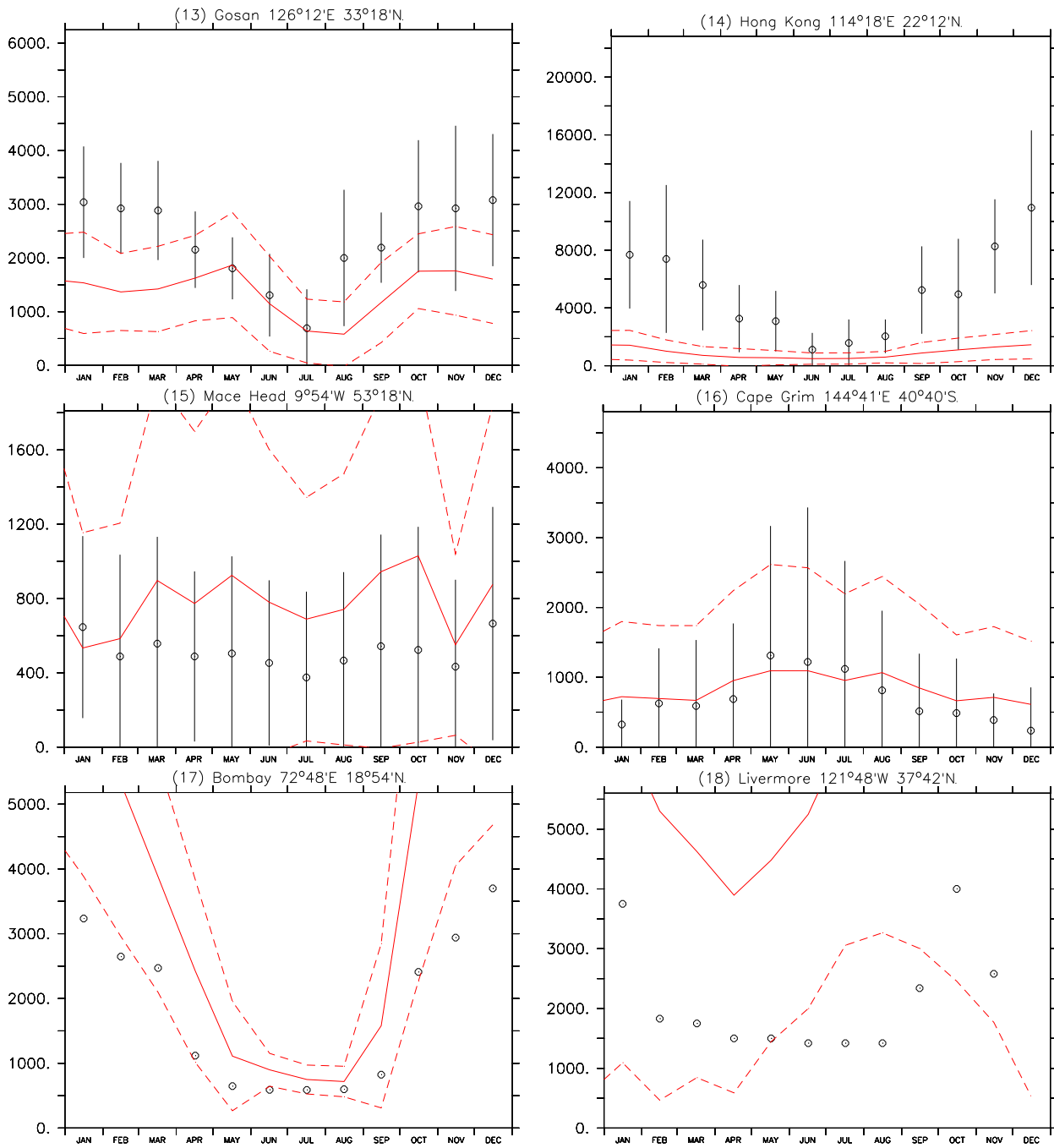


Figure 24: continued

References

- Emmons, L. K., Hauglustaine, D. A., Müller, J.-F., Carroll, M. A., Brasseur, G. P., Brunner, D., Staehelin, J., Thouret, V., and Marenco, A.: Data composites of airborne observation of tropospheric ozone and its precursor, *J. Geophys. Res.*, 105, 20 497–20 538, 2000.
- Jöckel, P., Tost, H., Pozzer, A., Brühl, C., Buchholz, J., Ganzeveld, L., Hoor, P., Kerkweg, A., Lawrence, M. G., Sander, R., Steil, B., Stiller, G., Tanarhte, M., Taraborrelli, D., van Aardenne, J., and Lelieveld, J.: The atmospheric chemistry general circulation model ECHAM5/MESSy1: consistent simulation of ozone from the surface to the mesosphere, *Atmos. Chem. Phys.*, 6, 5067–5104, <http://www.atmos-chem-phys.net/6/5067>, 2006.
- Novelli, P. C., Masarie, K. A., and Lang, P. M.: Distributions and recent changes in carbon monoxide in the lower troposphere, *J. Geophys. Res.*, 103, 19 015–19 033, 1998.
- Pozzer, A., Jöckel, P., Tost, H., Sander, R., Ganzeveld, L., Kerkweg, A., and Lelieveld, J.: Simulating organic species with the global atmospheric chemistry general circulation model ECHAM5/MESSy1: a comparison of model results with observations, *Atmos. Chem. Phys.*, 7, 2527–2550, <http://www.atmos-chem-phys.net/7/2527>, 2007.
- Randerson, J. T., van der Werf, G. R., Giglio, L., Collatz, G. J., and Kasibhatla, P. S.: Global Fire Emissions Database, Version 2 (GFEDv2.1), Tech. rep., Oak Ridge National Laboratory Distributed Active Archive Center, Oak Ridge, Tennessee, U.S.A, doi:10.3334/ORNLDaac/849, <http://daac.ornl.gov/>, 2007.
- Van der Werf, G. R., Randerson, J. T., L.Giglio, Collatz, G. J., and Kasibhatla, P. S.: Interannual variability in global biomass burning emission from 1997 to 2004, *Atmos. Chem. Phys.*, 6, 3423–3441, sRef-ID: 1680-7324/acp/2006-6-3423, 2006.
- Zhang, K., Wan, H., Zhang, M., and Wang, B.: Evaluation of the atmospheric transport in a GCM using radon measurements: sensitivity to cumulus convection parameterization, *Atmos. Chem. Phys.*, 8, 2811–2832, <http://www.atmos-chem-phys.net/8/2811/2008/>, 2008.